

AD-A222 881

DOCUMENTATION PAGE

Form Approved
OASD No. 0704-0188

Public reporting burden for this collection of information is estimated to average 1 hour per response, including the time for reviewing instructions, searching existing data sources, gathering and maintaining the data needed, and completing and reviewing the collection of information. Send comments regarding this burden estimate or any other aspect of this collection of information, including suggestions for reducing this burden, to Washington Headquarters Services, Directorate for Information Operations and Reports, 1215 Jefferson Davis Highway, Suite 1204, Arlington, VA 22202-4302, and to the Office of Management and Budget, Paperwork Reduction Project (0704-0188), Washington, DC 20503.

1. AGENCY USE ONLY (Leave blank)	2. REPORT DATE 7 May 1990	3. REPORT TYPE AND DATES COVERED Final Report/1 Sep 89-31 Aug 90	
4. TITLE AND SUBTITLE Support for the Forty-Second Annual Gaseous Electronics Conference		5. FUNDING NUMBERS 61102F/2301/A1	
6. AUTHOR(S) Dr. D. L. Huestis			
7. PERFORMING ORGANIZATION NAME(S) AND ADDRESS(ES) SRI International 333 Ravenswood Avenue Menlo Park CA 94025		8. PERFORMING ORGANIZATION REPORT NUMBER AFOSR-TR- 00 0644	
9. SPONSORING/MONITORING AGENCY NAME(S) AND ADDRESS(ES) AFOSR/NP Bolling AFB DC 20332-6448		10. SPONSORING/MONITORING AGENCY REPORT NUMBER AFOSR-89-0499	
11. SUPPLEMENTARY NOTES			
12a. DISTRIBUTION/AVAILABILITY STATEMENT Approved for public release; distribution is unlimited.		12b. DISTRIBUTION CODE	
13. ABSTRACT (Maximum 200 words) The Forty-Second Annual Gaseous Electronic Conference was held, as scheduled, on 16-20 October, 1989 in Palo Alto, CA.			
14. SUBJECT TERMS Gaseous, Electronics, Conference		15. NUMBER OF PAGES 217	
		16. PRICE CODE	
17. SECURITY CLASSIFICATION OF REPORT UNCLASSIFIED	18. SECURITY CLASSIFICATION OF THIS PAGE UNCLASSIFIED	19. SECURITY CLASSIFICATION OF ABSTRACT UNCLASSIFIED	20. LIMITATION OF ABSTRACT UL SAR

DTIC
ELECTE
MAY 31 1990
S O B D

G E C 89

*42nd Annual
Gaseous Electronics
Conference
17 – 20 October, 1989
Palo Alto, California*



Physical Sciences Building
SRI International, Menlo Park, CA

AEOSR-TR- 90 0644

42nd Annual Gaseous Electronics Conference

GEC89

16-20 October, 1989
Palo Alto, California

Approved for public release
distribution unlimited.

PROGRAM AND ABSTRACTS

A Topical Conference of the American Physical Society

Sponsored by:

SRI International

The American Physical Society: Division of Atomic, Molecular and Optical Physics

Executive Committee

James B. Gerardo, Chairman
Sandia National Laboratory

John H. Keller
IBM

William P. Allis, Honorary Chairman
Massachusetts Institute of Technology

James E. Lawler
University of Wisconsin

David L. Huestis, Secretary/Treasurer
SRI International

Chun C. Lin
University of Wisconsin

Ashok Bhattacharya
GE Lighting

William McConkey
University of Windsor

John P. Doering
Johns Hopkins University

Joseph M. Proud
GTE Laboratories

Douglas W. Ernie
University of Minnesota

Joseph T. Verdeyen
University of Illinois

Local Committee: SRI International

Young K. Bae, Philip C. Cosby, Donald J. Eckstrom, Marta C. Epp, Alison T. Gray,
Hanspeter Helm, A. Peet Hickman, David L. Huestis, Jay B. Jeffries, Donald C. Lorents,
James R. Peterson, Michel J. Rossi, Roberta P. Saxon, and Kenneth R. Stalder.

ACKNOWLEDGMENTS

The Gaseous Electronics Conference gratefully acknowledges the support of SRI International, and in particular the staffs of the Molecular Physics Laboratory and the Chemical Kinetics Department, for assistance with the local arrangements. Financial support for the Gaseous Electronics Conference has been provided by:

The Air Force Office of Scientific Research

The Army Research Office

The National Science Foundation

The General Electric Company

GTE Incorporated

The Gaseous Electronics Conference is a Topical Conference of the American Physical Society with sponsorship by the Division of Atomic, Molecular and Optical Physics.

CONTENTS

ACKNOWLEDGMENTS		ii
TECHNICAL PROGRAM		1
SESSIONS		
A	Diagnostics of Processing Discharges.....	27
BA	Hydrocarbon Plasmas.....	33
BB	Kinetic Models	39
BC	Electron Diffusion	43
CA	Plasma Processing.....	47
CB	Heavy Particle and Excited State Collisions.....	53
D	Workshop on the Reference System for RF Plasma Processing Research.....	57
E	Posters	59
FA	Ionization	85
FB	Laser Phenomena	89
GA	Arcs and Glows.....	95
GB	Electron and Heavy Particle Collisions.....	101
J	Posters	107
KA	Ar/Xe Lasers I	125
KB	Breakdown and Switching	131
LA	Ar/Xe Lasers II	137
LB	Cross Section Data I.....	143
MA	Fundamental Data from Plasmas.....	149
MB	Cross Section Data II.....	153
NA	Posters	159
NB	Novel Plasmas	177
P	Cross Sections I Wish I Knew.....	183
QA	Single Wafer Plasma Processing.....	189
QB	Collisions Between Atoms, Molecules, and Ions.....	195
RA	RF Discharges: Models and Experiments.....	201
RB	Optical Diagnostics	207
INDEX OF AUTHORS.....		213



	For
#1	<input checked="" type="checkbox"/>
ed	<input type="checkbox"/>
tion	<input type="checkbox"/>

Availability Codes	
Dist	Avail and/or Special
A-1	

TECHNICAL PROGRAM

FORTY SECOND ANNUAL GASEOUS ELECTRONICS CONFERENCE

REGISTRATION AND RECEPTION

6:30 PM - 9:30 PM
Monday, October 16, 1989
Hyatt Richeys Hotel
Camino Ball Room

INTRODUCTORY REMARKS

8:00 AM - 8:23 AM, Tuesday, October 17
Camino Ball Room C and D
Chair: D. L. Huestis, SRI International

8:00 - 8:10

WELCOME

Dr. George R. Abrahamson
Sr. Vice President
SRI International

8:10 - 8:23

REPORT ON NRC PLASMA SCIENCE COMMITTEE FOR PLASMA PROCESSING OF MATERIALS

J. M. Proud
GTE Laboratories

SESSION A. DIAGNOSTICS OF PROCESSING DISCHARGES

8:23 AM - 9:41 AM, Tuesday, October 17
Camino Ball Room C and D
Chair: H. H. Sawin, Massachusetts Institute of Technology

8:23 - 8:36

A-1

DETECTION OF ATOMIC CHLORINE IN RF PLASMAS BY LASER-EXCITED AMPLIFIED SPONTANEOUS EMISSION

A. D. Sappey and J. B. Jeffries

8:36 - 8:49

A-2

TWO-PHOTON DETECTION OF F AND F₂

G. W. Faris, M. J. Dyer, W. K. Bischel, and
D. L. Huestis

- | | | |
|-------------|-----|---|
| 8:49 - 9:02 | A-3 | LASER-INDUCED FLUORESCENCE
DIAGNOSTICS OF SILICON ETCHING
A. D. Sappey and J. B. Jeffries |
| 9:02 - 9:15 | A-4 | LASER-INDUCED-FLUORESCENCE
DETECTION OF SO AND SO ₂ IN 13.56-MHz
SF ₆ /O ₂ DISCHARGES
K. E. Greenberg and P. J. Hargis, Jr. |
| 9:15 - 9:28 | A-5 | S ₂ , SO, AND SO ₂ SPATIAL DISTRIBUTIONS IN
SF ₆ /O ₂ RADIO-FREQUENCY GLOW DISCHARGES
K. E. Greenberg and P. J. Hargis, Jr. |
| 9:28 - 9:41 | A-6 | ION CYCLOTRON RESONANCE MASS
SPECTROMETRY IN ECR PLASMAS
J. B. Friedmann, J. L. Shohet, A. E. Wendt,
and J. T. Brenna |

SESSION BA. HYDROCARBON PLASMAS

10:00 AM - 11:55 AM, Tuesday, October 17

Camino Ball Room C and D

Chair: L. W. Anderson, University of Wisconsin

- | | | |
|---------------|------|---|
| 10:00 - 10:25 | BA-1 | ROLE OF GAS DISCHARGE IN CHEMICAL
VAPOR DEPOSITION OF DIAMOND FILMS
Y. Tzeng
(Long Paper) |
| 10:25 - 10:38 | BA-2 | DIAMOND SYNTHESIS IN A 50 kW
INDUCTIVELY COUPLED ATMOSPHERIC
PRESSURE PLASMA
M. Gordon, T. Owano, C. H. Kruger, and
M. A. Cappelli |
| 10:38 - 10:51 | BA-3 | HYDROCARBONS FROM DISCHARGES IN
METHANE AND DISCHARGES OVER a-C:H FILMS
R. N. Rudolph and J. H. Moore |
| 10:51 - 11:04 | BA-4 | ABSOLUTE DENSITY AND SPATIAL
DISTRIBUTION OF THE FREE RADICAL CH ₃
AND CH ₂ IN A METHANE RF PLASMA
H. Sugai, H. Toyoda, and H. Kojima |
| 11:04 - 11:17 | BA-5 | MEASUREMENT METHOD OF THE SiH ₂
RADICAL DENSITY USING INFRARED LASER
ABSORPTION SPECTROSCOPY
T. Goto, N. Nishiwaki, N. Itabashi, K. Kato,
C. Yamada, and E. Hirota |
| 11:17 - 11:30 | BA-6 | INFRARED LASER ABSORPTION STUDIES OF
CF ₄ AND CH ₄ RF PLASMAS
J. Wormhoudt |

11:30 - 11:55 BA-7 PARTICULATE GENERATION IN SILANE/
AMMONIA RF DISCHARGES
H. M. Anderson and R. Jairath
(Long Paper)

SESSION BB. KINETIC MODELS

10:00 AM - 11:04 AM, Tuesday, October 17

Camino Ball Room B

Chair: B. M. Penetrante, Lawrence Livermore National Laboratory

10:00 - 10:25 BB-1 KINETIC MODELS OF GLOW DISCHARGES
W.N.G. Hitchon, T. J. Sommerer, and J. E. Lawler
(Long Paper)

10:25 - 10:38 BB-2 A MULTIGROUP APPROACH TO ELECTRON
KINETICS
S. Clark and E. E. Kunhardt

10:38 - 10:51 BB-3 TIME AND SPATIALLY DEPENDENT MONTE
CARLO SIMULATIONS OF PARTIALLY
IONIZED PLASMAS INCLUDING ELECTRON-
ELECTRON COLLISIONS
Y. Weng and M. J. Kushner

10:51 - 11:04 BB-4 THE EFFECTS OF PARTICULATE
CONTAMINATION ON ELECTRON
TRANSPORT IN GLOW DISCHARGES
M. J. McCaughey and M. J. Kushner

SESSION BC. ELECTRON DIFFUSION

11:04 AM - 12:08 PM, Tuesday, October 17

Camino Ball Room B

Chair: W.N.G Hitchon, University of New Mexico

11:04 - 11:29 BC-1 DIFFUSION THEORY OF ELECTRONS IN A
CONSTANT FIELD: TOF ANALYSIS
J. Ingold
(Long Paper)

11:29 - 11:42 BC-2 DGE ANALYSIS OF ASYMMETRIC TOF CURRENT
PULSES AT DIFFERENT DRIFT DISTANCES:
DETERMINATION OF V_d , D_L , D_3 AND D_4
C. A. Denman and L. A. Schlie

11:42 - 11:55 BC-3 BOLTZMANN AND MONTE CARLO
CALCULATIONS OF HIGHER-ORDER
TRANSPORT COEFFICIENTS
B. M. Penetrante and J. N. Bardsley

11:55 - 12:08 BC-4 NON-LINEAR DIFFUSION
E. E. Kunhardt

SESSION CA. PLASMA PROCESSING

1:30 PM - 3:18 PM, Tuesday, October 17

Camino Ball Room C

Chair: H. M. Anderson, University of New Mexico

- | | | |
|-------------|------|---|
| 1:30 - 1:55 | CA-1 | POWER DEPOSITION, DAMAGE MONITORING, AND END-POINT DETECTION USING PHOTOLUMINESCENCE SPECTROSCOPY IN RF GLOW DISCHARGES
R. A. Gottscho, A. Mitchell, S. J. Pearton, and G. R. Scheller
(Long Paper) |
| 1:55 - 2:08 | CA-2 | EFFECTS OF FEED GAS IMPURITIES ON THE PLASMA ETCHING OF POLYSILICON
G. Zau and H. H. Sawin |
| 2:08 - 2:26 | CA-3 | COMPUTER SIMULATION OF THE DYNAMICS OF PHYSICAL AND CHEMICAL PROCESSES ON SURFACES
W. L. Morgan
(Long Paper) |
| 2:26 - 2:39 | CA-4 | SURFACE REACTIONS OF ATOMIC CHLORINE ON POLYCRYSTALLINE Ni AND Si(110)
W. Mueller-Markgraf and M. J. Rossi |
| 2:39 - 2:52 | CA-5 | RADIATION DAMAGE TO SILICON BY COMBINED MICROWAVE AND RF PLASMA REACTIVE ION ETCHING
Y. Tzeng, T. H. Lin, and C. C. Tin |
| 2:52 - 3:05 | CA-6 | PLASMA ETCHING OF Y-Ba-Cu-OXIDE THIN FILMS
M. R. Poor and C. B. Fleddermann |
| 3:05 - 3:18 | CA-7 | POSITIVE ION FORMATION IN POSITIVE POLARITY SF ₆ CORONA DISCHARGES
I. Sauers and G. Harman |

SESSION CB. HEAVY PARTICLE AND EXCITED STATE COLLISIONS

1:30 PM - 3:28 PM, Tuesday, October 17

Camino Ball Room D

Chair: M. R. Flannery, Georgia Institute of Technology

- | | | |
|-------------|------|---|
| 1:30 - 2:05 | CB-1 | ASSOCIATION REACTIONS OF METASTABLE HELIUM ATOMS
J. Stevefelt
(Invited Paper) |
|-------------|------|---|

- | | | |
|-------------|------|---|
| 2:05 - 2:40 | CB-2 | HALF COLLISION STUDIES OF THE H + H ₂ TRANSITION STATE
P. C. Cosby and H. Helm
(Invited Paper) |
| 2:40 - 3:15 | CB-3 | STUDY OF LOW-ENERGY ELECTRON-MOLECULE INTERACTIONS USING RYDBERG ATOMS
F. B. Dunning
(Invited Paper) |
| 3:15 - 3:28 | CB-4 | RECOMBINATION OF Xe ⁺ IONS AND F ⁻ IONS IN AMBIENT HELIUM
H. S. Lee and R. Johnsen |

SESSION D. WORKSHOP ON THE REFERENCE SYSTEM FOR RF PLASMA PROCESSING RESEARCH

3:45 PM - 5:30 PM, Tuesday, October 17

Camino Ball Room C and D

Moderator: K. E. Greenberg, Sandia National Laboratories

A follow-up workshop is planned to review the progress made since last year's workshop on development of a "RF Reference Cell" for plasma processing research. The motivation for defining a specific design and a specific procedure for calibration is found in the observations that subtle differences in cell design may have profound effects on system characteristics and that calibration procedures are often insufficient to assure commonality of system characteristics, thus making data comparison difficult. Participants at last year's workshop agreed on an accepted specific design, "The Reference Cell" and an accepted calibration procedure, "The Reference Calibration," defining both cell design and a calibration tool set. Since then the discharge chamber design has been finalized and several systems are being constructed. It is expected that evaluation of several of these systems will be sufficiently far along by the time of this workshop to permit a meaningful comparison of results.

SESSION E. POSTERS

7:30 PM- 10:00 PM, Tuesday, October 17

Camino Ball Room A and B

Chair: H. Helm, SRI International

- | | |
|-----|---|
| E-1 | CYLINDRICAL SIMULATIONS OF RF PLASMA DISCHARGES AND PLASMA IMMERSION ION IMPLANTATION
M. V. Alves, V. Vahedi, and C. K. Birdsall |
| E-2 | PARTICLE SIMULATION CODE FOR MODELING PROCESSING PLASMAS
I. J. Morey, V. Vahedi, J. Verboncoeur, and M. A. Lieberman |

- E-3 DC SELF-BIAS VOLTAGES IN LOW PRESSURE DISCHARGES IN FINITE CYLINDRICAL CHAMBERS
M. A. Lieberman and S. E. Savas
- E-4 PARALLELIZING THE MONTE CARLO SIMULATION IN WEAKLY IONIZED PLASMAS
C. J. Wang and C. Wu
- E-5 THE PLASMA SHEATH TRANSITION IN AN ASYMMETRIC COLLISIONLESS PLASMA
H. van den Berg and K.-U. Riemann
- E-6 PARAMETRIC STUDIES OF Ar AND SF₆ RF DISCHARGES USING THE CONTINUUM MODEL, AND COMPARISON WITH EXPERIMENTAL DATA
E. Gogolides, J. Liu, and H. H. Sawin
- E-7 PIC SIMULATION AT HIGH PLASMA DENSITIES
R. K. Porteous and D. B. Graves
- E-8 ION BOMBARDMENT ENERGY DISTRIBUTIONS FROM RF DISCHARGES
M. F. Toups, D. W. Ernie, and H. J. Oskam
- E-9 A TUNED LANGMUIR PROBE FOR MEASUREMENTS IN RF GLOW DISCHARGES
A. P. Paranjpe, J. P. McVittie, and S. A. Self
- E-10 COLLISIONAL EFFECTS ON PLASMA FLOW ALONG THE DIVERGENT MAGNETIC FIELD OF AN ECR PLASMA STREAM SOURCE
M. Hussein and G. A. Emmert
- E-11 A COMPARISON OF THREE POWER MEASUREMENT TECHNIQUES IN A LOW PRESSURE RF DISCHARGE
R. B. Piejak and V. A. Godyak
- E-12 TIME-DEPENDENT EXCITATION IN A 13-MHz ARGON DISCHARGE
M. J. Colgan and D. E. Murnick
- E-13 TRANSIENT ELECTRON KINETICS IN CROSSED ELECTRIC AND MAGNETIC FIELDS AND CIRCULARLY POLARIZED MICROWAVE FIELD
P. Hui and G. Schaefer
- E-14 EXPERIMENTAL AND THEORETICAL LONGITUDINAL ELECTRON DIFFUSION COEFFICIENTS IN MOLECULAR GASES
J. L. Pack, R. E. Voshall, A. V. Phelps, and L. E. Kline

- E-15 PHOTODETACHMENT TECHNIQUE FOR MEASURING H⁻ VELOCITIES IN A HYDROGEN PLASMA
P. Devynck, M. Bacal, P. Berlemont, J. Brunteau, R. Leroy, and R. A. Stern
- E-16 FOKKER-PLANCK SWARM ENERGY SPECTRUM
N. J. Carron
- E-17 PARTICLE FOCUSING USING TWO-STAGE LASER ABLATION
K. D. Bonin and M. A. Kadar-Kallen
- E-18 TWO APPROXIMATE SHEATH SOLUTIONS FOR A PLANAR PLASMA ANODE
O. Biblarz
- E-19 THE UNIVERSAL RESPUTTERING CURVE
W. L. Morgan
- E-20 OPTICAL DIAGNOSTICS OF SPUTTERED METAL ATOMS IN DC AND RF DISCHARGES
G. M. Jellum and D. B. Graves
- E-21 ELECTRICAL CONDUCTIVITY OF HIGH PRESSURE IONIZED XENON
J. Koceić and S. Popović
- E-22 ELECTRIC FIELD IN SUPER-NARROW TUBE LOW PRESSURE Hg-Ar ELECTRIC DISCHARGE LAMPS
G. Zisis, P. Bénétruy, and J. J. Damelincourt
- E-23 LOW ELECTRIC FIELD MEASUREMENTS IN PLASMAS
J. R. Shoemaker
- E-24 MODELLING OF A SURFACE WAVE SUSTAINED HELIUM DISCHARGE AT LOW PRESSURE
S. Daviaud, G. Gousset, and J. Marec
- E-25 VUV SPECTROSCOPY OF AN ARGON SURFACE WAVE PLASMA WITH SUPERSONIC FLOW
M. E. Bannister, J. L. Cecchi, and G. Scoles
- E-26 SIMULATION OF ELECTRON AVALANCHES NEAR A GAS-SOLID INTERFACE
S. M. Mahajan and K. W. Lam
- E-27 CREATION OF AN ELECTROSTATIC IMAGE ON A DIELECTRIC SURFACE IN A SMALL GAP
V. Meytlis, T. Kegelman, and B. Fagen

- E-28 CONDUCTIVITY PROBE FOR HIGH PRESSURE PLASMAS
S. M. Jaffe, S. A. Self, and M. Mitchner
- E-29 OPTICAL EMISSION AND LANGMUIR PROBE DIAGNOSTICS OF A HYDROCARBON ARC JET PLASMA
K. R. Stalder and R. L. Sharpless
- E-30 IN-SITU DENSITY AND TEMPERATURE MEASUREMENTS OF VIBRATIONALLY-EXCITED HYDROGEN MOLECULES IN H⁻ ION SOURCE PLASMAS
G. C. Stutzin, A. T. Young, A. S. Schlachter, K. N. Leung, and W. B. Kunkel
- E-31 ATOMIC HYDROGEN MEASUREMENTS IN HYDROGEN BEARING PLASMAS
B. L. Preppernau, A. Tserepi, T. Czerny, and T. A. Miller
- E-32 DETECTION OF ATOMIC HYDROGEN NEAR A SURFACE BY RESONANT FOUR-PHOTON IONIZATION TECHNIQUE
G. Sultan, G. Baravian, J. Jolly, and P. Persuy
- E-33 STOCHASTIC PROPERTIES OF TRICHEL PULSE CORONA DISCHARGES IN O₂ AND Ne/O₂ MIXTURES
R. J. Van Brunt, S. V. Kulkarni, and V. K. Lakdawala
- E-34 ABSOLUTE TOTAL INELASTIC ELECTRON IMPACT EXCITATION OF He AND Ne
D. Spence and M. A. Dillon
- E-35 LOW ENERGY SHAPE RESONANCE IN THE GROUND ELECTRONIC STATE VIBRATIONAL EXCITATION OF SILANE AND DISILANE
H. Tanaka, L. Boesten, H. Sato, M. Kimura, M. A. Dillon, and D. Spence
- E-36 ELASTIC SCATTERING CROSS SECTION MEASUREMENTS FOR COLLISIONS OF 1.5-100 eV ELECTRONS WITH SILANE AND DISILANE
H. Tanaka, L. Boesten, H. Sato, M. Kimura, M. A. Dillon, and D. Spence
- E-37 POSITRON-CO COLLISIONS USING PARAMETER-FREE POSITRON CORRELATION POLARIZATION POTENTIAL
A. K. Jain
- E-38 CROSS SECTIONS FOR SOME CORE-EXCITED NaI QUARTET STATES
A. Z. Msezane

- E-39 ENERGETICS OF NEGATIVE ION FORMATION
VIA DISSOCIATIVE ATTACHMENT OF $e + \text{LiH}$
H. H. Michels and J. M. Wadehra
- E-40 LOW-ENERGY ELECTRON IMPACT
DISSOCIATION OF H_2 USING FULLY
CORRELATED TARGET WAVEFUNCTIONS
W. M. Huo
- E-41 THREE-BODY ASSOCIATION OF ATOMIC
IONS IN ATOMIC GASES
B. K. Chatterjee and R. Johnsen
- E-42 ION-MOLECULE REACTIONS OF
ATMOSPHERIC IONS WITH DIMETHYL-
METHYLPHOSPHONATE
R. Tosh, B. K. Chatterjee, and R. Johnsen
- E-43 ASSOCIATION REACTIONS IN $\text{C}_2\text{H}_2^+/ \text{C}_2\text{H}_2$
AND $\text{HC}_3\text{N}^+ / \text{HC}_3\text{N}$ SYSTEMS
A. D. Sen, V. G. Anicich, and M. J. McEwan
- E-44 DECAY PRODUCT AND ENERGY DISTRIBUTIONS
FROM H_3 $n=2$ RYDBERG STATES
P. Devynck, W. G. Graham, and J. R. Peterson
- E-45 NEAR ZERO PROJECTILE-FRAME KINETIC
ENERGY H^+ IN $\text{H}_2^+ - \text{He}$ COLLISIONS AT 4.0 keV
O. Yenen, L. Wiese, D. Calabrese, and D. H. Jaecks
- E-46 $\text{SO}_2 \cdot n\text{SO}_2$, $(\text{SO}_2 - \text{O}_2)^- \cdot n\text{SO}_2$ AND $(\text{SO}_2 - \text{O}_3)^- \cdot$
 $n\text{SO}_2$ CLUSTERS ($0 \leq n \leq 7$)
M. Jorda, E. Leduc, and M. Fitaire
- E-47 SPECTROSCOPIC STUDY OF A BOUND
TRIPLET STATE OF H_2 PERTURBED BY A
DOUBLY EXCITED STATE
L. J. Lembo, N. Bjerre, D. L. Huestis, and H. Helm
- E-48 TWO COLOR PHOTO-IONIZATION SPECTRA OF
 He_2 $a^3\Sigma_u^+$
N. Bjerre, L. Lembo, D. C. Lorents, and H. Helm

SESSION FA. IONIZATION

8:00 AM - 9:25 AM, Wednesday, October 18

Camino Ball Room C

Chair: S. K. Srivastava, Jet Propulsion Laboratory

- 8:00 - 8:35 FA-1 MEASUREMENTS OF ELECTRON IMPACT
IONIZATION CROSS SECTIONS
R. S. Freund
(Invited Paper)

- | | | |
|-------------|------|--|
| 8:35 - 9:00 | FA-2 | <p>THEORETICAL CALCULATIONS FOR ELECTRON-IMPACT IONIZATION OF METASTABLE STATES OF RARE-GAS TARGETS</p> <p>J. B. Mann, A. L. Merts, and G. Csanak
(Long Paper)</p> |
| 9:00 - 9:25 | FA-3 | <p>THE IDENTIFICATION OF RECOMBINATION PRODUCT EXCITATION STATES</p> <p>J.B.A. Mitchell, F. B. Yousif, P. van der Donk,
and T. J. Morgan
(Long Paper)</p> |

SESSION FB. LASER PHENOMENA

8:00 AM - 9:31 AM, Wednesday, October 18

Camino Ball Room D

Chair: L. A. Schlie, Air Force Weapons Laboratory

- | | | |
|-------------|------|--|
| 8:00 - 8:13 | FB-1 | <p>ARGON ION LASER EXCITED AT THE LOWER HYBRID FREQUENCY</p> <p>R. W. Boswell and P. Zhu</p> |
| 8:13 - 8:26 | FB-2 | <p>X-RAY PHOTOSWITCHED ARGON AND NEON DISCHARGES</p> <p>H. Brunet, B. Lacour, V. Puech, S. Mizzi,
S. Pasquiers, and M. Legentil</p> |
| 8:26 - 8:39 | FB-3 | <p>DETERMINATION OF THE ION TEMPERATURE IN A HeSe-LASER DISCHARGE FROM GAIN MEASUREMENTS AT DIFFERENT AXIAL MODES</p> <p>J. Mentel, N. Reich, and F. Gekat</p> |
| 8:39 - 8:52 | FB-4 | <p>LASER ACTION IN THE FLOWING AFTERGLOW OF A HOLLOW CATHODE DISCHARGE</p> <p>B. Wernsman and J. J. Rocca</p> |
| 8:52 - 9:05 | FB-5 | <p>PLASMA BREAKDOWN BEHAVIOR OF HYDROGEN AZIDE (HN₃) GAS MIXTURES</p> <p>M. W. Wright, L. A. Schlie, and C. A. Denman</p> |
| 9:05 - 9:18 | FB-6 | <p>THE EFFECT OF RETURN CURRENTS IN ELECTRON-BEAM EXCITED KrF LASERS</p> <p>M. J. Kushner</p> |
| 9:18 - 9:31 | FB-7 | <p>MICROSTREAMERS AS A TERMINATION MECHANISM IN KrF DISCHARGE LASERS</p> <p>M. J. Kushner</p> |

SESSION GA. ARCS AND GLOWS

10:00 AM - 11:31 AM, Wednesday, October 18

Camino Ball Room C

Chair: V. A. Godyak, GTE Laboratories

- | | | |
|---------------|------|--|
| 10:00 - 10:13 | GA-1 | INVESTIGATION OF DIELECTRIC BARRIER DISCHARGE UV-LAMPS
M. Neiger, H. Mueller, K. Stockwald, and V. Schorpp |
| 10:13 - 10:26 | GA-2 | EXCITATION OF RESONANCE LINES AND FORMATION OF EXCIMERS IN VARIOUS MERCURY/RARE GAS MIXTURES
B. Eliasson, B. Gellert, and U. Kogelschatz |
| 10:26 - 10:39 | GA-3 | TIME RESOLVED XUV EMISSION FROM HIGHLY IONIZED CAPILLARY DISCHARGES
J. F. Schmerge, J. J. Rocca, and M. C. Marconi |
| 10:39 - 10:52 | GA-4 | ELECTRIC FIELD AND EMISSION PROFILE MEASUREMENTS IN A HYDROGEN DISCHARGE AT LOW PRESSURES
B. N. Ganguly, J. R. Shoemaker, and A. Garscadden |
| 10:52 - 11:05 | GA-5 | PLASMA-ENHANCED PHOTOEMISSION FROM THE CATHODE IN A LOW PRESSURE DISCHARGE
M. B. Schulman and D. R. Woodward |
| 11:05 - 11:18 | GA-6 | TEMPERATURE MEASUREMENTS IN A NON-EQUILIBRIUM THERMAL PLASMA
T. Owano, M. Gordon, and C. H. Kruger |
| 11:18 - 11:31 | GA-7 | LIQUID COOLED, HIGH POWER (<5.4 kW), cw Hg UV LAMPS
L. A. Schlie, R. D. Rathge, and E. A. Dunkel |

SESSION GB. ELECTRON AND HEAVY PARTICLE COLLISIONS

10:00 AM - 11:07 AM, Wednesday, October 18

Camino Ball Room D

Chair: D. C. Lorents, SRI International

- | | | |
|---------------|------|---|
| 10:00 - 10:35 | GB-1 | LASER PROBING OF ION MOBILITY, VELOCITY DISTRIBUTIONS AND ALIGNMENT EFFECTS IN DRIFT FIELDS
S. R. Leone
(Invited Paper) |
| 10:35 - 10:28 | GB-2 | TERMOLICULAR ION-ATOM ASSOCIATION
M. R. Flannery and M. S. Keehan |

- | | | |
|---------------|------|---|
| 10:28 - 10:41 | GB-3 | IONIZATION CROSS-SECTION OF N ₂ O
C. B. Freidhoff and P. J. Chantry |
| 10:41 - 10:54 | GB-4 | DOUBLY DIFFERENTIAL CROSS SECTIONS
OF SECONDARY ELECTRONS EJECTED FROM
GASES BY ELECTRON IMPACT: 25-250 eV ON
O ₂
T. W. Shyn and W. E. Sharp |
| 10:54 - 11:07 | GB-5 | GAS PHASE ACIDITIES OF HPO ₃ AND HPO ₂
A. A. Viggiano, R. A. Morris, J. F. Paulson,
M. Henchman, T. Miller, and
A. E. Stevens Miller |

SESSION H. BUSINESS MEETING

11:30 AM - 12:00 Noon, Wednesday, October 18
Camino Ball Room D
Chair: J. B. Gerardo, Sandia National Laboratories

SESSION J. POSTERS

1:30 PM - 3:30 PM, Wednesday, October 18
Camino Ball Room A and B
Chair: Y. K. Bae, SRI International

- | | |
|-----|--|
| J-1 | MEASUREMENT OF THE I/V
CHARACTERISTICS OF A SYMMETRIC RF
DISCHARGE IN ARGON
R. B. Piejak and V. A. Godyak |
| J-2 | A NEW FAST ALGORITHM TO CALCULATE
OSCILLATORY STEADY-STATES OF A RF
PLASMA USING THE CONTINUUM MODEL
E. Gogolides, H. H. Sawin, and R. A. Brown |
| J-3 | COMPARISON OF CF AND CF ₂ LIF AND
ACTINOMETRY IN A CF ₄ DISCHARGE
L. D. Baston, J.-P. Nicolai, and H. H. Sawin |
| J-4 | SPATIAL PROFILE MEASUREMENTS OF
PLASMA SPECIES IN RADIO-FREQUENCY
GLOW DISCHARGES
P. J. Hargis, Jr. and K. E. Greenberg |
| J-5 | RF FREQUENCY DEPENDENCE OF PLASMA
PARAMETER AXIAL PROFILES IN A HELIUM
RF PLASMA
K. Terai, T. Kaneda, and J. S. Chang |
| J-6 | PARTICLE KINETICS IN PLASMAS
A. Garscadden |

- J-7 RF DISCHARGES AT VERY LOW NEUTRAL PRESSURES
N. Hershkowitz, M.-H. Cho, and A. Wendt
- J-8 A KINETIC DISCHARGE MODEL APPLIED TO THE RF REFERENCE CELL
T. J. Sommerer, W.N.G. Hitchon, and J. E. Lawler
- J-9 CYLINDRICAL MAGNETRON REACTIVE SPUTTERING FOR HERMETIC COATINGS OF FLUORIDE GLASS FIBERS
Z. Yu, P. A. Smith, G. J. Collins, D. W. Reicher, J. R. McNeil, B. Harbison, and I. Aggarwal
- J-10 THE FEASIBILITY OF USING NEURAL NETWORKS AND OTHER OPTIMIZATION ALGORITHMS TO OBTAIN CROSS SECTION DATA
W. L. Morgan
- J-11 SPACE AND TIME VARIATION OF STOCHASTIC HEATING IN A CAPACITIVE RF DISCHARGE
B. P. Wood, M. A. Liebermann, and A. J. Lichtenberg
- J-12 MEASUREMENT OF TARGET ION CURRENT IN PLASMA SOURCE ION IMPLANTATION
M. Shamim, J. T. Scheuer, and J. R. Conrad
- J-13 TEMPERATURE OF A HIGH PRESSURE MERCURY DISCHARGE
J. T. Dakin and R. P. Gilliard
- J-14 TEMPERATURE AND Na DENSITY IN AN AC Hg - NaI DISCHARGE PLASMA
A. Palladas, D. Karabourniotis, and A. Tsakonas
- J-15 PRODUCTION OF S₂F₁₀ FROM NEGATIVE GLOW CORONA IN SF₆
R. J. Van Brunt, J. K. Olthoff, J. T. Herron, and I. Sauers
- J-16 A KINETIC MODEL OF A DC DISCHARGE
D. J. Koch and W.N.G. Hitchon
- J-17 DETERMINISTIC CHAOS IN ELECTRICAL DISCHARGES IN GASES
D. Hudson
- J-18 SPECTROSCOPIC DIAGNOSTIC OF A He-Cd⁺ LASER DISCHARGE
Th. Wengorz and J. Mentel
- J-19 STREAMER TO ARC TRANSITION IN N₂
S. K. Dhali and A. Rata Booshanam

- J-20 ELECTRON IMPACT VIBRATIONAL
EXCITATION OF POLAR MOLECULES
S. Alston, G. Snitchler, and D. W. Norcross
- J-21 EMISSION OF THE FLUORINE RESONANCE
LINES FOLLOWING DISSOCIATIVE
ELECTRON IMPACT EXCITATION OF CCl_2F_2 ,
 NF_3 , CF_4 , AND SF_6
M. Roque, R. Siegel, K. E. Martus, and
K. Becker
- J-22 TOTAL ELECTRON-IMPACT CROSS SECTIONS
FOR AMMONIA
C. Ma, P. B. Liescheski, and R. A. Bonham
- J-23 MEASUREMENT OF COHERENCE
PARAMETERS IN ELECTRON-HEAVY NOBLE
GAS COLLISIONS
K. E. Martus and K. Becker
- J-24 ELECTRON-IMPACT DISSOCIATION OF Cl_2
MOLECULES
P. C. Cosby
- J-25 EXTREME ULTRAVIOLET EMISSION FROM
THE $b^1\Pi_u$ STATE OF N_2 EXCITED BY
ELECTRON IMPACT
G. K. James, J. M. Ajello, and D. E. Shemansky
- J-26 ELECTRON-IMPACT IONIZATION RATE
COEFFICIENTS AT VERY HIGH DENSITY-
NORMALIZED ELECTRIC FIELDS FOR
SEVERAL ALKANES AND FLUOROALKANES
G. N. Hays, J. B. Gerardo, and M. Ibrahim
- J-27 ELECTRON IMPACT IONIZATION OF ARGON
AND KRYPTON
R.E.H. Clark and G. Csanak
- J-28 ELECTRON IMPACT INFRARED EXCITATION
FUNCTIONS IN XENON
C. A. DeJoseph and J. D. Clark
- J-29 ELECTRON-EXCITATION CROSS SECTIONS
OF THE $4p^55p$ STATES OF KRYPTON AND
THEIR PRESSURE DEPENDENCE
J. E. Gastineau, M. P. Nesnidal, and T. G. Ruskell
- J-30 NEW COHERENCE DATA ON THE
EXCITATION OF HEAVY RARE GASES BY
ELECTRON IMPACT
P.J.M. van der Burgt, J. J. Corr, and
J. W. McConkey

- J-31 VUV FLUORESCENCE FOLLOWING
ELECTRON IMPACT ON DISCHARGE-
CREATED TARGETS
S. Wang and J. W. McConkey
- J-32 PRACTICAL APPLICATIONS OF
ELECTROSTATIC PROBES
N. Benjamin and B. Chapman

Laboratory Tours

4:15 PM - 6:00 PM, Wednesday, October 18
Molecular Physics Laboratory and Chemical Kinetics Department
SRI International

Social Hour and Banquet

6:00 PM, Wednesday, October 18
International Dining Room
SRI International

SESSION KA. Ar/Xe LASERS I

8:00 AM - 9:39 AM, Thursday, October 19
Camino Ball Room C
Chair: A. Garscadden, Wright Research and Development Center

- | | | |
|-------------|------|---|
| 8:00 - 8:35 | KA-1 | EARLY WORK IN HIGH-POWER Xe:Ar LASER RESEARCH
L. A. Newman and T. A. DeTemple
(Invited Paper) |
| 8:35 - 9:00 | KA-2 | EXPERIMENTAL STUDY OF THE e-BEAM AND e-BEAM SUSTAINED Xe:Ar LASER
A. Suda, B. L. Wexler, B. J. Feldman, and K. Riley
(Long Paper) |
| 9:00 - 9:13 | KA-3 | FISSION-FRAGMENT PUMPED ATOMIC XENON LASER
G. N. Hays, W. J. Alford, D. R. Neal,
D. A. McArthur, and D. E. Bodette |
| 9:13 - 9:26 | KA-4 | A PARAMETRIC STUDY OF THE ATOMIC XENON LASER
E. L. Patterson, G. E. Samlin, and
P. J. Brannon |
| 9:26 - 9:39 | KA-5 | PERFORMANCE CHARACTERISTICS OF THE X-RAY PREIONIZED Xe:Ar LASER
J. E. Tucker, B. L. Wexler, B. J. Feldman, and
T. McClelland |

SESSION KB. BREAKDOWN AND SWITCHING

8:00 AM - 9:43 AM, Thursday, October 19

Camino Ball Room D

Chair: L. E. Kline, Westinghouse Research & Development

- | | | |
|-------------|------|---|
| 8:00 - 8:25 | KB-1 | FORMATION OF CATHODE SPOTS BY UNIPOLAR ARCING
F. Schwirzke
(Long Paper) |
| 8:25 - 8:38 | KB-2 | TRANSPORT AND MULTIPLICATION OF CHARGED PARTICLES IN H ₂ AT VERY HIGH E/n
Z. Lj. Petrović and A. V. Phelps |
| 8:38 - 8:51 | KB-3 | APPLICATION OF A MULTI-DIMENSIONAL BEAM-BULK MODEL TO SIMULATION OF LOW PRESSURE PULSE POWERED DEVICES
H. Pak and M. J. Kushner |
| 8:51 - 9:04 | KB-4 | THEORETICAL ANALYSES OF HIGH PRESSURE SELF-SUSTAINED GLOW DISCHARGES WITH HIGH SWITCH RATIO
W. M. Moeny, A. E. Rodriguez, and J. M. Elizondo |
| 9:04 - 9:17 | KB-5 | EXPERIMENTAL RESEARCH ON HIGH PRESSURE SELF-SUSTAINED GLOW DISCHARGES WITH HIGH SWITCH RATIO
J. M. Elizondo, W. M. Moeny, J. W. Benze, B. R. Beckes, and K. Youngman |
| 9:17 - 9:30 | KB-6 | STREAMERS IN N ₂ : NEW EMPIRICAL RESULTS
F. E. Peterkin and P. F. Williams |
| 9:30 - 9:43 | KB-7 | STREAMER DYNAMICS
M-C. Wang and E. E. Kunhardt |

SESSION LA. Ar/Xe LASERS II

10:10 AM - 11:50 AM, Thursday, October 19

Camino Ball Room C

Chair: A. Garscadden, Wright Research and Development Center

- | | | |
|---------------|------|--|
| 10:10 - 10:23 | LA-1 | ENERGY SCALING OF THE ATOMIC Xe:Ar LASER
D. W. Trainor, L. Litzenberger, and M. McGeoch |
| 10:23 - 10:36 | LA-2 | TIME-RESOLVED SPECTROSCOPIC STUDY OF SELF-SUSTAINED DISCHARGE PUMPED Xe:Ar LASERS
K. Komatsu, E. Matsui, S. Takahashi, F. Kannari, and M. Obara |

10:36 - 10:49	LA-3	QUENCHING OF XENON LASER LEVELS ($6p[5/2]_2, 6p[3/2]_1$) BY RARE GASES W. J. Alford
10:49 - 11:02	LA-4	THE EFFECT OF He ADDITION ON THE PERFORMANCE OF THE Ar/Xe ATOMIC XENON LASER M. Ohwa and M. J. Kushner
	LA-5	POWER AND ENERGY LOADING EFFECTS IN SCALING OF THE ATOMIC XENON LASER M. Ohwa and M. J. Kushner
11:02 - 11:15	LA-6	UTILIZATION OF A COMMERCIAL DISCHARGE LASER FOR AN ATOMIC Xe LASER W. A. Neuman and J. R. Fincke
11:15 - 11:50	LA-7	CURRENT UNDERSTANDING AND REMAINING PHYSICS ISSUES OF THE Xe:Ar(He, Ne) LASER M. J. Kushner and M. Ohwa (Invited Paper)

SESSION LB. CROSS SECTION DATA I

10:10 AM - 12:04 PM, Thursday, October 19

Camino Ball Room D

Chair: R. A. Phaneuf, Oak Ridge National Laboratory

10:10 - 10:35	LB-1	CROSS SECTIONS FOR LOW-ENERGY ELECTRON MOLECULE COLLISIONS H. Pritchard, C. Winstead, K. Watari, M. Lima, and V. McKoy (Long Paper)
10:35 - 10:48	LB-2	ELECTRON SCATTERING FROM AND DISSOCIATIVE ATTACHMENT IN HALOGENATED SILANES H. X. Wan and J. H. Moore
10:48 - 11:13	LB-3	EXTREME ULTRAVIOLET EMISSION FROM N ₂ BY ELECTRON IMPACT: CROSS SECTIONS OF THE $c'_4 \ ^1\Sigma_u^+$ AND $b' \ ^1\Sigma_u^+$ STATES J. M. Ajello, G. K. James, and D. E. Shemansky (Long Paper)
11:13 - 11:26	LB-4	MEASUREMENTS OF ELECTRON-IMPACT CROSS SECTION FOR EXCITATION OUT OF THE He(2^3S) METASTABLE LEVEL R. B. Lockwood, F. A. Sharpton, L. W. Anderson, J. E. Lawler, and C. C. Lin
11:26 - 11:39	LB-5	A STUDY OF THE PAIS VARIATIONAL PHASE SHIFT APPROXIMATION AND ITS EXTENSION POTENTIALS WITH A PURE COULOMB TAIL S. R. Valluri and W. J. Romo

11:39 - 12:04 LB-6 INELASTIC 3S-3P AND SUPERELASTIC 3P-3S
ELECTRON SCATTERING
L. Vušković, T. Y. Jiang, M. Zuo, and B. Bederson
(Long Paper)

SESSION MA. FUNDAMENTAL DATA FROM PLASMAS

1:30 PM - 3:18 PM, Thursday, October 19
Camino Ball Room C
Chair: J. E. Lawler, University of Wisconsin

1:30 - 2:05 MA-1 OSCILLATOR STRENGTHS AND LIFETIMES
FROM TRANSFORM SPECTROMETER DATA
B. A. Palmer
(Invited Paper)

2:05 - 2:30 MA-2 ATOMIC TRANSITION PROBABILITY
MEASUREMENTS WITH AN INDUCTIVELY
COUPLED PLASMA
W. Whaling, T. R. O'Brian, M. W. Wickliffe,
J. E. Lawler, and J. W. Brault
(Long Paper)

2:30 - 3:05 MA-3 ELECTRON BEAM ION TRAPS (EBIT): A NEW
TOOL FOR STUDYING THE SPECTROSCOPY
OF MULTIPLY-CHARGED IONS
R. E. Marrs
(Invited Paper)

3:05 - 3:18 MA-4 EVAPORATIVE COOLING IN ELECTRON
BEAM ION TRAPS
B. M. Penetrante, M. A. Levine, and J. N. Bardsley

SESSION MB. CROSS SECTION DATA II

1:30 PM - 3:25 PM, Thursday, October 19
Camino Ball Room D
Chair: B. Bederson, New York University

1:30 - 1:55 MB-1 ATOMIC COLLISION PROCESSES IN THE EDGE
PLASMA OF MAGNETIC FUSION DEVICES
R. A. Phaneuf
(Long Paper)

1:55 - 2:08 MB-2 NEGATIVE AND POSITIVE ION FORMATION
BY ELECTRON IMPACT ON BENZENE
A. F. Fucaloro and S. K. Srivastava

2:08 - 2:33 MB-3 ELECTRON COLLISION CROSS SECTION
NEEDS FOR THE KrF LASER
D. C. Cartwright, P. J. Hay, and S. Trajmar
(Long Paper)

- | | | |
|-------------|------|--|
| 2:33 - 2:46 | MB-4 | e-CH ₄ COLLISIONS IN A STATIC-(EXACT) EXCHANGE PLUS PARAMETER-FREE POLARIZATION MODEL: ELASTIC AND ROTATIONAL EXCITATION PARAMETERS
P. McNaughten, D. G. Thompson, and A. Jain |
| 2:46 - 2:59 | MB-5 | DISSOCIATIVE ATTACHMENT IN THE CHLOROMETHANES
S. C. Chu and P. D. Burrow |
| 2:59 - 3:12 | MB-6 | TEMPERATURE DEPENDENCE OF THE VERTICAL-ONSET-DISSOCIATIVE ELECTRON ATTACHMENT OF CH ₃ Cl
P. G. Datskos, L. G. Christophorou, and J. G. Carter |
| 3:12 - 3:25 | MB-7 | INFERENCE OF HN ₃ ELECTRON ATTACHMENT CROSS SECTIONS FROM DRIFT VELOCITY AND ELECTRON ATTACHMENT RATE CONSTANT DATA
L. A. Schlie, C. A. Denman, and M. W. Wright |

SESSION NA. POSTERS

3:30 PM - 5:30 PM, Thursday, October 19
Camino Ball Room A and B
Chair: J. B. Jeffries, SRI International

- | | |
|------|--|
| NA-1 | PARTICLE SIMULATION OF A RF DISCHARGE: NONLOCAL EFFECTS
M. Surendra and D. B. Graves |
| NA-2 | PROBE POTENTIAL AND CAPACITANCE MEASUREMENTS IN A SYMMETRIC ARGON RF DISCHARGE DRIVEN AT 13.56 MHz
V. A. Godyak and R. B. Piejak |
| NA-3 | ELECTRON CYCLOTRON RESONANCE PLASMA SOURCE RESEARCH AT THE UNIVERSITY OF WISCONSIN-MADISON
H. M. Persing, N. Hershkowitz, A. Wendt, D. Diebold, and M.-H. Cho |
| NA-4 | OBSERVATION OF SUBMICRON PARTICLES IN RF PLASMAS
K. R. Stalder |
| NA-5 | POWER ABSORPTION BY ELECTRON CYCLOTRON RESONANCE
D. Carl, A. J. Lichtenberg, M. A. Lieberman, J. Steinhauer, and M. Williamson |
| NA-6 | STUDIES OF MICROWAVE BREAKDOWN PLASMAS IN AIR BY THE MICROWAVE CAVITY PERTURBATION TECHNIQUE
D. J. Eckstrom and M. S. Williams |

- NA-7 GROWTH OF DIAMOND IN A DC DISCHARGE
H. N. Chu, A. R. Lefkow, R. Redwing,
L. W. Anderson, M. G. Lagally, and J. E. Lawler
- NA-8 GENERATION OF CARBON ION BEAMS FROM
A SMALL MULTICUSP SOURCE
K. N. Leung, M. Lowenthal, W. Stockwell,
M. D. Williams, W. B. Kunkel, and J. M. Dawson
- NA-9 MULTI-SPECIES AMBIPOLAR DIFFUSION
T. Gist, A. Garscadden, and W. Bailey
- NA-10 KINETIC STUDY OF ELECTRON PROPERTIES
IN A CAPACITIVELY COUPLED RF-DISCHARGE
G. Frömling
- NA-11 ELECTRON DEGRADATION SPECTRA BY
SUBEXCITATION ELECTRONS IN GASEOUS-
AND SOLID-WATER
M. Kimura, M. A. Ishii, and M. Inokuti
- NA-12 MODEL OF PLASMA SOURCE ION IMPLANTATION
IN PLANAR, CYLINDRICAL AND SPHERICAL
GEOMETRIES
J. T. Scheuer, M. Shamim, and J. R. Conrad
- NA-13 GENERALIZED SHEATH CONDITION FOR
EMITTING AND REFLECTING WALLS
K.-U. Riemann
- NA-14 A MICRO-PYROMETER SYSTEM FOR MEASURING
THE TEMPERATURE OF F-LAMP ELECTRODES
A. Awadallah and A. K. Bhattacharya
- NA-15 MERCURY PRESSURE EFFECTS ON CONVECTION
IN HORIZONTAL DISCHARGES
M. E. Duffy and P. Y. Chang
- NA-16 SHORT-GAP BREAKDOWN IN He: THE EFFECT
OF IMPURITIES
J. P. Novak and R. Bartnikas
- NA-17 LINE BROADENING IN LASER-PRODUCED
OXYGEN PLASMAS
L. S. Dzelzkalns, W.A.M. Blumberg, P.C.F. Ip,
R. A. Armstrong, W. T. Conner, and C. C. Lin
- NA-18 TIME DEPENDENT SOLUTION OF BOLTZMANN
EQUATION IN SELF-SUSTAINED XeCl DISCHARGES
COUPLED TO PLASMA CHEMISTRY AND CIRCUIT
EQUATIONS
C. Gorse and M. Capitelli

- NA-19 STUDY OF UV AND VUV FLUORESCENCE OF HIGH PRESSURE RARE GASES EXCITED BY DIELECTRIC CONTROLLED DISCHARGE: THIRD CONTINUUM OF ARGON
C. Cachoncinlle, J. M. Pouvesle, F. Davenloo, J. J. Coogan, and C. B. Collins
- NA-20 MODEL OF ELECTRONS, IONS AND FAST NEUTRALS IN H₂ AT VERY HIGH E/n
A. V. Phelps
- NA-21 DENSITY MEASUREMENT OF THE METASTABLE Hg(6³P₂) IN A Hg-Ar LOW PRESSURE DISCHARGE
P. Moskowitz
- NA-22 STUDY OF NEGATIVE ION FORMATION BY ELECTRON IMPACT ON DICHLOROMETHANE, TOLUENE, XYLENE AND TRICHLOROETHANE
C. Timmer and S. K. Srivastava
- NA-23 PLASMA LINE BROADENING IN MOLECULAR SPECTRA IN D.C. GLOW DISCHARGES
W. T. Conner and R. C. Woods
- NA-24 STARK BROADENING IN HIGH PRESSURE HELIUM PLASMAS
L. W. Downes, S. D. Marcum, W. E. Wells, and J. O. Stevefelt
- NA-25 THE EFFECT OF RADIATIVE CASCADE ON CESIUM EXCITED STATE POPULATIONS IN THERMIONICALLY ASSISTED Ar-Cs DISCHARGES
M. L. Tackett, S. D. Marcum, and B. N. Ganguly
- NA-26 A STUDY OF THE INFLUENCE OF ³P₂ POPULATION OF MERCURY ON THE ELECTRON TEMPERATURE IN A Hg-Ar RF DISCHARGE
L. Maleki, B. Blasenheim, and G. Janik
- NA-27 MULTIPLY CHARGED NOBLE EXCIMERS
P. D. Haaland and R. A. Deemer
- NA-28 GLOBAL POTENTIAL ENERGY SURFACES OF H₂Cl⁺ AND COMPARISON WITH EXPERIMENTS
Th. Glenewinkle-Meyer, P. Knowles, Ch. Ottinger, P. Rosmus, and H. J. Werner
- NA-29 FORMATION OF XeCl AND Xe₂Cl DURING THREE BODY RECOMBINATION OF Xe₂⁺ AND Cl⁻
W. L. Morgan and D. R. Bates
- NA-30 RADIATION TRAPPING UNDER CONDITIONS OF LOW TO MODERATE OPTICAL DEPTH
T. Colbert and J. Huennekens

NA-31 COLLISIONAL RELAXATION OF $\text{NH}(^3\Sigma^-, v = 1-2)$
BY N_2 AND H_2
D. J. Flanagan, S. J. Lipson, J. A. Dodd,
W.A.M. Blumberg, J. Person, and B. D. Green

SESSION NB. NOVEL PLASMAS

3:45 PM - 5:16 PM, Thursday, October 19
Camino Ball Room D
Chair: C. B. Fleddermann, University of New Mexico

- | | | |
|-------------|------|---|
| 3:45 - 3:58 | NB-1 | RELATIVISTIC PLASMAS PRODUCED BY INTENSE LASERS
J. N. Bardsley and B. M. Peneirante |
| 3:58 - 4:11 | NB-2 | WIDE AREA DISC SHAPE PLASMA SOURCE FOR ENERGY ASSISTED CVD
Z. Yu, T. Sheng, H. Zarnani, B. Pihlstrom, and G. J. Collins |
| 4:11 - 4:24 | NB-3 | PLASMA PROCESSES IN SOFT VACUUM ELECTRON BEAMS USED FOR MICROELECTRONIC FILM PROCESSING
G. J. Collins |
| 4:24 - 4:37 | NB-4 | ELECTRON BEAM GENERATION BY ELECTRON BOMBARDMENT INDUCED CATHODE EMISSION
B. Szapiro, C. Murray, and J. J. Rocca |
| 4:37 - 4:50 | NB-5 | THE EFFECTS OF ADDING Xe TO A H_2 DISCHARGE
A. A. Mullan and W. G. Graham |
| 4:50 - 5:03 | NB-6 | REMOVAL OF SO_2 FROM FLUE GASES USING COMBINED PLASMA AND OPTICAL PROCESSING
J. H. Balbach, M. J. Rood, and M. J. Kushner |
| 5:03 - 5:16 | NB-7 | PLASMA OXIDATION OF SO_2 IN FLUE GAS
S. K. Dhali and I. Sardja |

SESSION P. CROSS SECTIONS I WISH I KNEW

7:30 PM - 10:00 PM, Thursday, October 19
Camino Ball Room C and D
Chair: C. C. Lin, University of Wisconsin

- | | |
|-----|---|
| P-1 | CROSS SECTIONS OF GREAT INTEREST TO AERONOMY AND ASTROPHYSICS
J. P. Doering
(Invited Paper) |
| P-2 | CROSS-SECTIONS I WISH I KNEW IN DISCHARGE LIGHT SOURCES
J. F. Waymouth
(Invited Paper) |

- P-3 ELECTRON-MOLECULE COLLISION CROSS SECTION NEEDS FOR ETCHING GASES
K. Becker
(Invited Paper)
- P-4 CROSS SECTION NEEDS FOR MODELING ETCHING AND DEPOSITION DISCHARGES
L. E. Kline
(Invited Paper)
- P-5 CROSS SECTIONS AND MOMENTS OF IMPORTANCE
A. Garscadden
(Invited Paper)
- P-6 A STATUS REPORT ON THE AVAILABILITY AND NEEDS OF ELECTRON IMPACT CROSS SECTIONS FOR MODELING PLASMA DEPOSITION
M. J. Kushner
(Invited Paper)

SESSION QA. SINGLE WAFER PLASMA PROCESSING

8:00 AM - 9:39 AM, Friday, October 20

Camino Ball Room C

Chair: J. H. Keller, IBM, East Fishkill

- | | | |
|-------------|------|---|
| 8:00 - 8:35 | QA-1 | ECR AND OTHER HIGH DENSITY PLASMAS FOR SINGLE WAFER PLASMA PROCESSING
W. M. Holber and J. Forster
(Invited Paper) |
| 8:35 - 9:00 | QA-2 | RF EXCITED DIFFUSION PLASMAS
R. W. Boswell
(Long Paper) |
| 9:00 - 9:13 | QA-3 | LOW PRESSURE RIE USING AN RF PLASMA SOURCE WITH SURFACE MAGNETIC CONFINEMENT
A. Wendt, M.-H. Cho, N. Hershkowitz, and H. Persing |
| 9:13 - 9:26 | QA-4 | CHARACTERISTICS OF INDUCTIVELY EXCITED DISCHARGES WITH A DRIFT SPACE
P. Bletzinger and M. E. Dunnigan |
| 9:26 - 9:39 | QA-5 | RF INDUCTION/MULTIPOLE LPSWE SYSTEM
J. H. Keller |

SESSION QB. COLLISIONS BETWEEN ATOMS, MOLECULES, AND IONS

8:00 AM - 9:30 AM, Friday, October 20

Camino Ball Room D

Chair: J. R. Peterson, SRI International

- | | | |
|-------------|------|--|
| 8:00 - 8:25 | QB-1 | IR EXCITATION CROSS SECTIONS FROM FAST O-ATOM COLLISIONS
G. E. Caledonia, B. L. Upschulte, R. H. Krech, B. Claflin, and G. Burgess
(Long Paper) |
| 8:25 - 8:38 | QB-2 | THE DEPENDENCE OF SPACECRAFT GLOW ON THE SPACECRAFT VELOCITY
R. J. Meyerott and G. R. Swenson |
| 8:38 - 8:51 | QB-3 | ION AND FAST NEUTRAL EXCITATION IN N ₂ AT VERY HIGH E/n
V. T. Gylys and A. V. Phelps |
| 8:51 - 9:04 | QB-4 | ROTATIONAL EXCITATION OF N ₂ ⁺ IN N ₂ AT E/n ≈ 100 Td
J. Borysow and A. V. Phelps |
| 9:04 - 9:17 | QB-5 | ENERGY TRANSFER IN THE B ² Π STATE OF NS
I. J. Wysong, J. B. Jeffries, and D. R. Crosley |
| 9:17 - 9:30 | QB-6 | TEMPERATURE DEPENDENT QUENCHING OF NO A ² Σ ⁺ AND B ² Π BY H ₂ O
G. A. Raiche, G. P. Smith, and D. R. Crosley |

SESSION RA. RF DISCHARGES: MODELS AND EXPERIMENTS

10:00 AM - 11:31 AM, Friday, October 20

Camino Ball Room C

Chair: M. A. Lieberman, University of California

- | | | |
|---------------|------|---|
| 10:00 - 10:13 | RA-1 | AN EXPERIMENTAL SYSTEM FOR RF DISCHARGE PHYSICS RESEARCH
V. A. Godyak, R. B. Piejak, and B. M. Alexandrovich |
| 10:13 - 10:26 | RA-2 | FREQUENCY EFFECTS IN A RF DISCHARGE
M. Surendra and D. B. Graves |
| 10:26 - 10:39 | RA-3 | DC SELF BIAS FORMATION IN SYMMETRIC PARALLEL-PLATE RF GLOW DISCHARGES
J. W. Butterbaugh and H. H. Sawin |
| 10:39 - 10:52 | RA-4 | THE SPATIAL AND TEMPORAL VARIATION OF PLASMA PARAMETERS IN AN RF DISCHARGE
C. A. Anderson and W. G. Graham |

- | | | |
|---------------|------|--|
| 10:52 - 11:05 | RA-5 | ION BOMBARDMENT ANGLE AND ENERGY
IN ARGON RF DISCHARGES
J. Liu, G. L. Huppert, and H. H. Sawin |
| 11:05 - 11:18 | RA-6 | PARTICLE MODELING OF AN ECR REACTOR
R. K. Porteous and D. B. Graves |
| 11:18 - 11:31 | RA-7 | TWO-DIMENSIONAL SIMULATIONS OF RF
GLOW DISCHARGES
J. H. Tsai and C. Wu |

SESSION RB. OPTICAL DIAGNOSTICS

10:00 AM - 11:43 AM, Friday, October 20

Camino Ball Room D

Chair: J. T. Dakin, GE Lighting

- | | | |
|---------------|------|--|
| 10:00 - 10:25 | RB-1 | UV EMISSION FROM A DISCHARGE IN N ₂ O
AND ELECTRON DETACHMENT
T. H. Teich
(Long Paper) |
| 10:25 - 10:38 | RB-2 | GAS TEMPERATURES FROM VIBRATIONAL
TEMPERATURES
M. Passow, M. L. Brake, and P. Lopez |
| 10:38 - 10:51 | RB-3 | TEMPERATURE PROFILES IN N ₂ AND N ₂ -Ar
DC DISCHARGES USING COHERENT ANTI-
STOKES RAMAN SPECTROSCOPY (CARS)
P. P. Yaney, B. L. Epling, and S. W. Kizirnis |
| 10:51 - 11:04 | RB-4 | TIME RESOLVED TWO-DIMENSIONAL EMISSION
SPECTROSCOPY OF A LF ASYMMETRIC H ₂
DISCHARGE
B. N. Ganguly, J. R. Shoemaker, and
A. Garscadden |
| 11:04 - 11:17 | RB-5 | EMISSION SPECTRA OF LASER PRODUCED
PLASMAS USED IN PRODUCING HIGH T _c THIN
FILMS
H. F. Sakeek, W. G. Graham, and T. Morrow |
| 11:17 - 11:30 | RB-6 | IMAGING OF LASER-PRODUCED PLASMAS USING
PLANAR LASER-INDUCED FLUORESCENCE
P. H. Paul, M. A. Cappelli, and R. K. Hanson |
| 11:30 - 11:43 | RB-7 | OPTOGALVANIC LINE PROFILE OF Cu
AUTOIONIZATION LEVELS
R. Shuker, M. Hakham-Itzhaq, and A. Ben-Amar |

SESSION A

8:23 AM - 9:41 AM, Tuesday, October 17

Hyatt Riskey Hotel - Camino Ball Room C and D

DIAGNOSTICS OF PROCESSING DISCHARGES

Chair: H. H. Sawin, Massachusetts Institute of Technology

A-1 Detection of Atomic Chlorine in rf Plasmas by Laser-Excited Amplified Spontaneous Emission, ANDREW D. SAPPEY and JAY B. JEFFRIES, SRI International--Laser-excited stimulated emission is used to detect atomic chlorine in an rf etching plasma. Two laser photons near 233.3 nm excite the spin-forbidden $3p^4 4p \ ^4S_0 \leftarrow 3p^5 \ ^2P^0$ transition. Amplified spontaneous emission (ASE) is observed from $3p^4 4p \ ^4S_0 \rightarrow 3p^4 4s \ ^4P_J$. The stimulated emission signals are compared to simultaneously acquired laser-induced fluorescence (LIF) from the same transition. For $J=1/2$ the ASE intensity is nearly 1000 times larger than the LIF. This strong, collimated stimulated emission provides a means to detect atomic chlorine which only requires a single optical access window.

*Supported by internal research and development funds of SRI International

A-2 Two-Photon Detection of F and F₂,* G. W. FARIS, M. J. DYER, W. K. BISCHSEL, and D. L. HUESTIS, SRI International--Optical detection of F and F₂ is of interest for diagnostics of plasma processing and for laser kinetics studies. F₂ is detected by excitation of the $F^1\Pi_g$ and $f^3\Pi_g$ states from the ground state with two photons near 207 nm and measurement of either VUV fluorescence or ionization by a third photon. Recent measurements with a VUV spectrometer have shown that the fluorescence occurs at 158 nm, corresponding to the F₂ laser transition. Detection of F atom emission at 776 nm resulting from two-photon excitation of the $^2D^{\circ}_j$ level was demonstrated previously¹, using the 170 nm 6th anti-Stokes wave of a doubled dye laser Raman shifted in H₂. We describe attempts to increase the sensitivity of the F atom detection by producing the 170 nm photons by Raman shifting an ArF laser in HD and using the 2nd anti-Stokes wave.

* Supported by AFOSR under Contract No. F49620-88-K-0003.

¹ G. C. Herring, M. J. Dyer, L. E. Jusinski, and W. K. Bischel, *Opt. Lett.* **13**, 360 (1988).

A-3 Laser-Induced Fluorescence Diagnostics of Silicon Etching, ANDREW D. SAPPEY and JAY B. JEFFRIES, SRI International- Laser-induced fluorescence is used to detect CF and SiF₂ radicals in an 13.56 MHz rf discharge of CF₄ and O₂ during the etching of a silicon wafer. Under conditions which minimize the reactive ion etching, the spatial gradients of concentration show that CF is lost from the gas phase to the silicon surface. Similar measurements on the SiF₂ radical show that it is produced on the surface and diffuses into the gas phase. Rotational and vibrational temperatures of CF are in equilibrium with one another and have a value similar to that estimated for the silicon wafer temperature.

*Supported by internal research and development funds of SRI International

A-4 Laser-Induced-Fluorescence Detection of SO and SO₂ in 13.56-MHz SF₆/O₂ Discharges, K. E. GREENBERG and P. J. HARGIS, JR., Sandia National Laboratories -- Laser-induced fluorescence (LIF) excited by a tunable KrF laser was used to detect SO and SO₂ in the active volume of SF₆/O₂ plasma etching discharges. Typical conditions for the 13.56-MHz, parallel-plate discharge were: 0.7 - 2.7 W/cm², 40 sccm SF₆, 0 - 6 sccm O₂, and 300 - 340 mTorr total pressure. SO was identified by using unfocussed KrF laser light to excite the SO v''=2 to v'=2 and v''=1 to v'=0 X-B transitions. When the laser was tuned near 248.0 nm, the v''=2 to v'=2 X-B transition was excited and the resulting fluorescence spectrum could be assigned to transitions from v'=2 of the B state to v''=3-19 of the X (ground) state. When the laser was tuned near 248.5 nm, the v''=1 to v'=0 X-B transition was predominantly excited and the fluorescence spectrum was dominated by transitions from v'=0 of the B state to v''=2-18 of the X state. SO₂ B¹B₁ emission was observed over the entire tuning range of the laser. Measurements of the SO₂ fluorescence lifetime indicate very fast quenching of the laser excited SO₂ states in our discharge system. Fast quenching is also supported by SO₂ LIF spectra recorded 1 μs after the laser pulse which show a red-shifted peak fluorescence emission. Estimates of the SO number density and comparisons with sulfur dimer measurements will be presented.

A-5 S₂, SO, and SO₂ Spatial Distributions in SF₆/O₂ Radio-frequency Glow Discharges,* K.E. GREENBERG and P.J. HARGIS, JR., Sandia National Laboratories -- A gated multichannel detector was used to measure spatially resolved laser-induced fluorescence from S₂, SO, and SO₂, in 13.56-MHz SF₆/O₂ discharges. Spatial profiles were measured across the gap between the parallel-plate electrodes, in the center of the discharge. Typical operating conditions were: 0.3 to 2.7 W/cm², 40 sccm SF₆, 0 to 80 sccm O₂, and 300 to 500 mTorr total pressure. Spatial profile measurements showed an enhancement of S₂ at both electrodes; a depletion of SO at both electrodes; and a minimum in the SO₂ density a few millimeters from the powered electrode. Etching a refractory metal (Ta) in the SF₆ discharge produced an order of magnitude increase in the S₂ density but no change in the S₂ spatial profile. A tunable dye laser was used to measure the distribution of the S₂(X) v''=0 and v''=1 states across the discharge gap. The effect of the interelectrode gap spacing (12, 18, or 25 mm) on profile measurements will also be reported.

*This work performed at Sandia National Laboratories supported by the U.S. Department of Energy under contract no. DE-AC04-76DP00789.

A-6 Ion Cyclotron Resonance Mass Spectrometry in ECR Plasmas* J.B. Friedmann, J.L. Shohet and A.E. Wendt, Engineering Research Center for Plasma-Aided Manufacturing, University of Wisconsin-Madison and J.T. Brenna, IBM Corporation, Endicott, New York. -- In-situ mass spectrometry measurements may be an effective means for process control of ECR plasmas. Mass measurements of active species in an ECR plasma reactor have been made using ion cyclotron resonance mass spectrometry. An ECR plasma, generated by a magnetron supply operating at 2.45 GHz, has been produced in a magnetic mirror geometry. The plasma is physically separated from a low pressure analysis cell. Plasma is coupled to the cell through a small orifice (0.0369 cm in diameter). The system has been operated in an Omegatron¹ configuration and mass spectra for Nitrogen, Helium, Argon and CF₄ have been obtained during ECR plasma production. Typical operating pressures are 5 x 10⁻⁵ torr in the analysis cell region and 3 x 10⁻² in the plasma production region.

* Work supported in part by the National Science Foundation under Grant No. CDR-8721545 and in part by IBM Corporation.

¹ D.E. Post and R. Behrisch, eds. Physics of Plasma-Wall Interactions in Controlled Fusion (Plenum Press, New York), 165 (1988).

SESSION BA

10:00 AM - 11:55 AM, Tuesday, October 17

Hyatt Rickeys Hotel - Camino Ball Room C and D

HYDROCARBON PLASMAS

Chair: L. W. Anderson, University of Wisconsin

BA-1 Role of Gas Discharge in Chemical Vapor Deposition of Diamond Films, Y. TZENG, Department of Electrical Engineering, Auburn University--We have investigated various plasma as well as non-plasma chemical vapor deposition (CVD) processes for deposition of diamond thin films. Gas discharges not only provide energetic electrons for dissociating large hydrocarbon molecules in mixtures with hydrogen and/or oxygen but also cause high fluxes of ions bombarding the substrates on which diamond is to be deposited. The role of these ions is unique for plasma CVD as compared with other non-plasma CVD processes such as the thermal CVD and combustion CVD of diamond. Depending on the ion energy distribution, ions can either promote or retard diamond deposition. In this paper, various diamond deposition processes will be reviewed with emphasis being put on the comparison among CVD's enhanced by different plasmas and between plasma and non-plasma CVD processes. From this comparison, the role of gas discharge in the chemical vapor deposition of diamond films will be discussed.

BA-2 Diamond Synthesis in a 50 kW Inductively Coupled Atmospheric Pressure Plasma,* M. GORDON, T. OWANO, C. H. KRUGER and M. A. CAPPELLI, Stanford University - Polycrystalline diamond coatings have been deposited on a variety of metal substrates using a 50 kW thermal plasma reactor. The growth morphology is found to vary significantly with reactor processing conditions. In this work, we explore the effects of varying the parameters controlling both the surface kinetics (substrate temperature) and gas phase chemistry (initial gas feed composition and plasma temperature). Scanning electron microscopy indicates that well faceted crystals are obtained with growth along the 100 and 111 planes. Raman scattering data is used to compare the bonding structure to that obtained by low pressure microwave plasma deposition.

* Work Supported in part by the Department of Energy (BES) and Office of Naval Research.

BA-3 Hydrocarbons from Discharges in Methane and Discharges over a-C:H Films,* R.N. RUDOLPH** and J.H. MOORE, Department of Chemistry and Biochemistry, University of Maryland -- Neutral hydrocarbons are observed from a microwave discharge in a fast flow of (a) 0.5 - 6% methane in argon, (b) 0.5 - 6% methane in hydrogen, and (c) hydrogen over a previously deposited a-C:H film. System (a) produces polyacetylenic and other hydrocarbons through C₈ by predominantly gas-phase reactions and deposits an a-C:H film. (b) and (c) produce hydrocarbon radicals and molecules with masses through 300 which in case (b) arise from both gas-phase reactions and film ablation, and in case (c) from film ablation alone. Proposals are made for the mechanisms of gas-phase polymerization, film deposition, and ablation. Hydrocarbon ions observed downstream from these discharges appear to arise from ionization of neutrals with a distribution determined by subsequent ion-molecule reactions and selective diffusion losses.

*Supported by NSF grant CHE-87-21744.

**on sabbatical from Adams State College, Alamosa, CO.

BA-4 Absolute Density and Spatial Distribution of the Free Radical CH₃ and CH₂ in a Methane rf Plasma,* H.SUGAI, H.TOYODA and H.KOJIMA, Nagoya University, Japan Neutral radical CH₃ and CH₂ in a capacitively coupled rf discharge in methane have been detected using threshold-ionization mass spectrometry.^{1,2} The absolute density of CH₂ radical in the 13.5 MHz-10 W discharge in 10 mTorr CH₄ is two orders of magnitude less than the CH₃ density (10¹¹ cm⁻³). Space-resolved density measurement of radical species shows the uniform distribution of the CH₃ density whereas the CH₂ density is higher near the powered electrode. Time-resolved density measurement of the afterglow of rf discharges provides the decay time of ~100 ms for CH₃ radical and ~10 ms for CH₂ radical. The CH₃ decay is well explained in terms of the recombination reaction CH₃ + CH₃ → C₂H₆. The CH₂ decay is attributed to surface loss (sticking coefficient ~0.025), in addition to gas phase loss due to the CH₂ reactions with CH₃ and CH₄.

*Work supported by a Grant-in-Aid for Scientific Research from the Ministry of Education, Science & Culture, Japan.

¹H. Toyoda, H. Kojima and H. Sugai, Appl. Phys. Lett. 54, 1507(1989).

²H. Kojima, H. Toyoda and H. Sugai, to be published in Appl. Phys. Lett.

BA-5 Measurement Method of the SiH₂ Radical Density Using Infrared Laser Absorption Spectroscopy*, T. GOTO, N. NISHIWAKI, N. ITABASHI and K. KATO, Nagoya Univ., C. YAMADA and E. HIROTA, Inst. for Molecular Science -- The SiH₂ radical density has never been measured for want of a measurement method. In this work, using the infrared diode laser absorption method, the measurement of the density of the SiH₂ radical formed from phenyl-silane by an ArF excimer laser has been carried out and first it has been shown to be able to determine the absolute value of the SiH₂ radical density. The glass tube of 12 cm diameter and 200 cm length has been used as an absorption cell. The phenyl-silane diluted with hydrogen in the cell has been decomposed by the ArF excimer laser traveling along the tube axis to form the SiH₂ radical. The transient absorption intensity of the P branch line of the SiH₂ ν_2 band has been observed at a phenyl-silane pressure of 10 mTorr, a hydrogen pressure of 830 mTorr and a hydrogen flowing rate of 500 sccm, and the SiH₂(X¹A₁) radical density has been determined to be 5×10^{11} cm⁻³ assuming a rotational temperature of 360 K.

*Supported by Grant-in-Aid for Scientific Research on Priority Areas of the Ministry of Education, Science and Culture.

BA-6 Infrared Laser Absorption Studies of CF₄ and CH₄ RF Plasmas*, J. WORMHOUDT, Aerodyne Research, Inc. -- Infrared tunable diode laser absorption studies of process plasmas are being carried out in a laboratory reactor which allows a long absorption path. Here we report studies of CF₄ and CH₄ radio frequency plasmas. The molecular species whose concentrations have been measured include CF₂ and C₂F₆ as well as CF₄ in CF₄ plasmas, and CH₃ and C₂H₂ as well as CH₄ in methane plasmas. Observations are made for ranges of reactor parameters, including RF power, dilution by Ar or H₂, total pressure, and O₂ addition. Spectroscopic determination of translational, rotational and vibrational temperatures will also be discussed.

*Work supported by the Air Force Office of Scientific Research under Contract F49620-87-C-0052.

BA-7 Particulate Generation in Silane/Ammonia RF Discharges, H.M. Anderson R. Jairath, Dept. Chem. Engr., University of New Mexico, Albuquerque, NM The rate of particle generation in a SiH_4/NH_3 rf discharge has been studied as a function of the discharge operating parameter space, electrode geometry, and power supply coupling mode. Measurements of the bulk quantity of particles produced in the discharge indicate the mode of coupling (capacitive or dc) and the electrode temperature significantly affect particle generation rates. Laser light scattering measurements made as function of the plasma power density also indicate that particle generation abruptly ceases at a threshold value sufficient to induce spark breakdown at the dc coupled electrode. Particle characterization of samples collected from the discharge chamber reveals that the primary particles are sub-micron, N-rich or Si-rich dependent on the feed gas ratio, and that substantial clustering of primary particles occurs in the gas phase simultaneous with particle growth. Based on the above observation implicating electrode interactions with particle generation rates, a new mechanism for the growth of particles in low pressure rf discharges for plasma processing is proposed.

SESSION BB

10:00 AM - 11:04 AM, Tuesday, October 17

Hyatt Rikeys Hotel - Camino Ball Room B

KINETIC MODELS

Chair: B. M. Penetrante, Lawrence Livermore National Laboratory

BB-1 Kinetic Models of Glow Discharges* W.N.G. Hitchon, T.J. Sommerer and J.E. Lawler, University of Wisconsin, Madison, Wisconsin 53706 U.S.A. -- Very efficient numerical solutions of kinetic equations^{1,2} have been applied to DC and RF discharges. The electron and ion distribution functions (in one spatial and two velocity variables (x, v, μ) $\mu \equiv v_x/v$) and the electric field are calculated self-consistently. Strong effects of varying frequency, voltage and secondary emission coefficient in RF discharges in He have been observed for $f = 10 - 13.56$ MHz, $V_a = 500-1000$ V (peak-to-peak), $\gamma = 0$ and $.1$, $p = 100$ mtorr. Conditions in the cathode fall and negative glow of a DC discharge in He, obtained using a detailed set of atomic processes, will be discussed. In particular, the peak negative glow electron density is related to the electron 'temperature' (measured as $\sim 10^{11}$ cm⁻³ and 0.1 to 0.2 eV) which are determined by elastic cooling and energy deposition by beam electrons.

1 W.N.G. Hitchon, D.J. Koch and J.B. Adams, J. Comp. Phys., (to be published).

2 T.J. Sommerer, W.N.G. Hitchon and J.E. Lawler, Phys. Rev. A, **39**, (1989) 6356.

* Work supported by the UW/NSF ERC in Plasma-Aided Manufacturing, Grant CDR-8721545.

BB-2 A Multigroup Approach to Electron Kinetics,* S. Clark and E. E. Kunhardt, Weber Research Institute, Polytechnic University. Given initial and/or boundary conditions, the behavior of an assembly of electrons in a gas can be obtained from solution of the kinetic equation for the distribution function, $f(v, r, t)$. By expanding the distribution in terms of localized functions in v -space, an equivalent formulation can be obtained in terms of the expansion coefficients. For a set of modulated gaussian functions, the expansion coefficients are proportional to the density of "electron groups" associated with the localized functions. Equations of evolution for these coefficients are explicitly derived. With this formulation, the dynamical behavior of the electrons in various regions of velocity space and the influence of the scattering process on these dynamics can be elucidated. This approach is illustrated by numerically solving the initial value problem for the amplitude equations.

* Work supported by the Office of Naval Research.

BB-3 Time and Spatially Dependent Monte Carlo Simulations of Partially Ionized Plasmas Including Electron-Electron Collisions. * Yilin Weng and Mark J. Kushner. University of Illinois, Urbana, IL.

Electron-Electron (e-e) collisions are important in describing the electron energy distribution at fractional ionizations $> 10^{-6}$. These collisions are typically not included in Monte Carlo Simulations (MCS) of partially ionized gases. We have developed a new method whereby e-e collisions may be included in time and spatially dependent MCS of partially ionized plasmas. The method is based on the use of a velocity resolved background electron fluid (BEF) as a species equivalent to heavy atoms. In doing so, we can use the same algorithms as used in treating e-neutral collisions to account for e-e collisions. Since momentum exchange occurs with the BEF, we periodically update the velocity distribution of the fluid using the intermediate results during the simulation. This method is made tractable by using a modified null cross section technique. As an example of the new method, we will present electron energy distributions for swarms in Ar and N₂.

*Work supported by NSF (ECS-88-15781).

BB-4 The Effects of Particulate Contamination on Electron Transport in Glow Discharges. * Michael J. McCaughey and Mark J. Kushner. University of Illinois, Urbana, IL. Glow discharge devices such as gas lasers or plasma deposition reactors are typically contaminated by particulate matter, or dust, which results from gas phase chemical reactions or sputtering. Sufficient large gas phase particulates ($> a few \mu m$) will develop negatively charged sheaths which act as scattering centers and which perturb electron trajectories. We report on a hybrid molecular dynamics-Monte Carlo computer simulation of electron transport in dusty plasmas to study these conditions. The sheath potential at the dust surface is self consistently solved for from the electron energy distribution (EED) by requiring a balance between electron and ion fluxes to the surface of the particles. The perturbation of the EED by the particulates, and the effect on electron impact rate coefficients and self sustaining E/N of glow discharges are presented.

*Work supported by the National Science Foundation (CBT88-03170).

SESSION BC

11:04 AM - 12:08 PM, Tuesday, October 17

Hyatt Riskey Hotel - Camino Ball Room B

ELECTRON DIFFUSION

Chair: W.N.G. Hitchon, University of New Mexico

BC-1 Diffusion Theory of Electrons in a Constant Field: TOF Analysis, JOHN INGOLD, GE Lighting, Cleveland, OH 44112--Electron diffusion theory is based on energy moments of the scalar equation for the isotropic part of the energy distribution, which is found by the spherical harmonic expansion method of solving the Boltzmann equation. The zeroth energy moment gives the particle balance equation, or diffusion equation, and the first energy moment gives the energy balance equation. These two equations are solved numerically in time and one space dimension along the electric field, including non-equilibrium regions near the electrodes, with a pulsed source of electrons at the incoming plane and a perfect sink at the outgoing plane. Calculated pulse widths for constant cross section are significantly less than those obtained from solution of the diffusion equation alone, using equilibrium values of diffusion coefficient and drift velocity. These results suggest that the concept of anisotropic diffusion is superfluous when energy balance is satisfied, i. e., when both density and average energy are allowed to vary in time and space.

BC-2 DGE Analysis of Asymmetric TOF Current Pulses at Different Drift Distances: Determination of V_d , DL , D_3 and D_4 † C. A. DENMAN and L. A. SCHLIE Advanced Laser Technology Division (WL\ARDI) Kirtland AFB, NM 87117-6008. -- Previously reported high-temporal-resolution electron time-of-flight (TOF) experiments in the noble gases have enabled the first observation of the higher-order asymmetric current pulse shape characteristics predicted by the density gradient expansion (DGE) theory. Preliminary analysis of these skewed current pulses utilizing the second-order diffusion approximation of the DGE yielded values for the drift velocity (V_d), longitudinal diffusion (DL) and the first reported values for the skewness diffusion (D_3). Because of the observed divergence of the second-order diffusion approximation for the largely skewed pulses, the analysis is extended to the third-order diffusion approximation yielding the higher-order diffusion coefficient D_4 . To further assess the temporal behavior of the electron current pulse as well as provide a consistency check of the analysis, the original drift distance of 15.7 cm is reduced by half. The unique feature of this sensitive high-resolution TOF apparatus is its virtual-ground current-to-voltage amplifier (4.4×10^7 V/A at 3 MHz BW) which detects the arrival-time-spectra of the electron current pulse.

†Supported by the Air Force Office of Scientific Research.

BC-3 Boltzmann and Monte Carlo Calculations of Higher-Order Transport Coefficients,* B. M. PENETRANTE and J. N. BARDSLEY, Lawrence Livermore National Laboratory -- The density gradient expansion theory is only asymptotically correct, and therefore can never adequately describe non-equilibrium boundary regions with strong density gradients. Nevertheless, the asymptotic values of the transport coefficients provide a practical means by which collisional cross sections can be inferred. The higher-order coefficients, such as the skewness, if measurable, may provide for a more unique inference of cross section data. We have performed Boltzmann and Monte Carlo calculations of electron transport in various gases in order to study the sensitivity of the higher-order transport coefficients to the energy dependence of the collision cross sections. We have also computed the arrival time spectra of the electron swarm under various drift tube conditions.

*Work performed under the auspices of the U.S. Department of Energy by the Lawrence Livermore National Laboratory under Contract No. W-7405-ENG-48.

BC-4 Non-linear Diffusion,* E. E. Kunhardt, Weber Research Institute, Polytechnic University. A continuity equation for the transport of electron density is derived using the concept of a macro-kinetic distribution (MKD) for electrons in a background gas.¹ In lowest order this distribution is shown to obey an equation that is equivalent to the steady-state Boltzmann equation with an equivalent field that is velocity dependent. An explicit form for the MKD is presented for the case of a quasi-Lorentz gas model. The MKD has been used to evaluate the electron current density and to obtain expressions for the mobility and diffusion coefficient. These coefficients are dependent on the electron density gradient, so that the resulting continuity equation is non-linear. The consequences of these results are illustrated for the case of constant collision frequency.

* Work supported by the Office of Naval Research.

¹ E. E. Kunhardt, J. Wu, and B. Penetrante, Phys. Rev. A37, 1654 (1988).

SESSION CA

1:30 PM - 3:18 PM, Tuesday, October 17

Hyatt Riskey Hotel - Camino Ball Room C

PLASMA PROCESSING

Chair: H. M. Anderson, University of New Mexico

CA-1 Power Deposition, Damage Monitoring, and End-Point Detection Using Photoluminescence Spectroscopy in rf Glow Discharges, R.A. GOTTSCHO, A. MITCHELL, S.J. PEARTON, and G.R. SCHELLER, AT&T Bell Laboratories -

Photoluminescence (PL) spectroscopy is used to measure wafer temperatures, damage, and process end-points during rf plasma etching of III-V compound semiconductors such as GaAs and AlGaAs. To discriminate against the plasma glow and minimize PL photo-degradation, we use pulsed excitation and gated electronic detection of the PL intensity. Exploiting the PL peak position dependence on temperature, we measure *in situ* wafer temperatures to better than 1°C from 25°C to 150°C. Thus, power deposition to the surface is determined as a function of discharge frequency, gas composition, applied power, and pressure. Because PL intensity is inversely proportional to surface state density, it is a useful and quantitative measure of surface damage and the effectiveness of damage passivation processes. We report results from BCl₃ plasma etching of AlGaAs and GaAs under a variety of conditions and show how plasma-induced damage is removed using H₂ plasma treatments. We also show how PL can be used in process end-point detection.

CA-2 Effects of Feed Gas Impurities on the Plasma Etching of Polysilicon, G. ZAU and H.H. SAWIN, M.I.T. -

The effects of different feed gas impurities on the polysilicon etching rate in several plasmas were measured. Changes in the polysilicon etching rate typically correlated well the ion flux and/or plasma induced emission. Impurities containing oxygen, water and molecular oxygen, can however cause abrupt etch stoppage. This is attributed to the formation of a surface oxide layer. Most impurities had little effect below 1000 ppm concentration. The most sensitive impurity was a stoichiometric mixture of hydrogen and oxygen used as a water substitute. This mixture reduce the etching rate of CF₄ and Cl₂ plasma at about 100 ppm. Water measurements were carried out using plasma induced emission and mass spectrometry. Both OH⁺ and H₂O⁺ ions were detected with the addition of the mixture. This indicates that water is formed in the plasma with the addition of the mixture.

CA-3 Computer Simulation of the Dynamics of Physical and Chemical Processes on Surfaces, W.L. MORGAN, JILA, Univ. of Colorado & NIST and Kinema Research, Monument, CO 80132--I will discuss the methodology behind simulating the dynamics of surface processes and will present results drawn from simulations of atomic collisions with silicon surfaces. The most exciting of these involve collisions of F atoms and F₂ molecules with Si. In such collisions reactive chemistry occurs which can locally heat the surface and which can cause etching of the surface with SiF_x molecules as reaction products. The development of two and three body potential functions¹ for the interactions of combinations of silicon and fluorine atoms now allows us to directly simulate the dynamics of such chemistry on surfaces.

¹F.H. Stillinger and T.A. Weber, Phys. Rev. B 31, 5262 (1985); J. Chem. Phys. 88, 5123 (1988); Phys. Rev. Letts. 62, 2144 (1989).

CA-4 Surface Reactions of Atomic Chlorine on Polycrystalline Ni and Si(110) WOLFGANG MUELLER-MARKGRAF and MICHEL J. ROSSI, Department of Chemical Kinetics, Chemistry Laboratory, SRI International, Menlo Park CA 94025--Gas-wall interaction studies of neutral transients are thought to be of prime importance in etching and deposition processes. We have studied in a controlled experiment the sticking coefficient and surface chemistry of Cl(²P_{3/2}) and Cl(²P_{1/2}) on polycrystalline Ni and Si(110) in the 10⁻³ Torr regime in a Knudsen cell. The Cl atoms were injected using a pulsed solenoid valve downstream from a microwave discharge in Cl₂ or CF₃Cl. The detection of both Cl species was performed by [3+2] Resonance Enhanced Multiphoton Ionization (REMPI) around 405 nm, whereas stable product species were monitored by on-line phase sensitive electron-impact mass spectrometry. In addition, a necessary ancillary experiment of Cl interaction with Teflon (PTFE) had to be performed in order to search for an "inactive" wall material. The results reveal a surprisingly large variation of the Cl sticking coefficient on the examined surfaces, ranging from 10⁻⁶ to essentially 1.0. Kinetic model calculations support the results in cases, where the Cl atom decays are complex. They thus reveal details of their interaction at substantial coverages, for example in the Cl/Ni case, where some thermodynamic data are known.

CA-5 Radiation Damage to Silicon by Combined Microwave and RF Plasma Reactive Ion Etching Y. TZENG, T.H. LIN and C.C. TIN, Department of Electrical Engineering, Auburn University--We have investigated the radiation damage caused by ion bombardment during reactive ion etching of silicon in a combined microwave and RF reactive ion etching reactor. Microwave plasma is used to generate high density reactive species. RF power is applied to a substrate for adjusting the RF self-bias as well as exciting plasma species in the down-stream of the microwave plasma. By controlling the substrate temperature, the rate of chemical reaction is adjusted. The ion bombardment enhanced the vertical etching rate and thus provide high etching anisotropy. The silicon wafer etched by this plasma is used to fabricate electronic devices for characterization. Current-voltage measurement as well as DLTS analysis are applied to correlate the plasma etching conditions with radiation damage. From this study, the etching of silicon using the combined microwave and RF plasma can be optimized.

CA-6 Plasma Etching of Y-Ba-Cu-Oxide Thin Films, M. R. POOR and C. B. FLEDDERMANN, Center for High Technology Materials, U. of New Mexico -- The commercial viability of electronic applications of high temperature superconducting ceramics will require the development of technologies for patterning thin films into devices. Studies of plasma etching of Y-Ba-Cu-Oxide thin films have been initiated using a dilute chlorine/helium mixture in a d.c. hollow cathode discharge configuration. Unannealed thin films deposited on alumina substrates are etched over a wide range of pressure, input power, substrate temperature and substrate bias. Energy dispersive spectroscopy (EDS) is used to detect the changes in stoichiometry undergone by the films during etching. The etch rate of these films is highly dependent upon substrate temperature, and our measurements show that the rates of etching of the metallic components of the film by chlorine are not the same: copper is most readily removed, followed by barium and yttrium. The dependence on discharge parameters of the etch rates of the individual metals as well as the overall film etch rates will be discussed.

CA-7 Positive ion formation in positive polarity SF₆ corona discharges. I. Sauers and G. Harman, Oak Ridge National Laboratory.--Positive ions were sampled into a mass spectrometer from a positive point-to-plane corona discharge in SF₆ in the pressure range 10-200 torr. Under moderately dry conditions (typically less than 100 ppm, H₂O) the ion fragments SF₅⁺, SF₃⁺, and SF₂⁺ were the major ions observed. The intensity ratios of SF₃⁺ and SF₂⁺ to SF₅⁺ are similar to those observed for electron-impact ionization of SF₆ at ~30 eV electron energy. A weak SF⁺ ion was also observed. Since the threshold for SF⁺ formation by electron impact is 31 eV, considerable electron energy is apparently available in the discharge. The absence of SF₄⁺ and possible reactions will also be discussed.

*Work supported by the Office of Energy Storage and Distribution, Electric Energy Systems Program, US Department of Energy under contract DE-AC05-84OR21400 with Martin Marietta Energy Systems, Inc.

SESSION CB

1:30 PM - 3:28 PM, Tuesday, October 17

Hyatt Riskey Hotel - Camino Ball Room D

HEAVY PARTICLE AND EXCITED STATE COLLISIONS

Chair: M. R. Flannery, Georgia Institute of Technology

CB-1 Association Reactions of Metastable Helium Atoms, J. STEVEFELT, GREMI/CNRS, U. of Orléans, France - Theoretical description of termolecular association of helium triplet atom with normal helium in a gas will be presented. The initial capture involves barrier tunneling in the He $a^3\Sigma$ state, and the subsequent relaxation of²highly excited vibrational and rotational states will be discussed. Results for the overall rate at which the product He₂ v=0 appears will be compared with measured reaction rates for the metastable atom-molecule conversion.

CB-2 Half Collision Studies of the H + H₂ Transition State
P. C. COSBY AND H. HELM, SRI International - Charge transfer of H₃⁺ in Cs produces an intense beam of H₃ molecules in the long-lived 2p²A₂" state. We have recently demonstrated¹ that these molecules can be photoexcited into other H₃ excited states which predissociate along the repulsive ground electronic state surface. The optical excitation completely defines the angular momentum, vibrational, and nuclear spin state of the dissociating molecule, as well as its total energy. The discrete energy releases that accompany the production of particular rovibrational levels in the H₂ photofragment are observed by explicit measurement of the velocity vectors of the correlated H + H₂ dissociation fragments. The rovibrational distribution in the H₂ fragment is found to be highly dependent on the transition state selected. Initial experiments have thus far probed only a few transition state configurations at energies 7.6 - 8.1 eV above the H + H₂(v=0) asymptote, however much lower energy regions of the ground state potential will be accessible using stimulated emission pumping with this technique.

¹P. C. Cosby and H. Helm, Phys. Rev. Lett. **61**, 298 (1988).

CB-3 Study of Low-Energy Electron-Molecule Interactions Using Rydberg Atoms,* F. B. DUNNING, Rice University -- Many collision processes involving atoms in high Rydberg states ($n \geq 40$) can be described by invoking the "essentially-free" electron model and considering only the interaction between the Rydberg electron and target particle. Thus, because the mean kinetic energy of a Rydberg electron is only a few meV, Rydberg atom collision studies provide a novel means to explore electron-molecule interactions at subthermal electron energies. Rate constants and cross sections for free electron capture by a variety of molecules have been derived from Rydberg atom studies. Translational energy release in dissociative electron capture has also been investigated in kinematic studies using a position sensitive detector. This work reveals that for some molecules (e.g. CH_3I) essentially all the excess energy of reaction appears in translation, whereas for others (e.g. CCl_4) much of this energy is stored as internal energy in the fragments. Kinematic studies also show that for intermediate n post-attachment interactions between the Rydberg core ion and product negative ion are important.

*Research supported by the NSF under Grant #PHY87-09637 and the Robert A. Welch Foundation.

CB-4 Recombination of Xe^+ Ions and F^- Ions in Ambient Helium*, H.S. Lee and R. Johnsen, University of Pittsburgh -- We have determined rate coefficients for ion-ion recombination of Xe^+ with F^- ions by observing the decay of the ionic conductivity in a photoionized helium afterglow plasma (helium pressures < 1 at.) containing admixtures of Xe and F_2 . In addition, we observed the fluorescence resulting from ion-ion recombination into the XeF^* excimer state, and we monitored the ion composition of the plasma by mass-spectrometric sampling of afterglow ions. The recombination coefficients were found to increase approximately linearly with helium pressure, reaching a value of about $1 \times 10^{-6} \text{ cm}^3/\text{s}$ at a helium pressure of 1 at.. The results will be compared to theoretical calculations by Flannery and Yang¹ and to Monte Carlo simulations by Morgan et al. .

1. M.R. Flannery and T.P. Young, Appl. Phys.Lett. **33**, 574, (1978)

2. W.L. Morgan et al. Phys. Rev. A **26**, 1696 (1982)

* Work supported by US Army Research Office

SESSION D

3:45 PM - 5:30 PM, Tuesday, October 17

Hyatt Richeys Hotel - Camino Ball Room C and D

**WORKSHOP ON THE REFERENCE SYSTEM FOR
RF PLASMA PROCESSING RESEARCH**

Moderator: K. E. Greenberg, Sandia National Laboratories

SESSION E

7:30 PM - 10:00 PM, Tuesday, October 17

Hyatt Richeys Hotel - Camino Ball Room A and B

POSTERS

Chair: H. Helm, SRI International

E-1

Cylindrical Simulations of RF Plasma Discharges and Plasma Immersion Ion Implantation*, M.V. ALVES**, V. VAHEDI, and C.K. BIRDSALL, ERL, UC Berkeley — A cylindrical many-particle simulation code, PDC1, has been used to model 1) RF discharges in which the electrodes have different areas, and 2) plasma immersion ion implantation, where the target has a transient negative bias. PDC1 is a 1D radial, electrostatic code. It has an external circuit with an RF source and RLC components and has an electron-neutral and ion-neutral collision model the same as in PDW1¹. The differences between having parallel planar and concentric cylindrical electrodes are examined. In particular, with RF discharges, the self-bias voltage at the powered electrode is measured and compared with theory².

*This work supported in part by DOE contract DE-FG03-86ER53220 and ONR contract N00014-85-K-0809

**On leave from INPE - S. J. Campos - SP - Brazil

[1] I. J. Morey, V. Vahedi, J. P. Verboncoeur, to be presented at this conference.

[2] M. A. Lieberman, *J. Appl. Phys.* **65**, 4186 (1989).

E-2

Particle Simulation Code for Modeling Processing Plasmas*, I.J. MOREY, V. VAHEDI, J. VERBONCOEUR and M. A. LIEBERMAN, ERL, UC Berkeley — The bounded plasma particle code PDW1¹ now has elastic, excitation, ionization and charge exchange collisions, so that a number of different processing plasmas can be simulated. RF discharge simulations have shown rectification of the plasma potential, ions responding to the average potential, sheath heating and joule heating. Both voltage and current driven RF discharges have been examined, and differences have been observed between the harmonic contents of the potential. Ion velocity distributions at the boundaries exhibit features due to charge exchange and ionization within the sheath regions. Plasma immersion ion implantation simulations will be compared with theory². The PC version of PDW1 has many quantitative diagnostics displayed in a window format, readily accessed using a menu system.

*This work supported in part by DOE contract DE-FG03-86ER53220 and ONR contract N00014-85-K-0809.

[1] W. S. Lawson, *J. Comp. Phys.* **80**, 253 (1989).

[2] M. A. Lieberman, to appear in *J. Appl. Phys.* (Oct 1989).

E-3

DC Self-Bias Voltages in Low Pressure Discharges in Finite Cylindrical Chambers, M.A. LIEBERMAN, University of California, Berkeley, and S.E. SAVAS, Applied Materials, Santa Clara — We have developed a theory of dc bias formation in low pressure capacitive rf discharges in finite cylindrical chambers where the powered electrode area is less than the area of the grounded and insulating walls. Results of analytical and numerical calculations are shown. Both of these assume that ionization is simply proportional to the electron density. The analytical model makes further assumptions that the ion mobility is constant and that the sheaths are purely capacitive in order to calculate the ratio $R = \text{plasma-to-powered} / \text{plasma-to-grounded electrode dc voltage}$. It is found that R is not proportional to any power of the electrode area ratio, as is so often assumed. The numerical results use a variable ion mobility and rf sheath model incorporating phase dependent admittance and capacitance to compute self-consistent values of R . Non-zero sheath admittance is found to have a small effect on R . Comparisons of the model with measurements^{1,2} will be presented.

1. J.W. Coburn and E. Kay, *J. Appl. Phys.* 43, 4965 (1972).
2. C.M. Horwitz, *J. Vac. Sci. Technol. A* 1, 60 (1983).

E-4

Parallelizing the Monte Carlo Simulation in Weakly Ionized Plasmas, C. J. Wang, Department of Electrical and Computer Engineering, U. of Colorado at Colorado Springs, and C. Wu, Electrical Engineering Department, Auburn University.--The Monte Carlo method is a useful technique to study the evolution of charged particle assembly. The simulation takes a considerable amount of time, even when few particles are used. However, this problem has inherent parallelism in nature. Parallel Monte Carlo techniques for simulating the evolution of an assembly of charged particles interacting with the background gas medium under the influence of the electrical field are presented. We have overcome three major difficulties: 1) the number of particles to be simulated is increasing over time due to the ionization process; 2) the conditional branching statements do not inhibit multiprocessing; 3) concurrency and vectorization are fully utilized through the new parallelized Monte Carlo method. The shared-memory vector multiprocessor Alliant FX/80 has been used for performance measurements. Significant speedup has been achieved on the simulation of an electron avalanche.

E-5 The Plasma Sheath Transition in an Asymmetric Collisionless Plasma. H. van den BERG, K.-U. RIEMANN. Ruhr-Universität Bochum, FRG. The plasma-sheath problem ($\lambda_D/L \rightarrow 0$) for an asymmetric warm collisionless plasma is solved in plane parallel geometry. To this end Emmert's model source term [1] is generalized to account for a superimposed plasma drift. The quasineutral plasma approximation results in a system of coupled integral equations which can be solved analytically. In contrast to Emmert's symmetric model one sheath edge shows the usual field singularity. At the other sheath edge we find a finite field strength and an oversatisfied Bohm criterion. These results are in full agreement with general relations on the Bohm criterion and on the sheath edge field singularity [2].

[1] G. A. Emmert et al., Phys. Fluids 23, 803 (1980).

[2] K.-U. Riemann, Phys. Fluids B1, 961 (1989).

E-6 Parametric Studies of Ar and SF₆ rf Discharges Using the Continuum Model, and Comparison with Experimental Data, E. GOGOLIDES, J. LIU, and H.H. SAWIN, MIT. -- A self-consistent continuum model¹ is used to simulate Ar and SF₆ discharges. Parameters that are varied in the model are pressure, rf current, and rf frequency. The effects of these parameters on the spatial and temporal profiles of particle densities, electron energies, ionization rates, electric fields, and other variables are examined. Model predictions of current-voltage waveforms, power deposition, ion fluxes and ion bombardment energies are in good agreement with experimental data. The characteristics of typical electropositive and electronegative discharges, Ar and SF₆, are contrasted. For example, as power is raised, the electron densities in both the Ar and SF₆ plasma increase, resulting in an increase of the current. In Ar, the voltage also increases while in SF₆ it remains approximately constant.

¹Gogolides *et al.*, J. Vac. Sci. Technol. A7, 1001 (1989).

E-7 PIC Simulation at High Plasma Densities,* R. K. PORTEOUS and D. B. GRAVES, Chemical Engineering, U. of California, Berkeley -- As the plasma density rises in a PIC simulation the number of Debye lengths increases and usually the grid spacing must be reduced to compensate. When the system contains more than 10^3 Debye lengths, or in multidimensional geometries, this represents a large overhead. Further, if the number of superparticles per cell is held constant, the total number of particles increases with the number of cells and inversely with the Debye length, i.e. as $n_e^{0.5}$.

The time for simulated plasmas to come to equilibrium is of the order of the ion residence time which is approximately independent of n_e . However the timestep must be kept at some fraction of the plasma period which decreases as $n_e^{-0.5}$. For $n_e > 10^{17} \text{m}^{-3}$ simulations may involve $10^6 - 10^7$ timesteps.

These combined increases in size and duration determine the limitations of practical simulations. Techniques for extending simulations of time-invariant plasmas to high densities, such as particle smearing and multi-timescaling, will be discussed and some results from such plasmas presented.

*Work supported in part by IBM.

E-8 Ion Bombardment Energy Distributions from RF Discharges, M. F. TOUPS, D. W. ERNIE, and H. J. OSKAM, U. of Minnesota--Experimental measurements of the energy distribution and the flux of ions bombarding an electrode of a parallel plate rf reactor were performed in various noble gases and noble gas mixtures using a hemispherical retarding grid energy analyzer. Quadrupole mass analysis was performed to identify the ions which were bombarding the electrode. Frequencies from 1 to 40 MHz and pressures from 0.025 to 1 Torr were studied. For a given amplitude of the applied rf potential, the frequency of the applied rf potential and the reactor gas pressure were found to be significant in determining the shape of the measured ion bombardment energy distributions. The total ion flux to the electrode surface was found to be determined by the frequency and amplitude of the applied rf potential and to be insensitive to the reactor gas pressure. These results will be discussed with reference to the physics of rf gas discharges.

E-9 A Tuned Langmuir Probe for Measurements in RF Glow Discharges, A.P. PARANJPE*, J.P. MCVITTIE** and S.A. SELF*,
*Dept. of Mechanical Engineering and **Dept. of Electrical Engineering, Stanford University, Stanford, CA 94305 -
Measurements of charged particle concentrations and the electron energy distribution function (EEDF) have been made in argon and SF₆ glow discharges using a tuned Langmuir probe technique. A simple passive circuit connected to the probe when properly tuned, increases the impedance between the probe and ground, thereby forcing the probe to follow the instantaneous plasma potential. In this manner RF induced distortion of the probe characteristic is mitigated. At 13.56 MHz the electron collection characteristic of a detuned probe is distorted by RF interference; the ion collection characteristic is unaffected. The EEDF is highly non-Maxwellian in argon discharges, but quite Maxwellian in SF₆ discharges. The mean electron energy increases with decreasing pressure and increasing power in argon discharges, but is independent of pressure and power in SF₆ discharges. The measured distribution functions and charged particle concentrations are in agreement with calculations.

E-10 Collisional Effects on Plasma Flow Along the Divergent Magnetic Field of an ECR Plasma Stream Source, M. HUSSEIN and G. A. EMMERT, University of Wisconsin-Madison--Plasma flow along decreasing magnetic field lines from the resonance cavity to the specimen plate in an ECR plasma stream source is numerically simulated. The approach is kinetic in which a Monte Carlo description for the ion dynamics, coupled with Boltzmann electrons is used to develop an iterative scheme for solution of the Vlasov equation and quasi-neutrality. Collisions between ions and neutrals are included in the context of Monte Carlo techniques. The effect of the divergent magnetic field on the plasma potential profile, the floating potential, and the energy distribution of the ions incident on the specimen are presented. Collisional effects are shown to produce a wider ion energy distribution than that obtained with a collisionless simulation(1).

(1) M. A. Hussein and G. A. Emmert, 16th IEEE Int. Con. on Plasma Science, Buffalo, N.Y., 22-24 May 1989.

E-11 A Comparison of Three Power Measurement Techniques in a Low Pressure RF Discharge, R. B. PIEJAK, V. A. GODYAK, GTE Laboratories Inc., Waltham, MA -- The power dissipated in a low pressure argon RF discharge driven symmetrically at 13.56 MHz has been measured in three different ways and compared. One measurement technique is just the product of the RMS voltage and current and the cosine of the phase shift between them. The second method of power measurement consists of taking the integral over one period of the voltage-current product. The third discharge power measurement is based on power meter measurements in the transmitting line (incident minus reflected power) with and without a discharge while having the matcher in both cases tuned to resonance. This enables the power dissipated in the discharge and that dissipated in the matcher to be calculated separately. All three measurements are compared versus the discharge voltage. The power dissipated in the matching system was found to be larger than the discharge power in some cases.

E-12 TIME - DEPENDENT EXCITATION IN A 13-MHz ARGON DISCHARGE, M.J. Colgan and D.E. Murnick, Physics Department, Rutgers University, Newark NJ 07102--The spatial and temporal dependence of ArI spectral lines are being measured in an argon discharge at 13-MHz using the time-to-amplitude conversion method on spatially resolved plasma-induced emission (PIE). Using single photon counting and fast phototubes, sub-nanosecond time resolution is achieved and radiative lifetime effects are observed. The discharge is maintained between parallel electrodes of equal area with applied r.f. power between 1 and 5 Watts at 1 Torr gas pressure. Previous measurements of this type have been reported for argon in a 50kHz discharge with asymmetric electrodes¹. Time-dependent electron collision excitation rates can be determined by deconvolution of PIE originating in 2p (Paschen notation) and higher-lying levels. These data may be used in combination with absolute 1s densities which we obtain by laser absorption spectroscopy to evaluate and improve fluid-type discharge models².

¹R.J. Seeböck and W.E. Kohler, *J. Appl. Phys.* **64**, 3855 (1988)

²D.B. Graves, *J. Appl. Phys.* **62**, 88 (1987)

E-13 Transient Electron Kinetics in Crossed Electric and Magnetic Fields and Circularly Polarized Microwave Field,* P. Hui and G. Schaefer, Weber Research Institute, Polytechnic University --The Monte Carlo Flux method¹ is used to calculate electron velocity distribution functions in cases where the distribution functions are fully 3-dimensional in velocity space. Examples are crossed electric and magnetic fields and circularly polarized microwave fields with and without crossed magnetic field. Steady state distributions and time dependent distributions after step-wise changes of the electric and the magnetic fields will be presented. The similarity relations between crossed electric and magnetic fields and microwave fields will be discussed.

*Work supported by the NSF

¹G. Schaefer and P. Hui, Submitted to J. Comp. Phys., to be published.

E-14 Experimental and Theoretical Longitudinal Electron Diffusion Coefficients in Molecular Gases, J. L. PACK,* R. E. VOSHALL, A. V. PHELPS⁺ and L. E. KLINE, Westinghouse STC, Pittsburgh, PA 15235 -- Values of the ratio of the longitudinal diffusion coefficient to mobility (D_L/μ) for electrons in D_2 , N_2 , H_2O , N_2O , NO_2 , CO , CO_2 and NH_3 were obtained during earlier measurements of electron mobility. The measured D_L/μ values agree well with predictions based on the theory of Parker and Lowke. The experimental values of D_L/D_T , where D_T is the transverse diffusion coefficient, are about 0.5 for D_2 , N_2 and CO in agreement the theory. The experimental D_L/D_T values for H_2O , N_2O and CO_2 are > 1 , also in agreement with theory. The occurrence of D_L/D_T values > 1 near and below the peak of the D_L/μ vs E/N curve is caused by the decrease in the momentum transfer cross section with increasing electron energy below the Ramsauer minimum. Calculated transport coefficients are given for E/N values from thermal E/N to 10 Td.

* Present address, 3853 Newton Drive, Murrysville, PA 15668.

+ Present address, Joint Institute for Laboratory Astrophysics.

E-15 Photodetachment Technique for Measuring H⁻ Velocities in a Hydrogen Plasma, P. DEVYNCK, M. BACAL, P. BERLEMONT, J. BRUNETEAU, R. LEROY, and R. A. STERN* Ecole Polytechnique, Palaiseau, France--We report work in progress on laser diagnostics of negative ion transport velocity in H⁻ ion volume sources. The plasma dynamics after the laser shot is discussed in detail, and the effect of the plasma potential perturbation on the H⁻ is evaluated. A method of evaluation of the H⁻ transport velocity from single laser beam photodetachment experiments is proposed. To substantiate this method, two laser beam photodetachment experiments have been developed. The velocities thus determined are pressure dependent; they correspond to H⁻ energies in the range 0.23 to 0.08 eV.

(Work supported in part by Direction des Recherches, Etudes et Techniques, and the Oak Ridge National Laboratory)

*Permanent address: University of Colorado, Boulder, CO

E-16 Fokker-Planck Swarm Energy Spectrum, N.J. CARRON, Mission Research Corp -- A Fokker-Planck expansion in energy space of the Boltzmann collision integral for electron swarms, valid for small fractional energy loss, is presented and studied. Treating angle variables in a two term Legendre series, there results a useful, physically meaningful, differential equation for the spectrum evolution in a time varying electric field. Elastic, inelastic and super-elastic collisions are included. The time independent solution in a constant field gives an approximate expression for the steady state swarm energy spectrum. The physical meaning of its functional form is made clear via ordinary convection-diffusion theory. Previous spectra by Wannier; Chapman and Cowling; Morse, Allis, and Lamar; Davydov; and Druyvesteyn are special cases. The new spectrum is exact in the limit of small quantum transition energies. The reasons for the inadequacy of the Continuous Slowing Down Approximation (CSDA) become apparent, and it is shown that the CSDA violates detailed balance. The spectrum is used with experimental cross sections to compute transport coefficients in O₂ and N₂, in which fractional energy loss is small at most energies. Agreement with swarm data is excellent from .01 to 100 Td for most coefficients.

E-17 Particle Focusing Using Two-Stage Laser Ablation,* K. D. BONIN and M. A. KADAR-KALLEN, Princeton U. — We have used two-stage laser ablation to produce a focused beam of neutrals, ions, and clusters.¹ The technique has enabled us to generate a collimated beam and beams which are focused in one and two dimensions. For a barium beam focused in two dimensions over a distance of 10.7 cm the on-axis density was measured to be 5×10^{15} atoms/cm³. An on-axis density of 10^{15} atoms/cm³ was measured for a collimated beam at the same distance. The particle beam is produced by a two stage process. In the first stage a pulse from the ablating laser ($\lambda = 532$ nm) strikes a barium slab in a vacuum chamber (10^{-6} torr) in front of a transparent substrate. The distance between the solid barium slab and the substrate is 0.5 cm. Material is removed from the barium slab and is deposited as a thin film on the substrate. A rotating stage then moves the barium and replaces it with a hole in front of the now coated substrate. The laser is pulsed again, ablating the barium deposited on the substrate and forming a beam which propagates freely. The particle beam's focusing properties are determined by the shape of the substrate's surface. Material deposited on a cylindrically or spherically curved glass substrate is focused to its center of curvature. A quartz crystal microbalance (QCM) was used to measure the total mass deposited by the focused barium beam. This technique should be especially useful to those interested in producing atomic beams of refractory elements.

*Supported by DOE LLNL/DOE S/C 1133303 and ARO DAAL-87-K-0068.

¹M. A. Kadar-Kallen and K. D. Bonin, *Appl. Phys. Lett.* **54**, 2296(1989).

E-18 Two Approximate Sheath Solutions for a Planar Plasma Anode, O. BIBLARZ, GTE Products Corporation, Danvers, MA 01923. -- Solutions to the anode sheath have been obtained when the electron and plasma temperature are equal and when the electron is substantially above the plasma temperature. A single, highly nonlinear equation for the electric field at the sheath is derived. A description for this electric field is used which does not satisfy all the conditions of the problem. The approximation can be improved by identifying the coefficients for the net production of charges a posteriori. This approach allows for largely non-numerical solutions of some validity. When the electron and plasma are at equal temperature, reasonable results are obtained for nitrogen which at sufficiently low currents are realistic. The second case, however, yields only unreasonable answers which are thought to be related more to the inadequacy of the planar geometry model than to the approximation of the electric field distribution. Conceivably, the reactivity of the sheath can also drive the problem to a multi-dimensional mode for equal electron and plasma temperatures.

E-19 The Universal Resputtering Curve, W.L. MORGAN, Kinema Research, Monument, CO 80132--Recent measurements¹ of the fraction of material resputtered during rare gas sputter deposition of metals have shown what appears to be a universal curve for fraction resputtered versus a dimensionless mass parameter for a wide range of metals and rare gases. I will present the results of Monte Carlo trajectory simulations and theoretical analyses that provide some insight into the reason for this universal behavior. The analysis provides a simple analytical model that can be used to estimate the contributions to resputtering from the target atoms being deposited and from the reflected rare gas atoms in the sputtering system.

¹D.W. Hoffman and J.S. Badgley, *J. Vac. Sci. Technol.* A 5, 1791 (1987); *ibid.* 6, 1691 (1988).

E-20 Optical Diagnostics of Sputtered Metal Atoms in DC and RF Discharges, G.M. JELLUM and D.B. GRAVES, Department of Chemical Engineering, University of California, Berkeley -- A study of the gas phase metal species sputtered from electrodes of DC and RF discharges has been carried out using various discharge diagnostics. In particular, time- and space-resolved laser induced fluorescence (LIF) and optical emission spectroscopy (OES); and space-resolved laser absorption and Langmuir probes. The discharge conditions, gases, and electrode materials have been varied to examine, systematically, the effects of electrode sputtering: the pressures have been varied from 0.03 to 3 torr and powers up to 1.5 W/cm². A dramatic difference is found between the spatially-resolved optical emission and laser induced fluorescence signals; this difference cannot be accounted for by considering only the electron density/energy dependence of the OES signal. A laser pump/probe experiment shows the gas phase metal species is not a neutral atom; we speculate that this species is a negatively charged metal cluster. The creation and loss mechanisms of this species are examined by combining the diagnostics with a pulsed discharge.

E-21 ELECTRICAL CONDUCTIVITY OF HIGH PRESSURE IONIZED XENON,* J. Koceić and S. Popović, Institute of Physics, Belgrade, Yugoslavia, -- Radial temperature distributions and voltampere characteristics were used to evaluate electrical conductivity of high pressure ionized xenon. This experiment confirms the influence of dense plasma conditions on transport properties of xenon plasmas. Possible contribution of excited states and ion-acoustic turbulences to the electron transport were also discussed.

*Submitted by L. Vušković

E-22 Electric Field in Super-Narrow Tube Low Pressure Hg-Ar Electric Discharge Lamps,* G.Zissis, P. Bénétruy, J.J.Damelinourt, C.P.A.Toulouse France -- We report here the first measured and calculated values of electric field strength in super narrow tube (diameter < 6 mm) low pressure Hg-Ar lamps. In our experimental apparatus, the cold spot temperature could be fixed to within $\pm 2^\circ\text{C}$ by using an oil circulation around the lamp. Measurements of electrical field have been carried out for three different diameters and for two different currents (20 and 40mA) using a high frequency power supply (28 kHz), the rare gas pressure was 15 Torr (24°C) in all cases. The experimental accuracy has been estimated to be $\pm 6\%$ in all cold spot temperature range (-15 to 85°C). We observe that, electric field remains almost constant (within $\pm 8\%$) as a function of cold spot temperature and its absolute value has been found to be several Volts/cm depending on the tube radius and discharge current. The electric field has also been calculated by using a self consistent collisional radiative model. Diffusion controlled positive column has been taken into account, and a non Maxwellian electron energy distribution function as proposed by Lagushenko¹, has been used. Our calculated values are in very good agreement (within $\pm 1\%$) with the experiment for $T_{cs} > 30^\circ\text{C}$, but important discrepancies have been found for the lower cold spot temperatures. This later may be explained by taking into account the possibility of rare gas ionization which may occur in these cases because the elevated electron temperature ($> 20000\text{K}$).

*Work supported in part by CIE Philips Eclairage, Pont-à-Mousson, France

¹R. Lagushenko and J. Maya, Journal of IES, 14, 306 (1984).

E-23 Low Electric Field Measurements in Plasmas.
J. R. SHOEMAKER, Wright Research and Development Center, WPAFB OH -- Low electric fields in plasmas have previously been measured using Inglis-Teller series termination and line broadening of high n (Rydberg) states of atoms. A misinterpretation in the definition of series termination, which has been propagated in the literature for the past 50 years is shown to change measured field values by a factor of two. The incorporation of instrumental resolution in the derivation of the series termination relation is shown to alter field values significantly. Problems with applying hydrogen line broadening theory to triplet and singlet helium are discussed, as well as a correction for hydrogen.

E-24 Modelling of a surface wave sustained helium discharge at low pressure, * S.DAVIAUD, G.GOUSSET, J.MAREC, LPGP, Univ. Paris-Sud, Orsay, FRANCE

A collisional radiative model has been realized to model helium surface wave discharges at low pressure (0.5-10 Torr) with an electron density of 10^{12} to 10^{13} cm^{-3} . The calculated values of the 2^3S and 2^3P densities are in good agreement with the densities measured by a selfabsorption technique. Furthermore, the model describes well the characteristics ν (effective collision frequency for momentum transfer) and θ (power needed to maintain an electron), which had been previously obtained experimentally¹. Using the model, the main mechanisms occurring in the discharge are studied: the plasma is stepwise excited by electron collisions.

*Work supported in part by Microcontrole, Evry, FRANCE

¹S.DAVIAUD, C.BOISSE-LAPORTE, P.LEPRINCE, J.MAREC, J. Phys. D (Appl. Phys.) 22(6) (1989) 770

E-25 VUV Spectroscopy of an Argon Surface Wave Plasma with Supersonic Flow*, M. E. BANNISTER, J.L. CECCHI, G. SCOLES, Princeton University -- The VUV emissions from the supersonic expansion of an argon plasma sustained by electromagnetic surface waves are studied. A 2.45 GHz surfatron¹ excites the plasma in a 4 mm I.D. quartz tube which is terminated by a converging nozzle, which produces supersonic flow into a vacuum chamber. Variations in the spectra in the 60-150 nm range, including features associated with Ar₂^{*} excimer emission, are investigated as functions of discharge pressure, nozzle diameter, and absorbed power. Emission spectra with and without a luminous expansion jet are compared. In addition, a scheme for the breakdown of the supersonic expansion is proposed based on experimental results.

*Work supported in part by U.S. Department of Energy Contract #DE-AC02-76CHO3073

¹M. Moisan, C. Beaudry, P. Leprince, *Phys. Lett.* 50A, 125 (1974).

E-26 Simulation of Electron Avalanches near a Gas-Solid Interface, S. M. Mahajan and K. W. Lam, Tennessee Technological University - - Electron avalanches near a solid dielectric surface in nitrogen gas (at 0.1 MPa) have been simulated. The electrons are assumed to propagate primarily in the gas. Nearby solid dielectric surface has been included in the simulation via (i) non-uniform electric field and (ii) photoemissive contribution to the ongoing avalanche in the gas. Photoemission from the solid dielectric surface has been assumed to be most effective near the tip of the ongoing avalanche. Field enhancement near cathode triple junction and field reduction near anode triple junction describes the non-uniform electric field along the length of the solid dielectric. Electron avalanches have been simulated with several different electric field profiles (linear, exponential, and step function), and at various values of electric fields.

Results indicate that if a nearby solid dielectric has reasonably high value of photoemission coefficient, then the surface flashover could occur at relatively low values of electric field. Experimental data on photoemission coefficient from various solid dielectrics is needed.¹ Electron avalanches in various non-uniform electric field profiles could provide information about the growth of electrons near a charged dielectric surface.

1. M. Tanaka, Y. Murooka, and K. Hidaka, *J. App. Phys.*, 61(9), 4471 (1987).

E-27 Creation of an Electrostatic Image on a Dielectric Surface in a Small Gap, V. Meytlis, T. Kegelman, B. Fagen, KCR Technology, Inc. - The discharge in an extremely small gap width (approx 10 μ m) is investigated experimentally and theoretically. The positive electrode has a metallic surface and the negative electrode is covered by a dielectric. The dielectric surface moves with respect to the fixed metal surface at a constant velocity. This allows creation of a sustained discharge between the surfaces. The positive charge which forms on the dielectric surface after a discharge creates a field concentration. The relationship between the applied and residual voltage (the positive charge on the dielectric) was obtained for different configurations of the metal anode and for different dielectric film thickness on the cathode. A converging surfaces model was used to describe the discharge under these conditions. Within this model it is possible to apply the Townsend Theory of Discharge to explain the experimental results.

E-28 Conductivity Probe for High Pressure Plasmas* S.M.Jaffe, S.A.Self, M.Mitchner Stanford University.--In our efforts to study three body recombination in afterglows at atmospheric pressure, we have developed a conductivity probe based on the capacitive coupling approach of Johnsen¹. The probe is a coaxial resonator operating at 250 Mhz with one end open to the plasma. The presence of plasma in this end reduces the signal transmission and this effect can be simply related to the plasma conductivity. Only a signal generator and diode detector are required. The measurable range of conductivity extends from 5×10^{-4} to 10^{-1} S/m. Afterglows of photoionized, high pressure plasmas have been measured with this probe and compared with kinetic models.

* Work supported by AFOSR

¹R.Johnsen, Rev. Sci. Inst 57, March 1986 P.428

E-29 Optical Emission and Langmuir Probe Diagnostics of a Hydrocarbon Arc Jet Plasma, K. R. STALDER AND R. L. SHARPLESS, SRI International--We have made spectroscopic measurements of an arc jet plasma used to synthesize polycrystalline diamond films on a silicon substrate. A subsonic plasma jet is ejected from the orifice of the arc chamber and impacts the substrate. Using 200 Torr hydrogen with 1% added CH₄, 900 watts discharge power and a substrate-orifice distance of 10 mm, we observed polycrystalline diamond films to grow at a rate of 1 micron per minute. Spectroscopic measurements show strong emission from C₂ and CH. Synthetic spectra fits to the C₂ emission show that the excited state C₂ temperature near the orifice is 5000 K, and drops to 4000 K 8mm downstream. The decrease in optical emission intensity is consistent with local thermodynamic equilibrium (LTE) conditions which are likely to prevail in this high pressure plasma. Langmuir probe measurements indicate the electron temperature is about 10,000 K, so this supports the LTE nature of this plasma.

E-30 In-Situ Density and Temperature Measurements of Vibrationally-Excited Hydrogen Molecules in H⁻ Ion Source Plasmas,* G. C. STUTZIN, A. T. YOUNG, A. S. SCHLACHTER, K. N. LEUNG and W. B. KUNKEL, Lawrence Berkeley Laboratory, University of California -- Production of vibrationally-excited hydrogen molecules has been postulated to be an intermediate step in H⁻ formation in ion source discharges, but until recently, measurements have been scarce. We have measured the rotational- vibrational distribution up to $v'' = 8$ and $J'' = 13$ (not simultaneously) using VUV laser absorption spectroscopy in a pure H₂ discharge. The vibrational populations appear to be well-described by a plateau in the vibrational distribution from $v'' \sim 5$ to $v'' \sim 11$. Further study of an ion source optimized for H⁻ production is in progress, in which the atomic and molecular populations as well as extracted H⁻ current and thermal electron characteristics will be measured at various discharge parameters. By correlating these data, one can attempt to determine the validity of the theoretical models for these sources.

* Supported by AFOSR and US DOE under Contract No. DE-AC03-76SF00098.

E-31 Atomic Hydrogen Measurements in Hydrogen Bearing Plasmas B. L. Preppernau, A. Tserepi, T. Czerny, and T. A. Miller, Ohio State University - - Hydrogen bearing plasmas are finding wide applications to the production of novel materials and properties. A recently developed laser probe diagnostic of atomic hydrogen concentrations has been applied to the study of the role of atomic hydrogen in various hydrogen bearing plasmas. The technique offers both excellent spatial and temporal resolution of atomic hydrogen profiles in these plasmas. The diagnostic has been shown to have a dynamic response capable of being utilized over a broad range of plasma conditions, particularly near plasma/surface interfaces.

E-32 Detection of atomic hydrogen near a surface by resonant four-photon ionization technique,* G. SULTAN, G. BARAVIAN, J. JOLLY, and P. PERSUY, L.P.G.P., (Associé CNRS), U. of PARIS-SUD 91405 ORSAY FRANCE - Hydrogen atoms are created in a flowing dc discharge in H₂. The gas pressure is in the range 0.1-10 Torr and the discharge current may be fixed between 1 and 100 mA. The H atoms produced in the discharge are driven out by the gas flow to the detection chamber, where a laser beam is focussed at few mm from a biased electrode. The laser wavelength is scanned in the range 364-366 nm, the value 364.7 nm corresponds to a resonance with 3 photons for atomic hydrogen. In this case the H atom is excited with 3 photons and ionized by a fourth one. The produced ions are collected in an applied field equal to about 30 V/cm and the intensity of the signal can be related to the H atom density. In this experiment the direct non resonance four-photon ionization of H and H₂ is negligible as compared with the resonance enhanced process. The resonance line is asymmetric and presents a FWHM between 0.05 and 0.2 nm.

* Work supported in part by DRET

E-33 Stochastic Properties of Trichel Pulse Corona Discharges in O₂ and Ne/O₂ Mixtures,* R.J. VAN BRUNT and S.V. KULKARNI, NIST, V.K. LAKDAWALA, Old Dominion Univ.—The stochastic behavior of ultra-violet sustained negative point-plane corona discharge pulses in O₂ and Ne/O₂ at atmospheric pressure have been investigated using a newly developed method¹ to directly measure various conditional discharge pulse-height and time-separation distributions. As in the case of negative corona pulses in air or N₂/O₂ mixtures, the strong correlation between pulse amplitude and time separation from the previous pulse can be explained by the influence of residual negative-ion space charge in reducing the electric field strength at the cathode. For Ne/O₂, the correlations between amplitudes of successive discharge pulses and between amplitude and time-to-initiation of the subsequent discharge pulse are the opposite of those found for O₂ and N₂/O₂ mixtures. It is argued that this difference between the stochastic behavior of corona pulses in Ne/O₂ and O₂ or N₂/O₂ can be attributed to the different relative roles played in these mixtures by residual metastables in enhancing both the ionization rate and secondary electron emission at the cathode. The influence of metastables appears to be more important O₂ and N₂/O₂.

*Work supported in part by U.S. Department of Energy.

¹R.J. Van Brunt and S.V. Kulkarni, Rev. Sci. Instrum. (in press, 1989).

E-34 Absolute Total Inelastic Electron Impact Excitation of He and Ne,* DAVID SPENCE and MICHAEL A. DILLON, Argonne National Laboratory--We have identified a previously unrecognized systematic error in the use of the "trapped electron method" which may have affected some previous measurements of inelastic electron scattering cross-sections. We have employed this technique to measure the total inelastic cross section in helium and neon from the first inelastic threshold to the ionization threshold. In our experiments, all experimental parameters are measured absolutely for the first time. Though our cross-section values are somewhat larger than some previous measurements, they are in excellent agreement (~5%) with recent R-matrix calculations^{1,2} over the whole energy range.

*Work supported in part by the U.S. Department of Energy, Office of Health and Environmental Research, under Contract W-31-109-Eng-38.

¹K. A. Berrington and A. E. Kingston, J. Phys. B 20, 6631 (1982).

²K. T. Taylor, C. W. Clark, and W. C. Fon, J. Phys. B 18, 2962 (1985).

E-35

Low Energy Shape Resonance in the Ground Electronic State Vibrational Excitation of Silane and Disilane, * H. TANAKA,† L. BOESTEN,† H. SATO,§ M. KIMURA, M. A. DILLON, and D. SPENCE, Argonne National Laboratory--Vibrational excitation functions and angular distributions obtained with electrons of ~ 1-7 eV incidence have been used to investigate resonance electron scattering from silane (SiH_4) and disilane (Si_2H_6). Calculations that use the discrete variable X_α multiple scattering model¹ show that a shape resonance with a maximum in the range of ~ 1.5-3.5 eV observed in the vibrational excitation functions of SiH_4 and Si_2H_6 arises from the decay of compound states with respective symmetries of t_2 and e_u .

*Work supported in part by the U.S. Dept. of Energy, OHER, under Contract W-31-109-Eng-38.

†General Sciences & Physics Dept., Sophia University, Tokyo 102, Japan.

§Physics Dept., Ochanomizu University, Tokyo 112, Japan.

¹H. Sato, M. Kimura, and K. Fujima, Chem. Phys. Lett. 145, 21 (1988).

E-36

Elastic Scattering Cross Section Measurements for Collisions of 1.5-100 eV Electrons with Silane and Disilane, * H. TANAKA,† L. BOESTEN,† H. SATO,§ M. KIMURA, M. A. DILLON, and D. SPENCE, Argonne National Laboratory--Energy and angular distributions for elastic collisions of electrons with silane (SiH_4) and disilane (Si_2H_6) have been measured for incident energies of 1.5-100 eV over a scattering angular range of 20-130°. Relative scattered electron intensities were normalized to helium cross sections by using the relative flow method. Experimentally determined cross sections are compared with theoretical results obtained from the discrete-variable X_α multiple scattering formulation.¹

*Work supported in part by the U.S. Dept. of Energy, OHER, under Contract W-31-109-Eng-38.

†Sophia University, Tokyo 102, Japan.

§Physics Dept., Ochanomizu University, Tokyo 112, Japan.

¹H. Sato, M. Kimura, and K. Fujima, Chem. Phys. Lett. 145, 21 (1988).

E-37 Positron-CO Collisions Using Parameter-Free Positron Correlation Polarization Potential. Ashok Jain, Florida A & M Univ., Tallahassee -- Recently, we¹ have proposed a parameter-free polarization potential for low-energy positrons collisions with atoms and molecules. This new potential is based on the correct asymptotic form ($-\alpha_0/2r^4$) which is smoothly joined with the positron-electron correlation energy $\epsilon_{corr}(r)$ at near-the-target distances. The $\epsilon_{corr}(r)$ is determined in an analytic form from *ab initio* calculations of the positron-electron correlated system. We employ this Positron Correlation Polarization (PCOP) potential for the positron-CO collisions below the Ps formation threshold energy under a close-coupling scheme. The converged cross sections are obtained in the multipole-extracted-Adiabatic-Approximation (MEAN). Our final total cross sections compare very well with measurements and improve upon all previously available calculations.

1. Ashok Jain, Phys. Rev. A39 (Aug. 1989 issue)

E-38 Cross Sections for Some Core-Excited NaI Quartet States*, Alfred Z. Msezane, Atlanta University -- Electron-impact excitation cross sections from ground $3s^2S$ and excited $2p^53s3p^4S$ states to the lowest core-excited quartet states of NaI arising from the configurations $2p^53s3p$, $2p^53s3d$ and $2p^53s4s$ are calculated and contrasted using a twelve-state R-matrix¹ method for energies from near threshold to 6 Ry. Extensive configuration interaction target wave functions are employed. Reach resonance structure characterizes the cross sections in the threshold region and the maxima of those from the $2p^53s3p^4S$ state dominate the corresponding ones from the ground state by at least two-orders of magnitude. The results may be important to the understanding of xuv lasers².

*Work supported in part by US DOE, Basic Energy Sciences, Division of Chemical Sciences.

¹K. A. Berrington et. al. Comput. Phys. Commun. 14, 367 (1978).

²D. E. Holmgren et. al. Phys. Rev. A31, 677.

E-39

Energetics of Negative Ion Formation via Dissociative Attachment of $e + \text{LiH}^*$, H. H. Michels, UTRC, and J. M. Wadehra, Wayne State U.---- The formation of H^- (Li^-) by dissociative attachment (DA) of $e + \text{H}_2$ (Li_2) is thought to be the dominant volume process in discharge type negative ion sources. The role of Li_xH_y (Cs_xH_y) molecules, which could be formed from seeding an alkali into a hydrogen plasma, is presently not well understood, but the addition of an alkali such as Cs appears to enhance the H^- production rate. This observation is interesting in light of the study by Gauyacq, et al¹, which indicates that charge transfer and collisional detachment processes should reduce H^- production in Na seeded plasmas. We have analyzed the electron attachment to LiH and $(\text{LiH})_2$ in terms of calculated potential energy curves. In agreement with previous studies, we find that the ground state of LiH^- is thermodynamically bound relative to $\text{LiH} + e$, with a calculated electron affinity of ~ 0.3 eV. The first excited state of LiH^- , which asymptotically correlates to $\text{Li}^- + \text{H}$, exhibits repulsive behavior in the region $3.0 \leq R \leq 6.0$ Å. Based on these preliminary studies, DA of $e + \text{LiH}$ to form Li^- should occur mainly for $E_{\text{coll}} > 3.0$ eV. The formation of $\text{Li} + \text{H}^-$ products may occur by non-adiabatic coupling of the $X^2\Sigma^+$ state of LiH^- to the continuum for $E_{\text{coll}} > 2.1$ eV. The role of LiH dimers is presently under study.

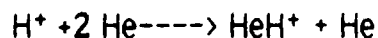
*Supported in part by AFOSR under Contract F49620-89-C-0019 and Grant AFOSR-87-0342.

¹J. P. Gauyacq, et al, Phys. Rev. A, **38**, 2284 (1988).

E-40

Low-Energy Electron Impact Dissociation of H_2 Using Fully Correlated target Wavefunctions W. M. HUO, NASA Ames Research Center, - The dissociation of H_2 by low-energy electron impact excitation to the $b^3\Sigma_u^+$ state has been studied using a two-state approximation with the target described by a full configuration-interaction (CI) wavefunction. The full CI treatment ensures that the molecule and dissociated products are described on an equal footing, an important consideration in calculating the dependence of the dissociation cross section on the initial vibrational state of the target. The different roles of target correlation and electron-target correlation will also be discussed.

E-41 Three-Body Association of Atomic Ions in Atomic Gases*. B.K. Chatterjee and R. Johnsen, University of Pittsburgh. -- We have derived a relatively simple formula to estimate three-body rate coefficients for association of atomic ions in atomic gases. While the derivation of this formula is rather crude, it reproduces available experimental data quite well and it may be useful for a quick estimation of rate coefficients, as is often needed for model calculations of discharges. We will outline the derivation and will present a comparison to available experimental data. We have also obtained new experimental data on the three-body association of protons (and the corresponding process for deuterons) in helium



at temperatures of 77 K and 300 K using a drift-tube apparatus. The results will be presented and will be compared to the theoretical formula.

* Work supported by ARO and NASA

E-42 Ion-Molecule Reactions of Atmospheric Ions with Dimethyl-Methylphosphonate*. R. Tosh, B.K. Chatterjee, and R. Johnsen, University of Pittsburgh. -- We will present the results of a series of measurements on reactions of O^+ , O_2^+ , N^+ , N_2^+ , NO^+ , NO^+ ($^3\Sigma_u$), H_2O^+ , and H_3O^+ ions with Dimethyl-methylphosphonate. (DMMP). Measured data include total rate coefficients into all product channels and product-ion branching ratios for ion energies (center-of-mass of the ion/reactant system) from 0.04 to about 1 eV. All measurements were carried out using a selected-ion drift-tube mass-spectrometer apparatus. Most reactions proceed by fast dissociative charge transfer (rate coefficients near $1 \times 10^{-9} \text{ cm}^3/\text{s}$) and lead to product ions similar to those observed in electron impact studies of DMMP. Ground-state NO^+ ions react by three-body association only while proton transfer is the only observed reaction of H_3O^+ ions.

* Work supported by the US Air Force (WPAFB)

E-43

Association Reactions in $C_2H_2^+/C_2H_2$ and HC_3N^+/HC_3N Systems, A. D. Sen, V. G. Anicich and M. J. McEwan, *JPL* — Rate coefficients of the association reactions, $C_4H_2^+ + C_2H_2$, $C_4H_3^+ + C_2H_2$ and $HC_5N^+ + HC_3N$ have been measured at pressure between 1×10^{-7} and 1×10^{-3} Torr by the ion cyclotron resonance technique. At low pressures the bimolecular association rates were $k_2 = 2.8 \times 10^{-10} \text{ cm}^3 \cdot \text{s}^{-1}$, $1.4 \times 10^{-10} \text{ cm}^3 \cdot \text{s}^{-1}$ and $5.1 \times 10^{-10} \text{ cm}^3 \cdot \text{s}^{-1}$ for $C_4H_2^+$, $C_4H_3^+$ and HC_5N^+ respectively. Above $\sim 5 \times 10^{-6}$ Torr termolecular association was observed with rate coefficients $k_3 = 5.7 \times 10^{-23} \text{ cm}^6 \cdot \text{s}^{-1}$, $1.3 \times 10^{-23} \text{ cm}^6 \cdot \text{s}^{-1}$ and $1.1 \times 10^{-22} \text{ cm}^6 \cdot \text{s}^{-1}$ for $C_4H_2^+$, $C_4H_3^+$ and HC_5N^+ respectively when the parent neutrals were the third bodies. The lifetimes for unimolecular dissociation were $\geq 73 \mu\text{s}$ for $(C_6H_4^+)^*$, $\geq 18 \mu\text{s}$ for $(C_6H_5^+)^*$ and $\geq 20 \mu\text{s}$ for $(H_2C_8N_2^+)^*$. The radiative stabilization rates were $3.7 \times 10^3 \text{ s}^{-1}$ for $(C_6H_4^+)^*$, $9.0 \times 10^3 \text{ s}^{-1}$ for $(C_6H_5^+)^*$ and $1.1 \times 10^4 \text{ s}^{-1}$ for $(H_2C_8N_2^+)^*$. It was also observed that the secondary ions $C_4H_2^+$, $C_4H_3^+$ and HC_3N^+ were produced with excess energy from $C_2H_2^+ + C_2H_2$ and $HC_3N + HC_3N$ reactions required collisional de-excitation before association with the parent neutrals.

E-44

Decay Product and Energy Distributions from H_3 $n=2$ Rydberg States,* P. DEVYNCK, W. G. GRAHAM,[†] and J. R. PETERSON, *SRI International*--The lowest bound states of H_3 , $2s A_1'$ and $2p A_2''$ are produced in keV beams from H_3^+ by near-resonant electron capture in Cs, and undergo rapid predissociative decay to the repulsive ground state. Translational spectroscopy is used on H^- atoms exiting the Cs oven along the beam axis to deduce the c.m. translational energies of the dissociation products. Both two-body and three-body energy distributions are observed, and the branching ratio is obtained from H_3 , D_3 , and HD_2 . The 3-body/2-body ratios depend on the rovibrational energy in the parent H_3^+ (beams were obtained from two different ion sources) and are smaller than those observed from dissociative recombination. The H_2 products are highly vibrationally excited, into the continuum. A distinct isotope effect is observed in the two-body decay of HD_2 .

*Research supported by AFOSR and NSF.

[†]Permanent address: Queens University, Belfast, Northern Ireland

E-45 Near Zero Projectile-frame Kinetic Energy H^+ in H_2^+ -He Collisions at 4.0 keV.* O. YENEN, L. WIESE, D. CALABRESE, and D. H. JAECKS, University of Nebraska-Lincoln--In some ion sources, one can quench upper vibrational states of H_2^+ by mixing Ne with H_2 in 5:1 ratio. We have inserted varying mixtures of Ne and H_2 in a duoplasmatron that we monitored by a quadrupole mass spectrometer just outside of the source, to alter the vibrational content of the H_2^+ beam. Using translational spectroscopy techniques in H_2^+ -He collisions at 4.0 keV, we found that the central peak of the H^+ lab energy distribution is shifted differently from $E_0/2$, depending upon the H_2/Ne ratio. Our results suggest that when high vibrational states are present, the dominant process for producing near zero projectile frame energy H^+ is electronic excitation from $1s\sigma_g$ to $2p\pi_u$ or $3d\sigma_g$ states. We also conclude that insertion of Ne in the duoplasmatron does depopulate the upper vibrational levels at least to a degree that other processes dominate the production of near zero energy H^+ in the c.m. of H_2^+ .
* Supported by NSF Grant PHY-8701905.

E-46 SO_2^- , nSO_2 , $(SO_2-O_2)^-$, nSO_2 and $(SO_2-O_3)^-$, nSO_2 clusters ($0 \leq n \leq 7$), M.JORDA, E.LEDUC, M.FITAIRE, LPGP, Univ. Paris-Sud, Orsay, FRANCE —Negative ion clusters have been identified in SO_2 and SO_2/O_2 mixtures ($p \sim 100$ Torr) with a previously described¹ experimental set-up (ionization by α -particules and detection with a mass spectrometer). Equilibrium constants of the reactions are measured as a function of gas temperature (253 K-390 K). This allows the determination of the enthalpy (ΔH) and entropy (ΔS) variations of the studied reactions. Mass discrimination between the observed ions has been done using O^{18} (for ex. ions of mass $112+n64$ could have been $(SO_3-O_2)^-$, nSO_2). In pure SO_2 , ΔH and ΔS which depend on the size of the clusters have values respectively between -3 and -7 kcal/mol (~ 0.2 eV) and -21.5 and -26 cal/mol/K ($\sim 10^{-3}$ eV/K).

¹C.V.SPELLER, M.FITAIRE, A.M.POINTU, J.Chem.Phys. 79 (1983) 2190

E-47

Spectroscopic Study of a Bound Triplet State of H₂ Perturbed by a Doubly Excited State L. J. LEMBO, N. BJERRE*, D. L. HUESTIS, AND H. HELM Molecular Physics Laboratory, SRI International, Menlo Park, CA -- A double-resonance technique is employed to measure the positions of energy levels of the 2³Π_g state of H₂. This state arises from the homogeneous interaction of the singly excited 1σ_g3dπ_g diabatic Rydberg state with the core-excited 2pσ_u2pπ_u state. This state was relied upon in a previous study to explain an unexpectedly intense photoionization behavior in triplet H₂ involving large changes in the vibrational quantum number. Some of these ionization lines correspond to 2³Π_g levels reported herein, which are observed to dissociate as well. The energy-level spacings are in good agreement with theoretical predictions. We also summarize all new information regarding the ionization transitions and levels.

This research was supported by the National Science Foundation under Grant No. PHY-8706332.

*Current Address: Institute of Physics, University of Aarhus, 8000 Aarhus C, Denmark.

E-48

Two Color Photo-ionization Spectra of He₂ a³Σ_u⁺, N. BJERRE,* L. LEMBO, D. C. LORENTS, and H. HELM, SRI International--A fast beam of He₂ a-state molecules produced by electron capture of He₂⁺ in cesium were two photon ionized by collinear photon beams from tunable lasers. Single photon transitions to intermediate states excited with a low power tunable laser were photo-ionized with a second strong time delayed laser beam of fixed wavelength. The resulting diatomic ions were detected as the first laser was scanned to obtain an absorption spectrum from the various ro-vibrational levels of the a state to the higher Rydberg states in the triplet manifold. Spectra in the 23-25000 cm⁻¹ range are dominated by a-e³Π_g and a-g³Σ_u⁺ transitions but several strong as yet unidentified transitions also appear. High Rydberg states of He₂ were studied by exciting, with the first laser, a transition to the c³Σ_u⁺ and with the second laser pumping Rydberg states lying above the ionization limit. Analysis and interpretation of these spectra in terms of the structure of He₂ is underway and will be presented.

*Institute of Physics, University of Aarhus, Denmark

SESSION FA

8:00 AM - 9:25 AM, Wednesday, October 18

Hyatt Richeys Hotel - Camino Ball Room C

IONIZATION

Chair: S. K. Srivastava, Jet Propulsion Laboratory

FA-1 Measurements of Electron Impact Ionization Cross Sections. R. S. FREUND, AT&T Bell Laboratories - As the principal collision process which sustains electrical discharges, electron impact ionization is of pervasive importance in gaseous electronics. Recently, molecular beam methods have provided accurate measurements of absolute partial ionization cross sections for atoms, molecules, and free radicals from threshold to several hundred eV, the energy region most important in gaseous electronics. Measurements are now available for single ionization of 43 atoms (almost all except the transition metals and rare earths), for double and triple ionization of many of the same atoms, and for ionization and dissociative ionization of several dozen molecules and a half dozen free radicals. This talk will review these recent measurements with an emphasis on species important in semiconductor plasma processing.

FA-2 Theoretical calculations for electron impact ionization of metastable states of rare-gas targets.* J. B. Mann, A. L. Merts, and G. Csanak, Los Alamos National Laboratory, Los Alamos, NM 87545. Electron impact ionization of metastable states of rare-gas atoms is of considerable scientific and practical interest for usage with the modeling of excimer lasers. We shall review the theoretical methods used in the past for the calculation of electron impact ionization cross sections of metastable atomic targets. This review shows that in the past, only plane-wave (Born) or binary-encounter type of theories were used for these problems. We shall present numerical results from distorted wave approximation (DWA) calculations for the ionization of the 2^1S and 2^3S states of helium as well as for the ionization of the $2p^53s$ configuration of neon, the $3p^54s$ configuration of argon, and the $4p^55s$ configuration of krypton. DWA calculation results will also be presented in some cases using the "maximum interference" DWA. Our results will be compared to other theoretical results and to the available experimental data.
*Work performed under the auspices of the USDOE.

FA-3 The Identification of Recombination Product Excitation States*, J.B.A. MITCHELL, F.B. YOUSIF and P. VAN DER DONK, The University of Western Ontario, T.J. MORGAN, Wesleyan University -- The dissociative recombination of molecular ions leads to the formation of atomic and radical fragments in a variety of states of potential and kinetic excitation. Two techniques for identifying product excitation states are currently under development in the merged beam laboratory at UWO. The first employs a time and position sensitive detector¹ to directly measure the kinetic energy and hence to deduce the potential energy of the products of diatomic molecular ion recombination. The second uses field emission detection to selectively ionize products formed in high principal quantum number states. Progress in the implementation of both these techniques will be discussed.

*Work supported by USAFOSR and Canadian NSERC.

1. D.P. de Bruijn and J. Los, Rev. Sci. Instrum. 53, 1020, 1982.

SESSION FB

8:00 AM - 9:31 AM, Wednesday, October 18

Hyatt Rickeys Hotel - Camino Ball Room D

LASER PHENOMENA

Chair: L. A. Schlie, Air Force Weapons Laboratory

FB-1

Argon Ion Laser excited at the lower hybrid Frequency.

R.W. BOSWELL and PEIYUAN ZHU, PRL, RSPHYS, Australian National University - Lasing action has been observed on the 488 nm line of the AII system in a 5 cm diameter rf excited magneto plasma. The gain is strongly peaked at magnetic fields for which the excitation frequency is equal to the lower hybrid frequency. The radial plasma density and gain profiles are very similar and have a full width half maximum of 1 cm. Theoretical analysis suggests that the rf antenna excites an $m = 1$ helicon (whistler) wave which is highly Landau damped and can produce an excess of electrons with ~ 20 eV energy, near that required to produce a population inversion in the upper 4P state of the 488 nm transition. The phenomenon appears similar to that observed in Tokamaks employing whistler waves for current drive.

FB-2

X-ray photoswitched argon and neon discharges.

H. BRUNET and B. LACOUR, Laboratoires de Marcoussis/CRCE and V. PUECH, S. MIZZI, S. PASQUIERS, M. LEGENTIL, LPGP Université Paris-Sud, FRANCE - The electric properties of X-ray phototriggered discharges in pure argon and neon have been investigated both theoretically and experimentally. The apparatus consists of a high pressure discharge cell ($1 \times 1 \times 50$ cm³) connected to a storage capacitor charged a few μ s before the application of the preionization pulse. The discharge breakdown is induced by a X-ray preionization pulse, 5 ns FWHM. The delay times from the onset of phototriggering to gas breakdown are reported as a function of the X-ray dose, reduced electric field E/N and gas pressure. A computer model integrating the time dependant equations for the electron and heavy particles kinetics and for the driving electrical circuit has been developed. The experimental versus theoretical comparison is satisfactory. It has shown the importance of background gas impurities, especially in neon discharges.

FB-3 Determination of the Ion Temperature in a HeSe⁺-Laser Discharge from Gain Measurements at Different Axial Modes, J. MENTEL, N. REICH, F. GEKAT, AEE0, Ruhr-Universität Bochum, FRG
A cw HeSe⁺-laser pumped by the positive column of a glow discharge is tuned by a birefringent plate on different laser lines which are emitted in the TEM₀₀-mode. The distance of the different axial modes is 217 MHz or less. They are tuned across the gain profile of the laser lines by the statistical variation of the resonator length. The different axial laser modes are recorded as intermediate frequencies in the GHz-region by a fast photodiode and a spectrum analyzer. Variable losses are inserted into the resonator by a pair of Brewster plates. From the dying out of the axial modes with increasing losses, gain profiles are determined. The measured Doppler profiles of different blue and green laser lines correspond to an ion-temperature of 1500 K.

FB-4 Laser Action in the Flowing Afterglow of a Hollow Cathode Discharge, B. Wernsman and J. J. Rocca, Electrical Engineering Department, Colorado State University-Previously, we reported CW laser action by electron-ion recombination in the 1.43 μm line of CdI in the flowing afterglow of a negative glow plasma.¹ Here, we report laser action in ArI, PbI, PbII, SnII, ZnI, NeI and H₂ in the supercooled afterglow plasma of a hollow cathode discharge. The CW ArI 1.27 μm laser line and the pulsed PbI and ZnI transitions at 1.31 and 1.315 μm are excited by three-body electron-ion recombination. The addition of H₂ sharply increased the laser output of the recombination laser lines by contributing to the cooling of the plasma. Variation of the laser characteristics as a function of the discharge parameters will be discussed.

¹This work was supported by AFOSR grant 87-0290.

¹Jorge J. Rocca, Appl. Phys. Lett., 47, 1145, (1985).

FB-5 Plasma Breakdown Behavior of Hydrogen Azide (HN₃)

Gas Mixtures†. M. W. WRIGHT†, L. A. SCHLIE, and C. A. DENMAN, Advanced Laser Technology Division (WL/ARDI), Kirtland AFB, NM 87117-6008.—Recent plasma and chemical kinetic studies of hydrogen azide gas mixtures have indicated their potential use in hybrid electro-chemical, high energy laser systems. To investigate the pertinent reaction schemes present, electrical breakdown experiments have been performed on mixtures of inert gases and hydrogen azide. As in the attachment studies done previously, strong N₂(C - B) ultraviolet emission was observed in Ar/HN₃ mixtures and to a lesser extent with Kr and Xe. Various geometries of the test region, ranging from a point-to-point discharge to a point-to-plane configuration were utilized. Under conditions involving a discharge region surrounded by a gaseous volume, detonation occurred whereupon the pressure increased in direct proportion to the amount of HN₃ present. Mass spectrometric analysis indicated the decomposition of HN₃ to H₂ and N₂ which stoichiometrically agrees with the observed pressure increase. Transient spectra suggests that the detonation follows a chemically activated chain reaction rather than being electrically or photo-induced. Other possible applications of these azide gas mixtures are chemical flashlamps in which the detonation acts as a photolytic pumping source.

† Funded by the Air Force Office of Scientific Research.

‡ Dept. of Physics, UNM, Albuquerque, NM 87131.

FB-6 The Effect of Return Currents in Electron-

Beam Excited KrF Lasers* , Mark J. Kushner, University of Illinois, Urbana, IL -- Space charge injected by the beam current in an electron-beam excited laser must return to the ground plane. The "return" current is driven by electric fields generated by the injected space charge. In large aperture laser systems (> 10's cm) the return current fields can exceed many Td. As a result electron impact rate coefficients of the bulk plasma and the spatial distribution of power deposition are altered. These devices then functionally resemble e-beam sustained discharges. The effects of return currents on the performance of fusion class electron beam excited KrF lasers are theoretically investigated. For these devices as much as 10-30% of the power near the walls is redistributed by the return currents and the electron temperature increases from 1.5 eV to as much as 2.5 eV. As a result low energy threshold processes, such as F₂ burnup, are significantly effected.

*Work supported by Los Alamos National Laboratory.

FB-7 Microstreamers as a Termination Mechanism in

KrF Discharge Lasers* Mark J. Kushner, University of Illinois, Urbana, IL -- The performance of electric discharge excimer lasers is typically limited by issues related to discharge stability rather than kinetics. Recent experimental observations of the premature termination of optical pulses in XeCl and KrF lasers while power is still being deposited have suggested microstreamers as a possible cause. In this paper the termination of optical pulses in a KrF discharge laser is theoretically investigated with a multidimensional computer model. The model simultaneously simulates both the bulk plasma and microstreamers by integrating the hydrodynamic conservation and laser kinetics equations. We find that disruption of the optical homogeneity of the medium from index variations resulting from microarcs terminate the laser pulse while only a few percent of the discharge power is being dissipated in the microstreamers.

*Work supported by the National Science Foundation.

SESSION GA

10:00 AM - 11:31 AM, Wednesday, October 18

Hyatt Rickeys Hotel - Camino Ball Room C

ARCS AND GLOWS

Chair: V. A. Godyak, GTE Laboratories

GA-1 Investigation of Dielectric Barrier Discharge UV-

Lamps.* M. NEIGER, H. MUELLER, K. STOCKWALD and V. SCHORPP

LTI, U. of Karlsruhe, FRG.--Dielectric barrier discharges

in excimer gas mixtures are capable of producing narrow band uv output with efficiencies of the order 10 %.^{1,2}

The measured dependence of current, uv output and efficiency ^{on} discharge parameters can be approximately described by a simple one-dimensional model of the individual microdischarge. However, space resolved measurements of uv emission within the gap exhibit large inhomogeneities which require a fully 2-dimensional modelling approach.

*Work supported by the German Ministry of R&D (B M F T).

¹ V. Schorpp, K. Stockwald and M. Neiger, 41st GEC (1988) Minneapolis, paper GA-6.

² H. Mueller and M. Neiger, 41st GEC (1988) Minneapolis paper E-26.

GA-2 Excitation of Resonance Lines and Formation of Excimers

in Various Mercury / Rare Gas Mixtures. B. ELIASSON, B. GELLERT and U. KOGELSCHATZ, ASEA BROWN BOVERI.

Corporate Research, 5405 Baden, Switzerland - We report on measurements and theoretical predictions of the intensities of the mercury resonance lines at 185 nm and 254 nm which have been excited in a silent discharge.

The calculations are based on our theory of microdischarge formation in silent discharges and include the solution of the stationary Boltzmann equation for the breakdown fields of such current filaments. The mercury emission was investigated in Xe, Kr, Ar, Ne and He. The total gas density, the gap spacing as well as the mercury partial pressure were varied within wide limits. The most intense radiation was found in a mercury/xenon mixture in qualitative agreement with theory. We have also determined an equivalent Boltzmann temperature from up to 8 excited Hg levels. It decreases with rising Hg vapour pressure confirming the theoretical model. Furthermore we measured line profiles for mercury mixtures with Xe, Ar, and He at various mercury temperatures. The highly resolved line profiles demonstrate the effects of optical thickness as well as excimer formation, e.g. HgXe*.

GA-3 Time Resolved XUV Emission from Highly Ionized Capillary Discharges, J.F. Schmerge, J.J. Rocca and M.C. Marconi, Electrical Engineering Department, Colorado State University-We have studied the extreme ultraviolet emissions from a lithium hydride capillary plasma 500 μm in diameter and several cm in length. The capillary is excited by a short (50-100 ns FWHM) pulse and single shot spectra with a temporal resolution of approximately 5 ns are obtained. Analysis of the data shows simultaneous line emissions from highly ionized (LiIII, OVI) and singly ionized (OII) species. This is consistent with the existence of a hot core plasma ($T_e > 25$ eV) surrounded by a cooler ($T_e < 5$ eV) plasma near the walls, in agreement with a model of a capillary plasma¹ in which ablation of the capillary wall material is assumed to form a high density plasma layer surrounding a less dense and hotter core. Diffusion of ions from the core plasma into the cooler boundary might lead to an annular region of high recombination in which extreme ultraviolet amplification might occur under optimized plasma conditions².

¹This work was supported by NSF grant ECS-8606226.

²R.A. McCorkle, *Appl. Phys. A*, 26, 261, (1981).

³M.Marconi and J.Rocca, *Appl.Phys.Lett.*, 54, 2180, (1989).

GA-4 Electric Field and Emission Profile Measurements in a Hydrogen Discharge at Low Pressures, B. N. GANGULY, J. R. SHOEMAKER and A. GARSCADDEN, Aero Propulsion and Power Lab, WPAFB, Ohio -- Spatially resolved electric field (E) and emission (I) profiles have been measured in an obstructed low current dc H₂ discharge, 2.5 cm diameter electrodes, all but the front surfaces dielectric shielded and 0.65 cm interelectrodes spacing. Stark splitting of polarization dependent H α and H β lines was used to measure E. The axial E was high and approximately constant over the entire interelectrode space. The radial variation of E and I show that the discharge is almost annular. H α spectra indicate that except in the anode spot region heavy particle excitations exceed electron impact excitations and that the kinetic energy of much of the excited atomic hydrogen was greater than 250eV. For these conditions (E > 3Kv/cm) the H β Stark emission measurements yield electric fields with absolute accuracy better than 6%.

GA-5 Plasma-enhanced Photoemission from the Cathode in a Low Pressure Discharge, M. B. SCHULMAN and D. R. WOODWARD, Philips Lighting Company, Lynn, MA -- Plasma-enhanced photoemission has been reported as an in situ method for electrode surface diagnostics in rf processing plasmas.^{1,2} We have used this non-intrusive method to study the effect of the plasma sheath on the emission properties of an oxide-coated tungsten-filament cathode in a low-pressure discharge lamp. Pulsed low-power laser beams at several wavelengths were used to induce photoemission from the cathode. The photoelectron pulses were detected as optogalvanic signals. The technique is shown to provide spatially and temporally resolved information on the effective work function of the cathode, which is influenced by the accelerating electric field at the cathode surface. The conditions under which thermionic emission become significant can also be determined.

¹G.S. Selwyn, B.D. Ai and J. Singh, *Appl. Phys. Lett.* 52, 1953 (1988).

²S.W. Downey, A. Mitchell and R.A. Gottscho, *J. Appl. Phys.* 63, 5280 (1988).

GA-6 Temperature Measurements in a Non-Equilibrium Thermal Plasma, T. Owano, M. Gordon, and C.H. Kruger, Stanford University -- Emission measurements of temperature and electron density have been made in a quartz reactor downstream of a 50 kW induction plasma torch at atmospheric pressure. Absolute and relative intensities of 8 argon lines, and the argon recombination continuum, have been separately interpreted to investigate non-equilibrium effects in a thermal plasma and their influence on temperature measurements. The data indicate non-equilibrium resulting from radiation escape and diffusion of electrons to the cooled walls. The results are interpreted in terms of a model of the bound and free electrons in partial-equilibrium at the Boltzmann temperature from relative line intensities. The partial-equilibrium hypothesis is supported by both the data, including the recombination electron-density measurements, and by calorimetric and total radiation source strength measurements. In contrast, absolute line-intensity and continuum temperatures based on LTE considerations depart from the Boltzmann temperature by as much as 1,000 K and are inconsistent with energy-balance requirements. These techniques have been applied to the diagnostics of a non-equilibrium discharge induced in the reactor by means of an auxiliary electrode.

GA-7 Liquid Cooled, High Power (<5.4 KW), cw Hg UV Lamps,++ L. A. Schlie, R. D. Rathge, and E. A. Dunkle**, Advanced Laser Technology Division, Weapons Laboratory (WL/ARDI), Kirtland AFB, NM 87117-6008—The performance of high power Hg vapor discharges (24 cm x 0.5 cm i.d) excited by cw, low ripple (<10%) microwaves (2.45 GHz) and cooled with an excellent UV transmitting liquid (di-methyl polysiloxane) is discussed. Very high volumetric power loadings (> 300 w/cc) in low pressure Hg vapors (≈ 15 torr) produce stable, uniform plasmas emitting intense UV radiation ($\lambda > 2400$ A). Using this liquid coolant, reliable operation of these type of lamps for high power UV emitters is possible. In an attempt to better understand these plasmas and establish the conditions for optimum UV emission, several investigations were performed. These include electron density measurements, UV intensity versus input microwave power, along with detailed electron Boltzmann kinetics analysis including high fractional excited state densities and electron-electron interactions. In addition, kinetic modeling of the excited states density is presented plus with a discussion of resonant trapping for the Hg 2537 A radiation. A discussion of the use of these lamps for cw photolytic atomic iodine lasers at 1.315 microns will be presented. ++ Funded by the Air Force Office of Scientific Research, Bolling AFB, D.C., ** Rockwell Power Services, 2021 Girard Ave, Albuquerque, NM 87117

SESSION GB

10:00 AM - 11:07 AM, Wednesday, October 18

Hyatt Richeys Hotel - Camino Ball Room D

ELECTRON AND HEAVY PARTICLE COLLISIONS

Chair: D. C. Lorents, SRI International

GB-1 Laser Probing of Ion Mobility, Velocity Distributions and Alignment Effects in Drift Fields, S. R. LEONE, JILA, NIST and U. of Colorado, Boulder, CO 80309-0440 -- A single frequency dye laser is used to probe the velocity distributions and alignment effects of ions in a well-characterized drift field of a flowing afterglow. The velocity distributions of Ba^+ in Ar and He are analyzed in terms of "moments" to obtain: (a) the mobility, (b) the average "temperature," or broadening of the Doppler velocity distribution in directions both parallel and perpendicular to the field, and (c) the "skewness" of the distribution, a measure of the degree non-Boltzmann character. Polarization studies on molecular ions, N_2^+ and trifluorobenzene cation, reveal that the ions become aligned by collisions due to the directed velocity and the anisotropy of the interaction potential. These results are discussed in terms of current theoretical formulations, which relate individual cross sections to the steady state transport results.

*Staff Member, Quantum Physics Division, National Institute for Standards and Technology.

GB-2 Termolecular Ion-Atom Association,* M. R. FLANNERY and M. S. KEEHAN, Georgia Tech--A theory of termolecular association, $Rg^+ + Rg + Rg' \rightarrow Rg_2^+ + Rg'$ of atomic rare gas ions in various rare gases is proposed. The $Rg^+ - Rg$ association is assumed to proceed via $Rg^+ - Rg'$ collisions. Ab-initio $Rg^+ - Rg$ interactions are used. Various simplifications to the proposed theory are investigated. Results are in good agreement with measurements.

*Research supported by AFOSR-84-0233.

GB-3 Ionization Cross-section of N₂O, C.B. FREIDHOFF and P.J. CHANTRY, Westinghouse STC, Pittsburgh, PA 15235--The mass-resolved positive ions formed from N₂O have been measured from their thresholds to 500 eV. Thresholds for the ions N₂O⁺, NO⁺, O⁺, N₂⁺, and N⁺ are measured to be 12.88, 14.70, 15.20, 17.25, and 19.50 eV, respectively. The individual cross-sections are derived from the relative signal strengths by reconciling their sum with the measured total ionization cross-section. Weighting factors accounting for the effect of ion collection efficiency of the fragment ion kinetic energies are used in the summation. Above 30 eV, this procedure indicates a substantial contribution to the total from ion products not measurable in the present experiment. Previous work¹ suggests that these ions result from delayed fragmentation of metastable N₂O⁺(*).

1. J.L. Olivier, R. Loch, and J. Momigny, *Chem. Phys.* **68**, 201 (1982).

GB-4 Doubly Differential Cross Sections of Secondary Electrons Ejected from Gases by Electron Impact: 25-250 eV on O₂,* T. W. SHYN and W. E. SHARP, University of Michigan, Space Physics Research Laboratory--We have measured the doubly differential cross sections of secondary electrons ejected from molecular oxygen by electron impact. A modulated crossed-beam method was used. The incident energies used were 25, 50, 75, 100, 150, and 250 eV. The energy and angular range covered for the secondary electrons were from 1.0 eV to one half of the incident energy and from 12 to 156°, respectively. Singly differential cross sections and total ionization cross sections have been obtained from the doubly differential cross sections. The present results are compared to the previous measurements by Opal et al. (*J. Chem. Phys.* **55**, 4100, 1971) and considerable discrepancies are found.

*This work was supported partially by NSF-Aeronomy.

GB-5 Gas Phase Acidities of HPO_3 and HPO_2 , A.A. VIGGIANO, R.A. MORRIS, AND J.F. PAULSON, GEOPHYSICS LABORATORY, IONOSPHERIC PHYSICS DIVISION, M. HENCHMAN, DEPT. OF CHEMISTRY, BRANDEIS UNIV., T. MILLER AND A.E. STEVENS MILLER DEPT. OF CHEMISTRY, UNIV. OF OKLAHOMA -- Proton transfer reactions usually proceed rapidly when exothermic and usually have no barriers to reaction. Proton transfer reactions have been used extensively to determine the gas phase acidity scale. However, the acidities of strong acids have proven difficult to measure. No acidities greater than that of HI have been measured, although some ordering of higher acidities has been made. We present here data on the gas phase acidities of HPO_3 and HPO_2 , the former being a stronger acid than HI. The data were obtained by measuring the rate constants for the endothermic proton transfer reactions of PO_3^- with HI and of PO_2^- with HCl as a function of kinetic energy in a variable temperature-selected ion flow drift tube. The rate constants are found to increase with increasing kinetic energy, and quasi-activation energies are derived. The activation energies are converted to endothermicities using a procedure derived from calibration against reactions of known endothermicities.

SESSION J

1:30 PM - 3:30 PM, Wednesday, October 18

Hyatt Richeys Hotel - Camino Ball Room A and B

POSTERS

Chair: Y. K. Bae, SRI International

J-1 Measurement of the I/V Characteristics of a Symmetric RF Discharge in Argon, R. B. PIEJAK, V. A. GODYAK, GTE Laboratories Inc., Waltham, MA -- I/V characteristics have been measured in a low pressure electroded RF discharge driven symmetrically at 13.56 MHz. The voltage was measured directly across the electrodes and the current was compensated for stray and fringe capacitance. The phase difference between V and I was measured very accurately by comparing the phase coefficients from a fast Fourier transform of the voltage and the current. These measurements provide accurate data of the equivalent resistance and capacitance of the discharge as well as the phase shift and impedance characteristic. Based on these measurements, the average plasma density and the sheath thickness are calculated. The current, resistance, capacitance and phase shift are shown versus discharge voltage for various gas pressures.

J-2 A New Fast Algorithm to Calculate Oscillatory Steady-States of a rf Plasma Using the Continuum Model, E. GOGOLIDES, H.H. SAWIN, and R.A. BROWN, MIT, -- Calculation of steady-states for rf plasmas using a continuum model is a very time consuming task, if the differential equations are integrated in time. Moreover criteria for determining steady-state are poorly defined, due to long transients in the bulk of the plasma. As a result of these constraints wide application of continuum models has been limited. We present here an algorithm which improves the convergence time of the continuum model between 2 to 3 orders of magnitude. We integrate in time for only one cycle and construct an objective function which contains the difference between the variables before and after the integration. We then proceed to zero that function, i.e. directly calculate the oscillatory steady-state. The technique when combined with parameter continuation methods, enables parametric studies of rf discharges to be carried out fast and on a regular workstation. In addition transients can still be followed in time, if desired, since the time integrator is preserved in the algorithm.

J-3

Comparison of CF and CF₂ LIF and Actinometry in a CF₄ Discharge, L. D. BASTON, J.-P. NICOLAI, and H. H. SAWIN, MIT-Relative ground state CF and CF₂ concentrations have been measured in a CF₄/Ar discharge using both laser induced fluorescence (LIF) and actinometric techniques. These measurements have been used to assess the validity of actinometry for CF and CF₂ in a CF₄ discharge. LIF detection of CF and CF₂ was achieved using CF (A²Σ-X²Π) and CF₂ (A¹B₁-X¹A₁) systems respectively. Actinometric measurements were obtained by monitoring the plasma induced emission (PIE) intensity of CF* (B²Δ-X²Π) at 202.4 nm, CF₂* (A¹B₁-X¹A₁) at 251.9 nm, and Ar* at 750.4 nm. The plasma conditions of the CF₄/5% Ar discharges studied ranged from 0.5-1 Torr pressure, 0.5-1.75 W/cm² power, 1.0 cm electrode separation, and 13.56 MHz RF excitation frequency. Application of actinometry for monitoring CF and CF₂ species concentrations in situ in a plasma is useful for studying kinetic mechanisms and rates, and has been previously reported.¹ Our results indicate that CF actinometry represents the relative CF concentration as measured by LIF in a CF₄ discharge under the studied conditions. CF₂ actinometry scales linearly with the relative concentration of CF₂ as measured by LIF.

¹R. d'Agostino, *et.al.*, Plasma Chemistry and Plasma Processing, 2(3), 213 (1982).

J-4

Spatial Profile Measurements of Plasma Species in Radio-frequency Glow Discharges,* P.J. HARGIS, JR. and K.E. GREENBERG, Sandia National Laboratories -- Spatial distributions of plasma species in a discharge were measured by imaging laser-induced fluorescence (LIF) radiation onto a gated multichannel diode-array detector. Spatial profiles, across the gap between the parallel-plate electrodes, were measured by exciting LIF with a vertical sheet of laser light. The LIF was imaged onto the entrance slit of a spectrometer and detected by the multichannel detector which replaced the exit slit. LIF from a static gas fill (~3 mTorr) of naphthalene (without a discharge) was used to correct the measured spatial profiles for nonuniformities in the laser beam and optical detection system. The spatial resolution of the system was measured by imaging the light emitted from a 100-μm diameter optical fiber placed in the center of the discharge chamber. 1024 point profiles with a spatial resolution of 0.3 mm were typically recorded in 10 to 100 s, depending on signal intensity. Examples of this technique, including measurements of the spatial distributions of CF₂ in CF₄, CF₄/O₂, CF₄/H₂, and CF₄/Ar discharges, will be presented.

*This work performed at Sandia National Laboratories supported by the U.S. Department of Energy under contract no. DE-AC04-76DP00789.

J-5

RF Frequency Dependence of Plasma
Parameter Axial Profiles in a Helium RF Plasma,

K.Terai and T.Kaneda, Tokyo Denki Univ. Tokyo, Japan,
J.S.Chang, McMaster Univ. Hamilton, Canada.--The
effect of RF frequency on the plasma parameter axial
profiles in a parallel plate capacitive coupling RF
helium plasma was experimentally investigated. The
electron temperature T_e and plasma density N were
determined by axially movable electrostatic double
probes. The results are obtained for the gas pressure
from 0.4 to 10 torr, the RF power from 5 to 30 watt and
the RF operating frequency from 300 kHz to 13.56 MHz.
The results show that: (1) the T_e profiles are inversely
proportional to the N profiles; (2) the T_e and N profiles
in lower RF frequencies were observed to be always a
symmetric compared with 13.56 MHz; (3) the T_e and N
profiles become nonmonotonic when gas pressures
exceed 2 torr for 13.56 MHz RF discharges; (4)
nonmonotonic T_e and N profiles were observed for 300
kHz RF discharges; (5) the T_e in a central region of RF
discharge has a nonmonotonic pressure and RF power
dependencies for all RF frequencies.

J-6

Particle Kinetics in Plasmas--ALAN
GARSCADDEN, Wright Research & Development
Center, OH, 45433--Particle contamination in
etching and deposition plasmas is a serious
problem accounting for many wafer rejections.
Estimates are made of the various effects due
to these particles in low pressure processing
plasmas. Macroscopic particles (0.1-10
microns diameter) act like very low mobility
negative ions in their transport properties
and also as surface recombination sinks of
charged species and of radicals. The particles
are at floating potential and are
electrostatically trapped in balance with
gravitational and thermophoretic forces. Many
of the gases form negative ions, with large
electron affinities and these have very long
residence times and can contribute to cluster
formation. External sources of particles, such
as aerosols and sputtering, also will be
causes of contamination. Vertical electrodes
that are immediately immediately reduced to
zero- or negative bias on switch-off are
recommended to reduce substrate contamination.

J-7 RF Discharges at Very Low Neutral Pressures,
N. HERSHKOWITZ, M-H CHO, A. WENDT, University of Wisconsin-Madison--We show that by taking advantage of surface multi-dipole fields, rf glow discharges can be maintained down to pressures at least as low as 5×10^{-5} torr. To our knowledge, this is well below the lowest previously reported rf glow discharge minimum operating pressure. Large effective electrode separation and good plasma uniformity can be achieved by making use of surface multi-dipole magnetic fields. Discharges employ only one conventional electrode. The line cusps replace the other electrode. Two different types of rf powered electrodes were explored -- conventional plates (diam. = 15 cm) and rods (diam = 0.64 and 1.3 cm). The powered electrodes were located sufficiently far from the magnets that the magnetic field could be ignored. Our experiments employed a second plate electrode. This plate was grounded and differs from the powered electrode in that it was located within the surface magnetic field. Adjustment of the separation of this plate from the magnet plane permits continuous variation of the maximum surface magnetic field (B_s) seen by plasma allowing continuous variation of the effective loss area at the electrode.
Work supported by the NSF ECS-8704529.

J-8 A Kinetic Discharge Model Applied to the RF Reference Cell* T. J. SOMMERER, W. N. G. HITCHON, and J. E. LAWLER U. of Wisconsin.—A kinetic description of discharges based on propagators (Green's functions) has previously been used to describe the electrons in the cathode fall of a helium dc glow discharge¹ and both the electrons and ions in a helium rf discharge.² We will present the predictions of this model for one pressure of the initial calibration conditions of the "RF Reference Cell"³: 0.1 torr argon, 200, 400, 600, and 800 V peak-to-peak applied voltage at 13.56 MHz, and a 2.54 cm gap. We will predict the I/V characteristics, as required for calibration of the Reference Cell, along with particle densities and other moments of the distribution function, and will investigate the nature of the heating of the discharge electrons.

*Supported by the AFOSR.

¹T. J. Sommerer, W. N. G. Hitchon, and J. E. Lawler. Phys. Rev. A **39** 6356 (1989).

²W. N. G. Hitchon, T. J. Sommerer, and J. E. Lawler. Proceedings of the Seventh IEEE Pulsed Power Conference, Monterey, CA, June 11-14, 1989 (in press).

³Proposed at the Forty-First Annual Gaseous Electronics Conference, Minneapolis, MN, October 18-21, 1988.

J-9 Cylindrical Magnetron Reactive Sputtering for Hermetic Coatings on Fluoride Glass Fibers,* Z. YU, P. A. SMITH and G. J. COLLINS, Colorado State University, D. W. REICHER and J. R. McNEIL, University of New Mexico, B. HARBISON and I. AGGARWAL, Naval Research Laboratory -Low temperature (<250°C), high speed coating is required for hermetic protection of fluoride glass fibers, which have broad transmittance range (0.3-7 μ m) and low optical loss (<0.01dB/Km). A cylindrical magnetron operated in the reactive sputtering mode has deposited AlN and MgO coatings on fluoride glass fibers. The fiber is located along the longitudinal axis within the reactive plasma, formed near the cylindrical cathode. A Mg cathode in a He-Ar-O₂ discharge is used for MgO deposition. While an Al cathode in a N₂ discharge is used for AlN coatings. Deposition rates of 1000Å/min and 500Å/min have been observed for MgO and AlN, respectively. Uniform thickness and full coverage of the film on the fiber is seen from electron microscope pictures. MgO and AlN films have been proven hermetic by measuring the growth of O-H band absorbance in the coating with water exposure.

*Work supported by the Naval Research Laboratory
Contract #N00014-87-C-2044.

J-10 The Feasibility of Using Neural Networks and Other Optimization Algorithms to Obtain Cross Sections from Swarm Data, W. L. MORGAN, Kinema Research, Monument, CO 80132--I will discuss preliminary findings on the use of neural network algorithms to obtain electron impact cross sections from measured drift velocities, characteristic energies, and other swarm data. I will discuss, in addition, results that I have obtained on model systems and on real atoms and molecules using creeping simplex and simulated annealing optimization algorithms.

*Research supported by the Wright Research and Development Center, Wright-Patterson AFB, Ohio.

J-11 Space and Time Variation of Stochastic Heating in a Capacitive RF Discharge. B.P. WOOD, M.A. LIEBERMAN AND A.J. LICHTENBERG, University of California, Berkeley — Low pressure (< 100 mTorr) capacitive rf discharges are widely used in the electronics industry. It has been shown^{1,2} that stochastic heating by the oscillating sheaths is the main electron energy deposition mechanism. We give an analytical model of the sheath motion which is then related to the space and time variation of the electron energy distribution and to the ionization rate in the discharge. Since the sheath motion and therefore the energy deposition is strongly nonuniform in space and time, ionization waves are found to emanate from the sheath and to propagate into the bulk plasma. We compare these results to particle-in-cell computer simulations and to experimental data.

1. M.A. Lieberman, *IEEE Trans. Plasma Sci.* 16, 638 (1988); 17, 338 (1989).
2. G.R. Misium, A.J. Lichtenberg, and M.A. Lieberman, *J. Vac. Sci. Technol. A* 7, 1007 (1989).

J-12 Measurement of Target Ion Current in Plasma Source Ion Implantation. M. SHAMIM, J. T. SCHEUER AND J. R. CONRAD, Plasma Source Ion Implantation Group, University of Wisconsin -- Average current per pulse to the target during Plasma Source Ion Implantation (PSII)¹ has been measured. Measurements were made for graphite, Cu, Al, and 304 Stainless Steel targets in spherical, cylindrical and planar shapes in H₂, He, N₂ and Ar plasmas. The target bias was varied from 15 to 40 kV and the density was varied from 10⁸ to 10¹⁰ cm⁻³. These parameters were chosen to investigate the effects of secondary electron emission at the target, ion mass, geometry and plasma density on the PSII process. The measured current has been found to be higher than that predicted theoretically.²

- ¹ J. R. Conrad, J. L. Radkte, R. A. Dodd and F. J. Worzala, *J. Appl. Phys.* 62, 4591 (1987).
- ² J. T. Scheuer, M. Shamim and J. R. Conrad, *Gaseous Electronics Conference*, Palo Alto, October 17-20, 1989.

J-13 Temperature of a High Pressure Mercury Discharge, J.T. DAKIN and R.P. GILLIARD*, GE Lighting, Cleveland, OH -- A variety of experimental techniques are used to determine the temperature in a high pressure mercury discharge. The arc tube has a bore of 2.35 cm, a gap of 9.0 cm, and operates at a power of 1000 W with an estimated pressure of 4.6 atm. The apparatus and some experimental results have been described previously. [1] Here the emphasis is on sources of error, and comparison of temperatures determined with different techniques. A Boltzmann plot showing the relative densities of the mercury atomic states is presented, and the degree of Local Thermodynamic Equilibrium is addressed. Implications for experimental studies involving measurement of temperature in mercury-dominated discharges are discussed.

1) J.T. Dakin and R.P. Gilliard, J. Appl. Phys., 60, p. 1281 (1986).

* current address ILC Technology, 399 Java Dr., Sunnyvale, CA

J-14 Temperature and Na-density distributions in an ac Hg-NaI discharge plasma*, A. PALLADAS⁺, D. KARABOURNIOTIS and A. TSAKONAS, Physics Dep't., Univ. of Crete, Iraklion, Crete, Greece.

- Time and space resolved emission measurements of the optically thin Hg 577- and Na 616-nm lines were conducted with a computer-automated system, in horizontal planes, of a high-pressure mercury arc discharge, containing sodium iodide as an additive. The purpose of these measurements was the determination of the time modulated plasma temperature as well as the density of sodium neutral atoms in the discharge, assuming LTE conditions. The temperature radial profiles and the arc pressure, were obtained from this experimental data, using the Hg 577-nm line. The Na-density radial profiles were then obtained, using the Na-616 nm line.

*Work supported by the Greek Ministry for Research and Technology.

+also with Centre de Physique Atomique, Univ. P. Sabatier, Toulouse, France.

J-15 Production of S₂F₁₀ from Negative Glow Corona in SF₆,^{*}
R.J. VAN BRUNT, J.K. OLTHOFF, and J.T. HERRON, NIST, I. SAUERS,
ORNL -- Disulfur decafluoride (S₂F₁₀) is formed in high-pressure electrical
discharges by reaction between SF₅ radicals produced by dissociation of SF₆.
The production rates for S₂F₁₀ in SF₆ during continuous glow-type negative
point-plane discharges have been measured as a function of discharge current
using a gas chromatograph-mass spectrometer. The yield curves for S₂F₁₀
production are found to be linear, thus suggesting that the production
mechanism is much faster than any destruction mechanisms. The magnitudes
of the measured S₂F₁₀ production rates are found to agree satisfactorily with
predictions based on a zonal model of the discharge chemistry which takes
into account the influences of O₂ and water vapor contamination. The model
predicts that S₂F₁₀ production will increase with increasing water vapor
content and is relatively unaffected by changes in O₂ content, provided
([O₂]/[SF₆]) < 2%.

*Supported by U.S. Department of Energy.

J-16 A Kinetic Model of a DC Discharge, D.J. Koch and
W.N.G. Hitchon, U. of Wisconsin-Madison, --- A self-
consistent model of a DC discharge is presented. This
model utilizes a Green's function solution¹ to a kinetic
equation which calculates the motion of all charged
particles in the discharge. The model yields ion and
electron densities that are consistent with the potential,
ionization and excitation rates. Results are given for
an argon DC discharge. A plasma chemistry submodel for
a DC silane discharge is also presented. This chemistry
submodel uses dissociation and ionization rates calculated
by the charged particle submodel to find densities and
and reaction rates of various gas phase neutral species.

¹W.N.G. Hitchon, D.J. Koch and J.B. Adams, *J. Comp. Phys.*,
(1989) in press.

J-17 Deterministic Chaos in Electrical Discharges in Gases, D. HUDSON, NSWC -- This work expands on the results of Braun et. al.¹ concerning observation of chaotic currents in DC discharges. The work of reference 1 is extended to more complex gases and gas mixtures. Improvements in the apparatus allow determination of gas pressure and electrical and optical diagnostics. It is observed that while some gases such as He follow a well defined path from smooth discharge via sinusoidal current perturbations, period doubling etc. to chaos, others such as CO₂ transition directly from smooth discharge to chaotic perturbations. Results of observations on various gases as well as any illuminating insights into their behavior will be presented.

¹T. Braun, J.A. Lisboa, R.E. Francke and J.A.C. Gallas, Phys. Rev. Lett. 59, 613 (1987)

J-18 Spectroscopic Diagnostic of a He-Cd⁺ Laser Discharge, Th.Wengorz and J.Mentel, AEEO, Ruhr-Universität Bochum, FRG -- The intensity of He-lines emitted from a positive column He-Cd⁺ laser discharge is measured end on by an afocal imaging optics in absolute units. Using Kirchhoff's law population density ratios are determined from the intensity of optical thick lines. The corresponding temperatures are approximately equal to electron temperature. For further investigations the He-Cd⁺ laser is operated by the discharge on the 441.6 nm laser line in TEM₀₀-mode. The different axial modes tuned across the gain profile by statistical variation of the resonator length are recorded as intermediate frequencies by a fast photodiode and a spectrum analyzer. The vanishing of the different axial modes with increasing losses inside the resonator is measured. Taking into account the isotope shifts and hyperfine splittings of Cd π 441.6 nm laser line emitted by cadmium of natural isotopic abundance gain profile and ion temperature are determined. On the basis of the temperature measurements and the radial profiles of line emission coefficients comments are made upon the radial diffusion of Cd-atoms and Cd-ions in the discharge.

J-19 Streamer to Arc Transition in N₂, S.K. DHALI and A. RATA BOOSHANAM, Southern Illinois University -- The numerical results of a streamer-to-arc transition model is presented for nitrogen at atmospheric pressure. The streamer phase of the calculation is performed by solving the electron and ion continuity equations along with the Poisson's equation¹. The plasma density ($\sim 10^{14}\text{cm}^{-3}$), the radial dimension (1/e radius of $\sim 0.4\text{mm}$), and the reduced electric field (E/N of 233 Td) are then used as initial condition for a transient glow model². The glow model, which includes gas heating, neutral gas dynamics, and electron-molecule and molecule-molecule collisions is solved in the radial dimension. Discussions on the plasma density, arc radius, and gas temperature and pressure are presented.

¹S.K. Dhali and P.F. Williams, J. Appl. Phys. 62, 4696 (1987).

²S.K. Dhali and L.H. Low, J. Appl. Phys. 64, 2917 (1988).

J-20 Electron Impact Vibrational Excitation of Polar Molecules,* S. ALSTON,[†] G. SNITCHLER, and D.W. NORCROSS,[‡] JILA, Univ. of Colo. and NIST -- The electron impact excitation of HF and HCL has been studied using a fully vibrational close-coupling (VCC) program. An exact treatment of exchange is used in the separable representation. Correlation and polarization are represented by a parameter-free model potential. Differential cross sections will be compared to recent experiments.

¹G. Knoth, M. Gote, M. Rädle, K. Jung, and H. Ehrhardt, Phys. Rev. Lett. 62, 1735 (1989); and unpublished data.

*Research supported by National Science Foundation grant PHY86-04504.

[†]Present Address: Dept. of Physics, Penn. State Univ., Lehmann, PA 18627

[‡]Staff Member, Quantum Physics Division, National Institute for Standards and Technology.

J-21 Emission of the Fluorine Resonance Lines Following Dissociative Electron Impact Excitation of CCl₂F₂, NF₃, CF₄ and SF₆*, M. ROQUE, R. SIEGEL, K.E. MARTUS and K. BECKER, City College of New York -- We report measurements of absolute emission cross sections and appearance potentials for the fluorine (2p⁴3s) 2,4P → (2p⁵) 2P⁰ resonance lines at 955 Å and 975 Å produced by dissociative electron impact excitation of SF₆, CF₄, NF₃ and CCl₂F₂. The cross sections are heavily influenced by 3p → 3s cascading¹⁻³. A detailed analysis of the low energy region of the cross sections revealed that different dissociation mechanisms lead to the formation of the excited fluorine atoms in the case of CCl₂F₂ compared to SF₆, CF₄ and NF₃. Partial fragmentation channels appear to play a very important role in the case of the CCl₂F₂ dissociation.

1. K.A. Blanks et al. J. Chem. Phys. **86**, 4871 (1987)
2. J.L. Forand et al., Can. J. Phys. **64**, 269 (1986)
3. S. Wang et al., Can. J. Phys. (1989), in press

*Supported by NSF through Grant No. CBT-8896249

J-22 Total Electron-impact Cross Sections for Ammonia, * Ce Ma, Phillip B. Liescheski and Russell A. Bonham, Chemistry, Indiana U. Total electron impact cross sections for Ammonia were measured from 4 to 50 eV by time-of-flight experiments. The primary electron pulses (< 1ns) generated wide energy range secondary electrons by hitting a graphite coated needle at the scattering center. Both primary and secondary electrons traveled 41 cm in the gas chamber before reaching an MCP chevron detector. The electronic signals from the detector and a LeCroy 4222 PDG start and stop a LeCroy 4208 TDC. A home made fast bus, that can host up to three 4208 TDCs, provided a memory storage of 4096 × 16 bits words for each TDC channel as well as 9.2 μsec fast data transmission for all 24 channels. The gas pressure was measured by an MKS SRG. The electron transmission spectra were measured in several different gas pressures and the total cross sections were determined by using the Beer's law.

* Work supported by the NSF through grant number CHE-8600746.

J-23 Measurement of Coherence Parameters in Electron - Heavy Noble Gas Collisions*, K.E. MARTUS and K. BECKER, City College of New York -- We report measurements of the P_1 and P_2 coherence parameters for excitation of the spin-orbit coupled " 1P_1 " and " 3P_1 " states of Ne, Ar and Kr by electron impact. Having demonstrated that the forward excitation in the regime of intermediate impact energies proceeds via direct excitation of the LS-coupled singlet component of the excited states¹, i.e. $P_1=+1$, the main emphasis of our current work are measurements of P_1 for very low impact energies where deviations from unity are expected caused by the LS-coupled triplet component of the excited states which makes its presence felt at energies close to threshold². We will also present P_1 and P_2 data for small angle scattering.

1. K.E. Martus and K. Becker, J. Phys. B, 22 (1989), in press
2. K. Bartschat and D.H. Madison, J. Phys. B 20, 5839 (1987)

*Supported by NSF through Grant No. PHY-8819510

J-24 Electron-Impact Dissociation of Cl_2 Molecules* P. C. COSBY, SRI International--Dissociation of chlorine molecules by electron impact is observed in a crossed beam apparatus in which the correlated neutral fragments are detected by a position and time sensitive detector. The fast beam of Cl_2 is produced by charge transfer neutralization of Cl_2^+ in chlorine gas and the state composition of the beam is probed by photofragment spectroscopy. The absolute cross section for the production of $Cl + Cl$ is found to rise from threshold (< 8 eV) to a maximum of $2.1 \pm 0.6 \text{ \AA}^2$ near 15 eV and decrease at higher electron energies. The translational energies of the fragments suggest that excitation to the repulsive $1^1\Pi_u$ state is the primary dissociation mechanism. Evidence is also found for predissociation to $Cl(^2P)+Cl(^2P)$ of Rydberg states converging to the ground state of Cl_2^+ .

*Supported by USAF Aero Propulsion Lab, Wright-Patterson AFB.

J-25 Extreme Ultraviolet Emission from the $b^1\Pi_u$ state of N_2 Excited by Electron Impact,* G. K. JAMES, J. M. AJELLO and D. E. SHEMAN-SKY, J.P.L. and U. of Arizona — The electron impact induced fluorescence spectrum of N_2 in the wavelength range 102 to 134 nm has been measured at a resolution of 0.05 nm. Emission cross sections have been determined for the vibronic transitions of the $b^1\Pi_u \rightarrow X^1\Sigma_g^+$ Birge - Hopfield I band system at 20 eV and 100 eV electron impact energy. A comparison of excitation and emission cross sections shows that, with the exception of the $v' = 1$ level, all other vibrational levels of the $b^1\Pi_u$ state predissociate with a predissociation to radiation branching ratio of between 0.98 and 1.00. Predissociation of the $b^1\Pi_u$ state alone contributes approximately 14% to the total dissociation cross section of N_2 at 100 eV. The excitation function of the $b(1,2)$ transition at 103.28 nm has been measured from threshold to 400 eV. Application of a modified Born approximation analytic model to the $b^1\Pi_u$ excitation function data yields a band system oscillator strength of 0.365.

*This work supported by the Air Force Office of Scientific Research and the National Science Foundation (grant # ATM 8715709), and NASA.

J-26 Electron-Impact Ionization Rate Coefficients at Very High Density-Normalized Electric Fields for Several Alkanes and Fluoroalkanes,* G. N. HAYS and J. B. GERARDO, Sandia National Laboratories; M. Ibrahim, Atlanta University--We report electron-impact ionization rate coefficients at very high values of density-normalized electric field (E/N up to 10^5 Td, $1Td=10^{-17}Vcm^2$) for several alkanes, and fluoroalkanes. The electrical properties of the former series of molecules is of interest for thin-film diamond-like deposition, for example, while those of the latter series of molecules is of interest because of their widespread use in the manufacture of microelectronic circuits as well as their use as high-voltage gaseous insulators. The measurements were made in an electrodeless cell contained in an S-band waveguide immersed in a dc magnetic field and subjected to a pulsed rf electric field at cyclotron resonance. We have previously shown that our measurements are equivalent to experiments in dc electric fields. This experimental approach circumvents complications due to electrode effects at extremely high values of E/N .

*Supported by USDOE under contract DE-AC04-76DP00789.

J-27 Electron Impact Ionization of Argon and Krypton,*
R. E. H. CLARK and G. CSANAK, Los Alamos National
Laboratory - The extensive Coulomb-Born ionization cross
sections of Sampson and coworkers¹ have been fitted as a
function of n and ℓ . The resulting fit is applied to
ionization of the $3p^6$, $3p^54s$ and $3p^54p$ configurations of
argon and the $4p^6$, $4p^55s$ and $4p^55p$ configurations of
krypton. Comparisons are made with the binary encounter
theory² and distorted wave approximation (DWA) of Mann.³
A simple prescription for obtaining the differential
cross section with respect to ejected electron energy is
compared with the calculated DWA differential cross
sections. For all integral cross sections, the inner-
shell excitation autoionization contribution is included
and is shown to be a significant part of the total
ionization cross section.

*This work was performed under the auspices of the U.S.
Department of Energy.

¹R.E.H. Clark and D.H. Sampson, J. Phys. B, 17 (1984)
and references therein.

²H.A. Hyman, Phys. Rev. A, 20, 855 (1979).

³J.B. Mann (Private Communication).

J-28 Electron Impact Infrared Excitation Functions in
Xenon, C. A. DeJoseph, Jr., Wright-Patterson A.F.B., OH
45433 and J. D. Clark, Wright State University, Dayton, OH
45430 - Electron impact excitation functions over an electron
energy range of 10-150eV have been measured on a number
of transitions in Xenon over the spectral range of approxi-
mately 0.9-4 μ m. These include the 1.73, 2.03, 2.48, 2.65,
3.11, 3.27 and 3.51 μ m lasing transitions observed in the He-
Xe and the Ar-Xe lasers. Measurements were made using a
low energy electron gun designed and built in-house together
with a commercially built Fourier Transform Spectrophoto-
meter.

J-29 Electron-Excitation Cross Sections of the 4p⁵5p States of Krypton and their Pressure Dependence.* JOHN E. GASTINEAU, MICHAEL P. NESNIDAL, and TODD G. RUSKELL, Lawrence University—The energy dependence (10-100eV) of the optical emission cross sections of the ten Paschen 2p levels of krypton have been measured using the optical method. The cross sections show some pressure dependence in the range of 100 μ T to 5 mT, but to a smaller degree compared to Paschen 2p emission cross sections of xenon¹. The pressure dependence is strongest at energies above 35 eV, and cross sections below 25 eV are essentially independent of pressure effects. The higher energy cross sections for the 2p₂, 2p₃, 2p₇, and 2p₉ levels reach low pressure limits by 200 μ T and the absolute apparent cross sections have thus been determined. Estimates for the other 2p apparent cross sections are obtained by extrapolation. The apparent cross sections range from 1 to 7·10⁻¹⁸ cm².

*Supported by a William and Flora Hewlett Foundation Grant of Research Corporation and by Lawrence University.

¹Gastineau *et al*, 39th Gaseous Electronics Conference p.90.

J-30 New Coherence Data on the Excitation of Heavy Rare Gases by Electron Impact.* P.J.M. VAN DER BURGT, J.J. CORR and J.W. McCONKEY, University of Windsor, Canada. -- We report continuing measurements of the Stokes parameters for excitation of the resonance lines of the heavy rare gases following electron impact. These will extend previous measurements reported from this laboratory^{1,2} and are particularly aimed at elucidating spin-related effects such as exchange or spin-orbit interaction. Particular attention will be paid to the in-plane polarization correlation parameter from which the so-called height of the excited state charge cloud is deduced.

* Research supported by the Natural Sciences and Engineering Research Council of Canada.

1. M.A. Khakoo and J.W. McConkey, *J. Phys. B* **20**, 5541 (1987).
2. P. Plessis, M.A. Khakoo, P. Hammond and J.W. McConkey, *J. Phys. B* **21**, L483 (1988).

J-31 VUV Fluorescence Following Electron Impact on Discharge-Created Targets. * SHOUYE WANG and J.W. McCONKEY, University of Windsor, Canada. -- An RF discharge source is used to produce a gas beam with a significant metastable content and, in the case of molecular parent species, a significant dissociation fraction. This is crossed with a magnetically-focussed electron beam which produces high currents in the near threshold region. The resultant radiation is observed orthogonal to both beams using a Seya-Namioka monochromator - channel electron multiplier combination. Data obtained as a function of incident electron energy will be presented at the Conference for N₂ and other targets.

* Research supported by the Natural Sciences and Engineering Research Council of Canada.

J-32 Practical Applications of Electrostatic Probes, N. BENJAMIN and B. CHAPMAN, Lucas Labs --The Electrostatic Probe was introduced by Irving Langmuir in order to research the ionized gaseous state of matter he called "plasma" in the 1920s. Since then, probes have been primarily restricted to research applications right up to the present day. This paper describes some of the more pragmatic features of Electrostatic Probe use, principally directed towards applications in Plasma processing for thin film and semiconductor production. We shall indicate how various practical problems of application to process may be resolved. Examples will be given of the use of a Probe for process characterization and the determination of process reproducibility, as well as it's use for determining spatial profiles in the reactor. Finally we shall discuss the potential of probes in future applications for manufacturing process control.

SESSION KA

8:00 AM - 9:39 AM, Thursday, October 19

Hyatt Riskey Hotel - Camino Ball Room C

Ar/Xe LASERS I

Chair: A. Garscadden, Wright Research and Development Center

KA-1 Early Work in High-Power Xe:Ar Laser

Research^{*}, L.A. Newman^{**} and T.A. DeTemple, U. of Illinois--The 1.73 micron line of xenon in an argon buffer has emerged as one of the most efficient and powerful electrically excited atomic laser lines. The research leading up to the discovery of these features, the post discovery experiments, and the initial identification of the underlying physical processes responsible for the strong emission will be reviewed.

^{*}Research originally supported by the National Science Foundation and the United States Air Force WPAFB.

^{**}United Technology Optical Systems

¹ L.A. Newman and T.A. DeTemple, Appl. Phys. Lett. 27, 678 (1975).

KA-2 Experimental Study of the e-Beam and e-Beam Sustained Xe:Ar Laser.

A. Suda^{*}, B.L. Wexler, B.J. Feldman, and K. Riley^{*}, NRL.--Experimental studies of the electron-beam and electron-beam sustained Xe:Ar laser have been carried out to evaluate performance and provide data for kinetics analysis. Small signal gain and saturation intensity have been measured and compared with calculated values. The pulse shapes and energy in the 1.73, 2.03, 2.63, and 2.65 μm lines have been observed with nonselective and single-line cavities. Data have been taken as a function of pump rate, pressure, and xenon concentration. Various electron and heavy particle collision processes can be suggested to explain the data. The e-beam pumped laser produced 1.7 J/l at 4 atm with 2.3% efficiency. With the e-beam sustained discharge, 3.5 J/l was obtained with 3.2% efficiency and an enhancement factor of 4.5. When the e-beam pump power was reduced, the enhancement increased to 10 but the laser output dropped significantly. With the addition of helium to the Xe:Ar mixture, the 2.03 μm output increases dramatically and becomes dominant. The effects of adding krypton and neon were also observed.

^{*} Geo-Centers, Inc.

KA-3

Fission-Fragment Pumped Atomic Xenon Laser,*
G. N. HAYS, W. J. ALFORD, D. R. NEAL, D. A. McARTHUR,
and D. E. BODETTE, Sandia National Laboratories--We
report on laser characteristics of atomic xenon
(1.7-3.5 μm), in a rare-gas buffer, pumped by fission
fragments from U^{235} , under bombardment by thermal
neutrons. Energy efficiency up to 3% has been reported
for low-pump-rate ($< 10 \text{ W/cc}$), long pulse (several
msec) excitation of xenon utilizing this pumping
mechanism¹. We will present results of the effects of
buffer gas composition and pump rate on the performance
of several laser lines of interest. We find that
dilution of an Ar/Xe gas mixture with helium has
dramatic effects on the output spectrum, whereas
dilution with neon has little or no effect.

*This work performed at Sandia National Laboratories,
supported by the U. S. Department of Energy under
Contract Number DE-AC04-76DP00789.

¹W. J. Alford and G. N. Hays, J. Appl. Phys. 65, 3760
(1989).

KA-4

A Parametric Study of The Atomic Xenon Laser,*
E. L. PATTERSON, G. E. SAMLIN, and P. J. BRANNON, Sandia
National Laboratories -- Operation of the atomic Xe laser at average
e-beam pump rates between 0.04 and 1.0 kW/cm^3 with buffer gases
of Ar, Ar/He, or Ne is described. The pump time for these
experiments is 1 ms, providing an average energy loading of up to
1 J/cm^3 . The 2.6 μm transitions dominate in all cases where the
laser cavity feedback is not wavelength selective (for these
measurements we could not discriminate between the 2.63 and
2.65 μm lines). In all cases the laser pulsewidth (full width at 10%
peak power) decreased with increasing pump power. With optics
selected to favor the 1.73 μm line and the use of 0.5% Xe, laser
termination occurred with an average energy loading of 0.16 J/cm^3
for Ar buffer gas and occurred with an energy loading of
 $\sim 0.25 \text{ J/cm}^3$ for Ne buffer gas. Higher resolution measurements
have shown that, with either Ar/Xe or Ar/He/Xe mixtures and
pump rates up to 900 W/cm^3 , the 2.65 μm line dominates over the
2.63 μm line. The ratio of intensity of the 2.65 to 2.63 μm line
increases with increasing Xe concentration or decreasing pump rate.

*This work supported by the U.S. Department of Energy under
contract number DE-AC04-76DP00789.

KA-5 Performance Characteristics of the X-ray Pre-ionized Xe:Ar Laser, J.E. Tucker, B.L. Wexler, B.J. Feldman, and T. McClelland, NRL -- X-ray preionization has allowed discharge pumping of the Xe:Ar laser at 4 atm pressure¹. Increased output and pulse length have been observed with a new laser head, with 0.4 J obtained from a 40 cm long x 5 cm high discharge having a nominal 2 cm width, in a 1% Xe, 3 atm Ar mixture. This compact device also definitively demonstrates the suppression of surface flashover by electric field uniformity and shaping in the laser head. The impedance mismatch between the Marx bank and the discharge results in a ringing discharge and a modulated output. The total laser pulse length observed is inversely proportional to pressure and xenon concentration, and continues for more than 5 μ s for a 0.1% Xe in 1 atm Ar mixture. With a nonselective cavity, 70% of the output occurs at 1.73 μ m and 20% at 2.63 μ m. The remainder occurs in the 2.03 and 2.65 μ m lines. Line competition effects have also been observed. When helium is added, the 2.03 μ m line becomes dominant as the other lines are suppressed.

¹J.E. Tucker, B.L. Wexler, B.J. Feldman, and T. McClelland, to be published in IEEE Phot. Tech. Lett., Aug., 1989

SESSION KB

8:00 AM - 9:43 AM, Thursday, October 19

Hyatt Richeys Hotel - Camino Ball Room D

BREAKDOWN AND SWITCHING

Chair: L. E. Kline, Westinghouse Research and Development

KB-1 Formation of Cathode Spots by Unipolar Arcing.

F. SCHWIRZKE, Naval Postgrad. Sch. - Breakdown and plasma formation on electrodes is a fundamental process in pulsed power technology. The initial "explosive" plasma formation on the surface of a cathode of a vacuum diode and many other discharges is highly non-uniform. Micron-sized cathode spots form within ns. Laser produced unipolar arcs¹, UPA, ignite and burn on a ns time scale. Similar UPA craters have now been observed on the cathode surface of a pulsed vacuum diode. Field emitted electrons ionize desorbed neutrals above an emitting spot. Plasma pressure gradients then naturally lead to electric fields which ignite and drive the UPA². Power dissipation for an UPA is considerably larger than for field emitted or space charge limited current flow. The high current density of an UPA provides explosive plasma formation. Unipolar arcing represents a fundamental form of discharge which contributes to breakdown and formation of cathode spots in a unique way. This report was sponsored by NRL and the Naval Postgraduate School.

¹F. Schwirzke, Laser Induced Unipolar Arcing, in Laser Interaction and Related Plasma Phenomena, Vol 6, H. Hora and G. H. Miley, eds., Plenum Publ. Corp., New York, 1984

²F. Schwirzke, J. Nucl. Mater., 128 & 129 (1984) 609.

KB-2 Transport and Multiplication of Charged Particles

in H₂ at Very High E/n,* Z.Lj. PETROVIĆ** and A.V.

PHELPS, JILA, University of Colorado and NIST. --

Current waveforms were taken for pulsed-laser initiated, non-selfsustained discharges in hydrogen at E/n from 0.5 to 45 kTd. The change from H₃⁺ to H₂⁺ for E/n of 0.5 kTd to 3 kTd causes a very slow change with E/n in the duration of a single avalanche. Integrated currents yield¹ the charge that crosses the gap in electron (Q_e) and ion (Q_i) transit times and in vacuum (Q_c). Q_e/Q_c and Q_i/Q_c ratios are fitted to equilibrium models for E/N ≤ 1 kTd and non-equilibrium models for E/n ≥ 3 kTd. Apparent secondary electron coefficients are higher than published values.² The ionization cross section of the non-equilibrium model is reduced to fit Q_e/Q_c ratios. Fits to Q_i/Q_c data at the higher E/n yield secondary electron coefficients which depend on E/n only as expected when secondaries are due to H₂⁺ and fast H₂.

*Work supported in part by NSF.

**Permanent address: Institute of Physics, Belgrade.

¹V.T. Gylys, B.M. Jelenković and A.V. Phelps, J. Appl. Phys. 65, 3369 (1989).

²M.A. Folkard and S.C. Haydon, Aust. J. Phys. 24, 527 (1971).

KB-3

Application of a Multi-Dimensional Beam-Bulk Model to Simulation of Low Pressure Pulse Powered Devices. * HOYOUNG PAK and MARK J. KUSHNER, University of Illinois, Urbana, IL--A computer model has been developed to simulate low pressure pulse power devices such as conventional thyratrons, pseudo-sparks and electron beam sources. The simulation is a 2-1/2 dimensional time-dependent continuum model using rectilinear or cylindrical coordinates. Gas pressure, gas composition, applied voltage, and geometry are user definable. To account for nonequilibrium electron transport, a beam-bulk methodology has been developed. In this model the electron distribution is separated into a low energy component (the "bulk"), described by the electron continuity and energy equations, and a high energy component (the "beam") representing ballistic electrons. Results are presented for optically triggered pseudo sparks and low pressure beam sources during which we demonstrate when non-equilibrium effects must be considered.

*Work supported by Defense Nuclear Agency

KB-4

Theoretical Analyses of High Pressure Self-sustained Glow Discharges with High Switch Ratio. * W. M. MOENY, A. E. RODRIGUEZ, and J. M. ELIZONDO, Tetra Corporation, Albuquerque. --Tetra Corporation has recently developed high pressure glow discharge gas mixtures with high switch ratios, (ratio of the breakdown voltage to the glow voltage). This involved detailed engineering of excited-state ionization, attachment and recombination processes within the mixtures to achieve these results. The gas mixtures are composed of a dominant monatomic gas used as a buffer and energy donor, another monatomic is used as an electron donor, with a third one used as a secondary electron donor. A fourth gas element is added as a buffer or attacher. The gas elements were selected from those that show a coincidence in the power flow from primary metastable states to Penning ionization processes. In this paper, we describe the theoretical analyses that led to the development of these mixtures.¹

*Research supported by SDI/IST and managed by ONR

¹See companion paper, these proceedings

KB-5

Experimental Research on High Pressure Self-Sustained Glow Discharges With High Switch Ratio,*
J. M. ELIZONDO, W. M. MOENY, J. W. BENZE, B. R. BECKES,
and K. YOUNGMAN, Tetra Corporation of Albuquerque, New
Mexico —Experimental measurements of glow voltage,
breakdown voltage, and maximum current were made of
pulsed high pressure, self-sustained glow discharges
with high switch ratios, that is, a high ratio of the
breakdown voltage to the glow voltage. The best
results achieved to date are a switch ratio of 3.7 with
a breakdown voltage of 4.6 kV per cm, glow voltage of
1.25 kV per cm, and current densities of 7-8 amps per
square cm. One gas mixture was tested for lifetime
performance in a closed loop, performing an excess of
700 discharges at a repetition rate of a pulse every 5
seconds. In this paper, we describe specific
experiments with mixtures of nitrogen, neon, helium,
argon, xenon, and CF₄.¹

* Research supported by the SDI/IST and managed by
ONR.

¹See companion paper, these proceedings

KB-6

Streamers in N₂: New Empirical Results, F.E.
Peterkin and P.F. Williams, University of Nebraska—We
have obtained streak and high speed shutter photographs
of streamers in a trigatron spark gap filled with N₂ at
pressures around atmospheric, main gap charging voltages
ranging from about 50% to 99% of the breakdown voltage,
V_{SB}, and both charging polarities, producing cathode-
and anode-directed streamers. The streamers propagate
with a non-constant velocity which, for charging voltage
near V_{SB}, ranges from $\approx 2 \times 10^8$ cm/sec initially to more
than 10^9 cm/sec. Surprisingly, we find that cathode-
directed streamers propagate faster than anode-directed
streamers. For charging voltage near V_{SB}, cathode-
directed streamers have a diameter of ≈ 2 mm and anode-
directed streamers are somewhat thinner and have a more
feather-like appearance. For lower charging voltages,
cathode-directed streamers remain well-defined, whereas
the anode-directed streamers become more diffuse. We
observe a jump in the main gap current when the streamer
approaches the distant main gap electrode. From the
magnitude of this jump and the streamer body diameter we
can estimate the free electron density in the streamer
to be in the range $10^{14} - 10^{15}$ cm⁻³.

KB-7 Streamer Dynamics,* M-C. Wang and E. E. Kunhardt, Weber Research Institute, Polytechnic University. The dynamics of anode and cathode directed streamers have been investigated using the 2-D numerical simulation scheme of Wu and Kunhardt.¹ An analytical approach based on process competition is utilized to elucidate the transition between transient and steady-state streamer behavior. Using this approach, the fundamental dynamics responsible for the differences between anode and cathode directed streamers are examined. We have also investigated the instability of axial streamers and their transition to annular streamers. The critical condition for this instability is derived analytically and the dominant process is determined.

*Work supported by the Office of Naval Research and National Science Foundation.

¹C. Wu and E. Kunhardt, Phys. Rev. A37, 4396 (1988).

SESSION LA

10:10 AM - 11:50 AM, Thursday, October 19

Hyatt Rikeys Hotel - Camino Ball Room C

Ar/Xe LASERS II

Chair: A. Garscadden, Wright Research and Development Center

LA-1 Energy Scaling of the Atomic Xe:Ar Laser, DANIEL W. TRAINOR, L. LITZENBERGER, M. McGEOCH, Avco Research Laboratory, Inc.-- The atomic xenon laser has been scaled from the 80J level reported by Basov et. al.¹ to 650J using a large two-sided electron-beam pumped device. These experiments were conducted at a pump rate temporally and spatially averaged) of 70 kW/cm³ with energy delivered to the laser gas (spatially averaged) of 115 J/l. An aluminum primary mirror and an uncoated fused silica output coupler were aligned to form a stable flat-flat resonator. The laser cavity dimensions are 50 x 65 x 300 cm³. Energy measurements were made with full aperture calorimeters. The temporal pulse shape of the 1.73 μ m laser output was measured with a spectrally filtered germanium photodiode. The device was operated at gas pressures ranging from 20 to 40 psi with argon/xenon mixtures containing experimentally optimized xenon partial pressures. The maximum energy was obtained at an intrinsic efficiency of 0.57%. A maximum efficiency of 0.85% was observed during a shorter e-beam pulse at a reduced energy output of 495J.

¹N. G. Basov, et. al, IEEE J. Quant. Electron. QE-21, 1756 (1985).

LA-2 Time-Resolved Spectroscopic Study of Self-Sustained Discharge Pumped Xe:Ar Lasers, K.KOMATSU, E.MATSUI, S.TAKAHASHI, F.KANNARI AND M.OBARA, Dept. of Electrical Engineering, Keio U.,--The atomic Xe:Ar laser operates with multilines in the near-infrared region of the spectrum. To experimentally understand the complicated kinetics¹ involved in the excitation and quenching, the time-resolved spectroscopic measurement was carried out for a *self-sustained discharge -pumped Xe:Ar laser*. The time-resolved spectroscopy of the laser lines was performed as a function of the diluent (Ar,He), excitation rate, pumping duration and mixture pressure. The discharge laser is with a discharge volume of 2x2x50 cm³ and a UV preionizer. The results will be compared to the direct electron-beam-pumped and electron-beam-sustained discharge-pumped Xe:Ar lasers.

¹M.J. Kushner, M. Ohwa, T.J. Moratz: Technical Digest of Conference on Lasers and Electro-Optics, Baltimore, Maryland, (1989) p.252

LA-3 Quenching of Xenon Laser Levels ($6p[5/2]_2$, $6p[3/2]_1$) by Rare Gases, * W. J. ALFORD, Sandia National Laboratories--Quenching rates of the xenon $6p[5/2]_2$ and $6p[3/2]_1$ levels by rare gases (He, Ne, Ar, Kr, Xe) have been measured. The quenching rates are obtained from the $6p$ fluorescence decay following two-photon excitation. Quenching by Ar is found to be much larger for the $6p[5/2]_2$ level than for $6p[3/2]_1$. Helium shows the opposite behavior: larger for the $6p[3/2]_1$ than for $6p[5/2]_2$. Quenching due to three body collisions have been observed for Ar and Kr quenching of $6p[3/2]_1$. In addition, radiative lifetimes have been measured. Results will be presented and compared to previous measurements. Quenching of the $6p$ manifold by rare gases may be the dominant kinetic process in determining which wavelength(s) lase in high pressure xenon lasers.

*This work performed at Sandia National Laboratories, supported by the U. S. Department of Energy under Contract Number DE-AC04-76DP00789.

LA-4 The Effect of He Addition on the Performance of the Ar/Xe Atomic Xenon Laser. * Mieko Ohwa and Mark J. Kushner, University of Illinois, Urbana, IL--Ar buffered gas mixtures for xenon lasers operate efficiently and predominantly on the $1.73 \mu\text{m}$ transition. The $2.03 \mu\text{m}$ transition is virtually absent. When He is added to an Ar/Xe mixture, the laser power obtained at $2.03 \mu\text{m}$ increases and that at $1.73 \mu\text{m}$ decreases while the total laser power remains nearly constant. This behavior is attributed to a rapid quenching of the lower level of the $2.03 \mu\text{m}$ transition initiated by He. For He addition, He/Ar/Xe mixtures have a lower electron number density at a given power deposition, and lower gas temperature for a given energy loading. The power deposition which results in the reduction of lasing due to electron collision mixing between the upper and lower levels therefore shifts to a higher value. We will discuss the possible mechanisms responsible for this behavior in He/Ar/Xe mixtures. We will also discuss extraction of high energy by comparing this system with Ar/Xe mixtures.

*Work supported by Sandia National Laboratory.

LA-5 Power and Energy Loading Effects in Scaling of the Atomic Xenon Laser.* Mieko Ohwa and Mark J. Kushner, University of Illinois, Urbana, IL--The atomic xenon laser can be efficiently operated at moderate power loadings leading to quasi-steady state lasing. At high power deposition, though, electron collision mixing between the 5d and 6p manifolds (upper and lower levels) reduces the population inversion. Optimum performance is obtained with $n_e/N \leq 2-3 \times 10^{-6}$. High energy loading at even moderate power deposition results in gas heating. The rate of ion association reactions, and the rate constants for dissociative recombination of diatomic ions, which populate the upper laser level, decrease with increasing gas temperature. The result is that the electron density and rate of electron collision mixing of the laser levels increase which may eventually impact laser oscillation. We will discuss the scaling of laser power and energy efficiency of the xenon laser as a function of power deposition and gas heating resulting from high energy loading.

*Work supported by Sandia National Laboratory.

LA-6 Utilization of a Commercial Discharge Laser for an Atomic Xe Laser.* W. A. Neuman and J. R. Fincke, EG&G Idaho, Inc., Idaho National Engineering Laboratory--A commercial excimer laser discharge system has been used to pump an atomic Xe laser. The line strengths and temporal behavior of the 5d \rightarrow 6p laser transitions have been experimentally measured for a variety of buffer gases and pressures. Because the discharge system has a uv preionizer, the discharge behavior favored helium buffers, which result in domination of the 2.03 μm line. Line competition has been studied for mixtures of Ar/He, Ar/Ne, He/Ne and Ar/He/Ne as well as the individual buffers, at various pressures up to 2 atm. Comparison of kinetic calculations with observed experimental results will be presented. The discharge pulse width is 20 ns. Typical extracted energy on all lines is 15 mJ.

*Work performed under the auspices of the U.S. Department of Energy.

LA-7

Current Understanding and Remaining Physics

Issues of the Xe:Ar(He, Ne) Laser* Mark J. Kushner and Mieko Ohwa, University of Illinois, Urbana, IL -- The high pressure (≥ 0.5 atm) atomic xenon laser ($5d \rightarrow 6p$) has demonstrated high intrinsic efficiencies (3-5%) over a wide range of pressures and power deposition. The laser spectrum (6 major lines may oscillate) and efficiency, though, are separately sensitive functions of gas mixture, power deposition, and energy loading. Parametric experimental data obtained over the last 15 years has given insight to the important kinetics pathway for exciting and quenching the laser. Our current understanding of the operation of the xenon laser based on these results, and computer modeling, will be discussed. In particular, we will highlight the areas where we lack sufficient understanding of the kinetics to optimally scale the laser and conjecture on the potential performance of the system.

*Work supported by Sandia National Laboratory and National Science Foundation.

SESSION LB

10:10 AM - 12:04 PM, Thursday, October 19

Hyatt Richeys Hotel - Camino Ball Room D

CROSS SECTION DATA I

Chair: R. A. Phaneuf, Oak Ridge National Laboratory

LB-1 Cross Sections for Low - Energy Electron Molecule Collisions, H. PRITCHARD, C. WINSTEAD, K. WATARI[†], M. LIMA[‡], V. MCKOY, California Institute of Technology. The Schwinger Multichannel method has recently been used to study several low-energy electron-molecule collision processes with special emphasis on the effects of channel coupling. Examples to be reported include $1\pi_u \rightarrow 1\pi_g$ excitations of N_2 leading to the $A^3\Sigma_u^+$, $W^3\Delta_u$, $w^1\Delta_u$, $a^1\Sigma_u^-$, and $B'^3\Sigma_u^-$ electronic states and analogous $1\pi \rightarrow 2\pi$ excitations in CO. Cross sections for excitation of selected electronic states of H_2O at the two-channel level will also be presented along with the results of studies of polarization phenomena in elastic scattering by the polyatomics NH_3 , CH_4 , and SiH_4 .

*Supported by NASA-Ames Cooperative Agreement NCC 2-319, NSF Grant PHY- 8604242, and the Innovative Science and Technology Program of SDIO Contract DAAL 03-86-K-0140.

[†]Supported by CNPq(Brazil).

[‡]Permanent address: University of Campinas, Campinas, Brazil.

LB-2 Electron Scattering from and Dissociative Attachment in Halogenated Silanes*, H.X. WAN and J.H. MOORE, Department of Chemistry and Biochemistry, University of Maryland --Total scattering cross-sections and dissociative attachment cross-sections for 0.2 - 12 eV electrons have been measured for silane (SiH_4) and the chlorinated silanes (SiH_nCl_{4-n}) and tetrahalosilanes (SiX_4). The scattering cross-sections are large, ranging from 10 to over $100 \times 10^{-16} \text{ cm}^2$ in this energy range. Broad resonances associated with temporary negative ion states are observed and assigned. In contrast to the case of the halogenated methanes, the dissociative attachment cross sections are very small, even at threshold, and the scattering resonances do not give rise to enhanced dissociative attachment.

*Supported by NSF grant CHE-87-21744.

LB-3 Extreme Ultraviolet Emission from N₂ by Electron Impact: Cross Sections of the c'₄¹Σ_u⁺ and b'¹Σ_u⁺ States,* J. M. AJELLO, G. K. JAMES and D. E. SHEMANSKY, J.P.L. and U. of Arizona — Emission cross sections have been measured for each of the vibrational transitions of the c'₄¹Σ_u⁺ → X¹Σ_g⁺ Carroll-Yoshino and b'¹Σ_u⁺ → X¹Σ_g⁺ Birge Hopfield II band systems of N₂ excited by electron impact at 100 eV in the wavelength range 82 to 110 nm. The c'₄¹Σ_u⁺ and b'¹Σ_u⁺ states strongly perturb one another by homogeneous configuration interaction, leading to vibrational excitation cross sections with a v' dependence that is strikingly different to the variation of deperturbed Franck-Condon factors. Excitation function measurements of the c'₄(0,0) and b'(16,0) transitions have been performed from threshold to 400 eV. A modified Born approximation analytic model has been applied to these measurements yielding accurate band system oscillator strengths. Comparison of the emission and excitation cross sections shows that the c'₄¹Σ_u⁺ state is less than 10% predissociated; the predissociation yield for the b' state is 84%. These results represent a substantial improvement in the available data base.

*This work supported by the Air Force Office of Scientific Research and the National Science Foundation (grant # ATM 8715709), and NASA.

LB-4 Measurements of Electron-Impact Cross Section for Excitation out of the He(2³S) Metastable Level.* R. B. LOCKWOOD, F. A. SHARPTON, L. W. ANDERSON, J. E. LAWLER, and CHUN C. LIN, Univ. of Wisconsin, Madison—In this experiment metastable He(2³S) atoms formed in a hollow-cathode discharge flow out of the hollow cathode through an orifice into a vacuum collision chamber. The vertical metastable-atom beam is crossed by a horizontal electron beam of energy up to 16 eV. Radiation from the He(n³L) atoms produced by electron excitation out of the 2³S metastable level is measured and utilized to determine the optical emission cross sections. Absolute calibration of the cross section is facilitated by a laser-induced fluorescence experiment which gives the ratio of the electron excitation cross section to the known 2³S→3³P optical absorption cross section. Apparent excitation cross sections and excitation functions have been obtained for several n³L levels. The direct excitation cross sections for the 3³P level are found to be much smaller than those for 3³S and 3³D.

*Work supported by the Air Force Office of Scientific Research.

LB-5A Study of the Pais Variational Phase Shift Approximation and Its Extension Potentials with a Pure Coulomb Tail, S. R.VALLURI, Dept. of Appl. Math., U. of Western Ontario, CANADAand W. J. ROMO, Ottawa-Carleton Inst. for Phys., Carleton U.,CANADA, -- The accuracy of a variational approximations scheme for

calculating phase shifts in potential scattering problems that was devised by Pais¹ is investigated. Calculations indicated that the method gives fairly accurate results for all but the very lowest partial waves. The partial derivative of the phase shift with respect to the angular momentum ($\partial\delta_l/\partial l$) can be calculated for a variety of potentials in the Pais approximation. This is of importance since this partial derivative is directly proportional to the deflections angle which has played an essential role in the analysis of 'rainbows' in heavy ion collision². The Pais approximation can be of use in computational physics since the scattering processes can be formulated in terms of a Sturmian Bessel set of functions³. The extension of the Pais formula to the pure Coulomb potential has been studied and some simple applications have been worked out. The analysis of 'rainbows' is now under study.

1. A. Pais, Proc. Camb. Phil. Soc., 42 (1946) 45.
2. K. W. McVoy et al; Nucl. Phys. A455 (1986) 118.
3. S. Weinberg, Phys. Rev. 131 (1963) 400.
G. H. Rawitscher, Phys. Rev. C25 (1982) 2196.

LB-6Inelastic 3S-3P and Superelastic 3P-3S Electron

Scattering,* L. VUŠKOVIĆ, T.Y. JIANG, M. ZUO, and B.

BEDERSON, New York U., -- We report on "time inverse"

processes, the inelastic 3S-3P and the superelastic 3P-

3S absolute differential cross sections for 3 and 20 eV

unpolarized electron scattering by sodium over an

angular range of about 0-20°. Inelastic process corre-

sponds to electron scattering with all atomic sublevels

of initial and final state present, while in the

superelastic case the atoms are initially prepared by

circularly or linearly polarized laser light which

result in unequal initial state population. Accordingly

detailed balancing cannot be directly invoked to compare

the inverse reactions, and in fact our results do reveal

significant differences between those processes.

Experiments were performed using crossed-beam electron

and photon recoil technique¹. Absolute cross sectionsare obtained² by a suitable analysis of deflection beam

profiles taking into account all relevant beam and

apparatus parameters.

*Work supported by NSF

¹B. Jaduszliwer et al., Phys. Rev. a 30, 1255 (1984).²L. Vušković et al., to appear, Phys. Rev. A 40, XXX (1989); T.Y. Jiang et al., to be published.

SESSION MA

1:30 PM - 3:30 PM, Thursday, October 19

Hyatt Riskey Hotel - Camino Ball Room C

FUNDAMENTAL DATA FROM PLASMAS

Chair: J. E. Lawler, University of Wisconsin

MA-1 Oscillator Strengths and Lifetimes from Transform Spectrometer Data, B. A. Palmer, Los Alamos National Laboratory – A Fourier transform spectrometer (FTS) has been used in the past to measure branching ratios. The FTS data can also be used to augment oscillator strengths and lifetimes because of the inherent intensity accuracy, the high resolution, and the wide spectral coverage. It does however rely on previous measurements, and this may be the limiting factor in absolute accuracy. The various analysis techniques will be discussed as well as the inherent problems, the largest being the lack of LTE in any laboratory source that works well with the instrument. The sources that are commonly used, the hollow cathode and the inductively coupled plasma, will be examined and the problems with each will be discussed. Because of the accuracy in the FTS, some of the problems with these sources can be overcome in the analysis of the data. Examples of these techniques will be given.

MA-2

Atomic Transition Probability Measurements with an Inductively Coupled Plasma, W. WHALING *Caltech*, T. R. O'BRIAN, M. W. WICKLIFFE, J. E. LAWLER *U. of Wisconsin*, J. W. BRAULT *NOAO/NSO*. – The 1-m. Fourier Transform spectrometer at the National Solar Observatory (Kitt Peak) has been used extensively by many guest scientists to measure the emission branching fractions by which atomic level lifetimes can be converted into individual atomic transition probabilities (ATP). This conventional method of measuring ATP's uses a tiny fraction (usually $\ll 1\%$) of the spectral information in an FTS spectrum. The inductively coupled argon spectral source (ICP) provides a way to make more efficient use of the immense amount of information in a typical FTS spectrum. We show that the population of excited levels in the ICP approximates closely the Boltzmann exponential dependence on excitation energy. Measured lifetime values for only a few levels spread over a wide range of excitation energy determine the excitation temperature of the ICP source. Once the relative populations of excited levels are known, it becomes possible to find the ATP *for every line that can be classified* in the ICP spectrum by simply measuring the emission line strength. Application of this method to Mo and Fe will be reported, including the computer techniques required to measure and analyze the thousands of transitions accessible by this method.

MA-3 Electron Beam Ion Traps (EBIT): A New Tool for Studying the Spectroscopy of Multiply-Charged Ions.* R. E. MARRS, Lawrence Livermore National Laboratory--An Electron Beam Ion Trap (EBIT) at LLNL is being used to produce and trap ions with up to 82 electrons removed (e.g. neonlike U^{82+}) for x-ray spectroscopy measurements. In EBIT highly charged target ions are prepared in a selected ionization stage and bombarded with a monoenergetic electron beam. The available electron energy range is presently $0.5 \leq E_e \leq 30$ keV. This technique has been used to obtain precise energy level (i.e. Lamb shift) measurements, to obtain electron-ion collision cross sections for impact excitation¹ and dielectronic recombination², and to study x-ray line ratios used for plasma diagnostics.

*Work performed under the auspices of the US Department of Energy by Lawrence Livermore National Laboratory under contract No. W-7405-ENG-48.

¹R.E. Marrs et al., Phys. Rev. Lett 60, 1715 (1988)

²D.A. Knapp et al., Phys. Rev. Lett 62, 2104 (1989)

MA-4 Evaporative Cooling in Electron Beam Ion Traps.*

B. M. PENETRANTE, M. A. LEVINE⁺ and J. N. BARDSLEY, Lawrence Livermore National Laboratory -- Evaporative cooling has been used successfully in EBIT to extend the containment time for neon-like gold to several hours. We have developed a computer model to elucidate the mechanisms which affect the energy and charge balance of the trapped and coolant ions. With this model we are able to self-consistently determine the (a) ion density as a function of charge state, (b) spatial extent of the various ionic species, (c) heating rate of the ions by the electron beam, (d) energy transfer from the highly-charged ions to the coolant ions, (e) energy distribution among the coolant ions, and (f) energy escape rate of the ions. Thus, for each set of operating parameters and amount of coolant, we are now able to predict the resulting number of trapped ions and their trapping times, and study the relative efficiencies of different coolants.

*Work performed under the auspices of the U.S. Department of Energy by the Lawrence Livermore National Laboratory under Contract No. W-7405-ENG-48.

⁺Lawrence Berkeley Laboratory

SESSION MB

1:30 PM - 3:25 PM, Thursday, October 19

Hyatt Richeys Hotel - Camino Ball Room D

CROSS SECTION DATA II

Chair: B. Bederson, New York University

MB-1 Atomic Collision Processes in the Edge Plasma of Magnetic Fusion Devices, R.A. PHANEUF, Oak Ridge National Laboratory* -- The importance of atomic processes in the hot central core of magnetic fusion plasmas such as tokamaks has received much attention over the past decade. However, it has only recently been recognized that a detailed understanding of the behavior of the cooler edge region near the physical boundary of the vacuum chamber is critical to effective plasma confinement and heating. This region is characterized by electron temperatures in the 1-100 eV range, and relatively large densities of neutral species such as H, H₂ and hydrocarbons of the type C_mH_n. Accurate low-energy cross-section data for atomic processes such as excitation, ionization, recombination, dissociation, interchange reactions and charge transfer are required for modelling the edge plasma.¹ A survey of data needs will be presented.

*Operated by Martin Marietta Energy Systems, Inc., for the U.S. Department of Energy under contract No. DE-AC05-84OR21400.

1. H. Tawara and R. A. Phaneuf, *Comm. At. Mol. Phys.* **21**, 177-93 (1988).

MB-2 Negative and Positive Ion Formation by Electron Impact on Benzene*, A.F. FUCALORO[†] and S.K. SRIVASTAVA, Jet Propulsion Laboratory, California Institute of Technology--We have utilized a crossed electron beam and molecular beam collision geometry to study the ionization, dissociative ionization and dissociative attachment properties of benzene by electron impact. A large number of dissociated fragments (both positive and negative) have been identified for the first time. Threshold energies and cross sections for the production of various fragments have been measured. Threshold energies have also been calculated from the knowledge of heats of formation and compared with the measured ones. This comparison provides information on the bond structures of the various radical fragments. These data will be presented at the conference.

*Work supported in part by Air Force Wright Aeronautical Laboratories.

[†]On leave from Joint Sciences Department, Pitzer College, Claremont, CA 91711.

MB-3 Electron Collision Cross Section Needs for the KrF Laser, D.C. CARTWRIGHT and P. J. HAY, Los Alamos National Laboratory, and S. TRAJMAR, JPL CalTech -- Electron Collision processes play a critical role in the KrF laser. These processes contribute to the formation and the destruction of the excimer molecule and/or have critical importance in determining the behavior and performance of the laser system.

Although some information on electron collision cross sections pertinent to KrF laser exists in the literature, for a rather large variety of processes only fragmentary data or no information at all is available. The problem is especially serious for collision processes involving excited (mostly metastable) species. Here we briefly review the needs in general and specifically describe procedures we have used for estimating electron collision cross sections for quenching of metastable Ar and Kr and for dissociation of molecular fluorine.

The estimation of quenching cross sections is based on the principle of detailed balance and results will be presented for both Ar and Kr for electrons in the zero to 2.5 eV kinetic energy range.

Estimation of F₂ dissociation cross section is based on very fragmentary electron-impact energy-loss spectra, the similarity of the F₂ and N₂ molecule and the available cross sections for electron impact excitation of N₂.

MB-4 e-CH₄ collisions in a Static-(Exact) Exchange plus Parameter-free Polarization Model: Elastic and Rotational Excitation Parameters. P. McNaughten and D. G. Thompson, Queen's Univ., Belfast, N. Ireland and Ashok Jain, Florida A & M Univ., Tallahassee.-- We report differential, integral and momentum transfer cross sections for the elastic, rotational excitation and rotationally summed processes in an exact static-exchange plus nonadjustable polarization model of Jain and Thompson¹. The inhomogeneous scattering equations are solved iteratively² for all the symmetries (A₁, E, T₁ and T₂) considered here. We compare our results with recent experimental data in the whole energy region (0.1 - 10 eV). The agreement with expt. data is excellent and much better than all previous calculations. In particular, our results on the total and differential cross sections are very good below 1 eV where polarization and exchange effects are very crucial.

1. A. Jain and D. G. Thompson, J. Phys. B15, L631 (1982)
2. P. McNaughten and D. G. Thompson, J. Phys. B21, L703 (1982).

MB-5 Dissociative Attachment in the Chloromethanes,*
S.C. CHU and P.D. BURROW, U. of Nebraska, Lincoln--

Using a newly modified electron beam apparatus with provisions for counting the ion fragments, we have re-examined the dissociative attachment cross sections of CH_3Cl , CH_2Cl_2 , CHCl_3 and CCl_4 at low energies. The cross sections are normalized to that for O^- from CO_2 at the 4.4 eV peak.¹ Because the cross section for CH_3Cl is so small, contamination of the gas bottles or from the gas handling method can lead to an overestimate of the low energy peak. We have found direct evidence for both these problems. Our cross section is substantially smaller than that derived recently from swarm measurements² and differs in energy dependence.

*This work was supported by NSF.

¹G.J. Schulz, Phys. Rev. 128, 178 (1962).

²Z.L. Petrovic, W.C. Wang and L.C. Lee, J. Chem. Phys. 90, 3145 (1989).

MB-6 Temperature Dependence of the Vertical-Onset-Dissociative Electron Attachment to CH_3Cl *, P. G. DATSKOS, L. G. CHRISTOPHOU, AND J. G. CARTER, Oak Ridge National Laboratory and the University of Tennessee - The low-energy (< 1 eV) dissociative electron attachment process in CH_3Cl exhibits a vertical onset behavior. At 300K the total electron attachment rate constant $k_a(\langle\epsilon\rangle, T)$ for CH_3Cl in N_2 is $< 10^{-14} \text{ cm}^3 \text{ s}^{-1}$. As T is increased to 750K, $k_a(\langle\epsilon\rangle, T)$ shows a remarkable (by over 4×10^3 times) increase which depends on $\langle\epsilon\rangle$; two negative ion states contribute to $k_a(\langle\epsilon\rangle, T)$, at thermal energies and at ~ 0.7 eV. At $T = 750\text{K}$, the $k_a(\langle\epsilon\rangle, T)$ is $\sim 4 \times 10^{-11} \text{ cm}^3 \text{ s}^{-1}$. The exceedingly small $k_a(\langle\epsilon\rangle, T)$ at 300K and the profound increases in $k_a(\langle\epsilon\rangle, T)$ with small increases in T (which may indicate infrared photoenhanced electron attachment) make CH_3Cl and its mixtures with buffer gases candidates for pulsed power switches.

*Research sponsored by the U.S. Department of Energy under Contract No. DE-AC05-84OR21400 with Martin Marietta Energy Systems, Inc.

MB-7 Inference of HN_3 Electron Attachment Cross Sections From Drift Velocity and Electron Attachment Rate Constant Data,++ L. A. Schlie, C. A. Denman, and M. W. Wright**, Advanced Laser Technology Division (WL/ARDI), Kirtland AFB, NM 87109-6008

Recently, it was reported that the energetic azide HN_3 molecule is electronegative. In an attempt to further understand this electron attachment process, detailed electron attachment rate constant data plus other TOF (Time-of-Flight) experimental results (V_d , D_1 , and D_3) were measured over a wide range of E/N values and all of the inert gases. Such data indicates the very strong influence of this electron attachment process on such gas mixtures. In addition, the results indicate that threshold energies greater than 0.2 eV exists. Using the Boltzmann equation to describe the electron kinetics, these data are used to infer the energy dependence of the this particular process. The algorithms used are discussed in detail.

++ Funded by the Air Force Office of Scientific Research, Bolling AFB, D.C.

** Dept. of Physics and Astronomy, University of New Mexico, Albuquerque, NM 87131

SESSION NA

3:30 PM - 5:30 PM, Thursday, October 19

Hyatt Richeys Hotel - Camino Ball Room A and B

POSTERS

Chair: J. B. Jeffries, SRI International

NA-1 Particle Simulation of a RF Discharge: Nonlocal Effects.*
M. SURENDRA and D. B. GRAVES, University of California, Berkeley - A self-consistent 1D2V particle-in-cell simulation of a RF discharge will be presented. Collision effects included in the model are elastic and ionizing electron-neutral collisions using realistic differential cross sections and ion-neutral charge exchange. The detailed nature of the model is suited to an in-depth study of the RF plasma and sheath dynamics. Fluid models typically require the use of swarm parameters either in the local field approximation¹ or in an energy balance approach². The accuracy of these simplifying assumptions are examined by comparing transport properties and inelastic rates predicted by the particle simulation to their local field values. Furthermore, the effects of power and neutral gas density will be discussed. Ion energy distributions at the electrode under various operating conditions are also presented.

*Work supported in part by San Diego Supercomputer Center.

1J. P. Boeuf, Phys Rev A **36**, 2782 (1987).

2A. D. Richards et al., Appl. Phys. Lett. **50**, 492 (1987)

NA-2 Probe Potential and Capacitance Measurements in a Symmetric Argon RF Discharge Driven at 13.56 MHz. V. A. GODYAK, R. B. PIEJAK, GTE Laboratories Inc., Waltham, MA -- The DC voltage and various RF voltage components on a wire loop probe located at the mid-plane of an RF discharge have been measured using RF probes with different input capacitance. The measurements showed that the RF component on the loop probe was almost entirely composed of the second harmonic of the driving frequency. The values of RF and DC components of the probe potential were found to mainly depend upon the input capacitance of the RF probes. Measuring the potential with RF probes of different input capacitance enabled us to determine values of plasma-probe capacitance and to calculate true values of DC and RF potentials. The DC and RF probe potentials were compared with predictions from various RF electrode sheath models. The values of probe-plasma capacitance and the RF voltage are important in designing an electronic circuit for probe diagnostics in an RF discharge.

NA-3 Electron Cyclotron Resonance Plasma Source Research at the University of Wisconsin-Madison, H. M. Persing, N. Hershkowitz, A. Wendt, D. Diebold, M. H. Cho, University of Wisconsin-Madison, Electron cyclotron resonance (ECR) plasmas have recently been used for a number of applications such as low temperature chemical vapor deposition, plasma etching, ion beams, etc. We are investigating two such sources: a commercially available source which is employed as an etcher and a device built to achieve overdense ($\omega_{pe} \gg \omega_{rf}$) target plasmas with $n_e=10^{13}$. In both instances, we are intent on characterizing the plasma sources by measuring the radial, axial, and azimuthal distributions of density (n_e), electron temperature (T_e), and plasma (ϕ_p) and floating (ϕ_f) potentials as functions of magnetic field configuration, microwave power, and neutral gas composition and pressure. Further investigations will include measurements of the electron and ion "endloss" currents and their energy distributions. The latest results will be presented.

NA-4

Observation of Submicron Particles in RF Plasmas, K. R. STALDER, SRI International--We have observed submicron size particles in an parallel plate rf plasma. The particles were grown while etching silicon wafers in $\text{CCl}_2\text{F}_2/\text{Argon}$ plasmas. The particles were observed in situ by a laser scattering apparatus which made vertical scans between the plates. Particles tended to stratify in the discharge, with the maximum particle density located at the lower sheath-plasma boundary. The particle sizes, calibrated against Rayleigh scattering from test gases, are less than 0.4 microns in diameter. These particles are smaller than those reported by Selwyn, et al.¹ in a similar experiment. Possible explanations for the discrepancies include differences in electrode temperatures, electrode materials and degree of discharge confinement. We have not yet made chemical analyses of the particles, but we note that they were only observed while etching silicon. Nucleation, growth and transport processes in plasmas will be discussed.

1. G. S. Selwyn, J. Singh and R. S. Bennett, to be published in J. Vac. Sci. Tech. A (July/August, 1989).

NA-5 Power Absorption by Electron Cyclotron Resonance, D. CARL, A.J. LICHTENBERG, M.A. LIEBERMAN, J. STEINHAUER, AND M. WILLIAMSON, University of California, Berkeley — Electron cyclotron resonance (ECR) discharges are widely used for the fabrication of integrated circuits. ECR power absorption on a magnetic beach is calculated from linear wave theory and from nonlinear single particle heating theory. The two results are found to be in reasonable agreement in the weak absorption limit where the nonlinear calculation can be performed. The calculations predict a rather sharp cut-off of absorbed power with decreasing incident power due to the plasma becoming transparent to the incident radiation. Over most power levels of interest, however, the ECR power is strongly absorbed. A simple discharge model is constructed based on these results. The theoretical results and the model are compared with experimental measurements.

NA-6 Studies of Microwave Breakdown Plasmas in Air by the Microwave Cavity Perturbation Technique,* D. J. ECKSTROM AND M. S. WILLIAMS, SRI International—We have used a 329 MHz microwave cavity to make very sensitive measurements of the electron densities and collision frequencies in air following pumping by a high-power pulsed 2.86-GHz microwave source at LLNL. The S-band source was focused through 23-cm diameter holes in the cavity endwalls. The pressure was varied from 0.01 to 30 torr; microwave pump power and pulse length were adjusted to minimum values required to produce measurable electron densities, which ranged from 2×10^5 to $1 \times 10^7/\text{cm}^3$. Threshold pump powers were slightly lower than values for critical breakdowns, and followed similar trends with pulse length (decreasing power but increasing energy with increasing pulse length). Electron density decay rates were about $10^2/\text{sec}$ from 0.01 to 0.3 torr and then increased linearly with higher pressures (slower than 3-body electron attachment rates in air). Collision frequencies could not be measured below 1 torr. They corresponded to calculated values for $T_e = 800$ K at 1 torr, decreasing to 300 K at 3 torr and 100 K at 30 torr. The latter value may reflect a contribution of negative ions to the conductivity.

*Work supported by AFGL through LANL.

NA-7 Growth of Diamond in a DC Discharge,* H. N. CHU, A. R. LEFKOW, R. REDWING, L. W. ANDERSON, M. G. LAGALLY and J. E. LAWLER, Department of Physics, University of Wisconsin, Madison, WI 53706--Diamond films have been grown using DC discharges. We have studied the growth of diamond using both a Ta spiral hollow cathode and a abnormal glow discharge using a Cu cathode. The diamond is grown on a Si(100) substrate with a feed gas of 0.5-1.0% CH₄ in H₂ at a pressure of 30 Torr, with a flow rate of 80sccm, with 150V cathode to anode potential difference, and a cathode to anode spacing of 0.5-2.0 cm. The substrate is heated resistively to 900°C. The growth rate is about 0.5 micron/hour. The diamond is identified using both Raman Scattering and a scanning electron microscope. Spatially resolved emission measurements will be reported. We observe a glow near the cathode, a dark space, and second glow near the anode.

*Research Supported by NSF Grant No. CDR-8721545 in support of the Engineering Research Center - Plasma Aided Manufacturing.

NA-8 Generation of carbon ion beams from a small multicusp source* -- K.N. LEUNG, M. LOWENTHAL, W. STOCKWELL, M.D. WILLIAMS, and W.B. KUNKEL, Lawrence Berkeley Laboratory, and J.M. DAWSON, UCLA -- Carbon ion beams are used in some experiments to form diamond-like films. Negative carbon ions are required in Accelerator Mass Spectrometry applications. In most cases, the carbon ions are generated either by dissociation of gas molecules such as CO, CO₂ or CH₄ or by sputtering graphite targets with energetic Cs⁺ ions. We would like to report a novel method of producing C⁺ or C⁻ ions without the use of gases or cesium. The experiment was performed in a 7.5-cm-diam. multicusp source. A graphite hairpin filament was used to generate the background carbon vapor as well as the primary ionizing electrons. Preliminary results showed that almost pure steady-state C⁺ ion beams could be obtained without employing any supporting gas for the discharge. An ample amount of C⁻ ions has also been observed when the source was biased for negative ion extraction.

* This work is supported by the U. S. DOE under Contract Number DE-AC03-76SF00098.

NA-9 Multi-Species Ambipolar Diffusion^{*},
T. Gist and A. Garscadden, Wright Research and
Development Center (WRDC), and W. Bailey, Air
Force Institute of Technology (AFIT). An
improved model of multi-species ambipolar
diffusion has been developed. Previous models
based on Schottky's single species ambipolar
diffusion¹ require assumptions that cannot be
justified from the physical situation, or can
produce only numerical solutions. The new
model, based only partly on Schottky's
development, produces analytic solutions for a
range of realistic systems, and numerical
solutions are often much simpler than
previously.

Development of the new model is discussed.
Analytic and numerical solutions for realistic
cases are presented. Validity and necessary
conditions for proportionality are discussed.

*Work supported in part by WRDC and AFIT.

¹Diffusion Theory and the Positive Column, W.
Schottky, Zeitschr. f. Phys., October 1924.

NA-10 Kinetic study of electron properties in a capacitively
coupled RF-discharge. G. FROMLING, Ruhr-Universität Bochum,
FRG. -- The electron distribution function is investigated in the
frequency range $\nu_e \lesssim \omega \ll \nu_m$ where ν_e/m are the collision frequencies
of energy or momentum exchange, respectively.

The energy supply necessary to sustain the discharge is modeled
by the reflection of the electrons at the oscillating space charge potential.
Since the thermalization of these electrons occurs far from this space
charge region in the energy exchange zone, the problem is nonlocal.
The ultimate goal is the correction of the Boltzmann factor of the
electron density and the Hertz-Knudsen formula for the electron
current. We present first the numerical results.

NA-11 Electron Degradation Spectra by Subexcitation Electrons in Gaseous- and Solid-Water, M. KIMURA, M. A. ISHII,[†] and M. INOKUTI, Argonne National Laboratory-- Electrons whose kinetic energies are below the electronic-excitation threshold are termed subexcitation electrons. Knowledge of the behavior of these electrons is essential in radiation physics and chemistry. We have conducted a systematic study of the moderation of the subexcitation electrons in H₂O (gas and solid) using the Spencer-Fano theory and its simplified treatment, the continuous slowing-down approximation within time-dependent and time-independent representations. Our study shows that while the general shapes of two degradation spectra arising from the gaseous and condensed phases are similar, detailed structures as well as magnitudes are quite different because of additional energy-loss processes in the condensed phase.

*Work supported in part by the U.S. Department of Energy, Office of Health and Environmental Research, under Contract W-31-109-Eng-38.

[†]Summer student, Department of Educational Programs, ANL.

NA-12 Model of Plasma Source Ion Implantation in Planar, Cylindrical and Spherical Geometries, J. T. SCHEUER, M. SHAMIM and J. R. CONRAD, Plasma Source Ion Implantation Group, University of Wisconsin -- A model of transient sheath propagation has been developed and applied to Plasma Source Ion Implantation.¹ This model assumes that the transient sheath obeys the Child-Langmuir law² for space charge limited emission at each instant during the propagation. The model predicts the final sheath extent and average current to the target during each high negative voltage pulse for planar cylindrical and spherical geometries.

¹ J. R. Conrad, J. L. Radkte, R. A. Dodd and F. J. Worzala, J. Appl. Phys. 62, 4591 (1987).

² I. Langmuir, Phys. Rev. 21, 419 (1923); I. Langmuir and K. Blodgett, Phys. Rev. 22, 347 (1923); I. Langmuir and K. Blodgett, Phys. Rev. 24, 49 (1924).

NA-13 Generalized Sheath Condition for Emitting and Reflecting Walls. K.-U. RIEMANN, Ruhr-Universität Bochum, FRG. In the asymptotic limit of a small Debye length ($\lambda_D \rightarrow 0$) the problem of the plasma boundary layer is splitted up into the separate problems of a collision free sheath and quasineutral presheath. For the case of completely absorbing walls the well known Bohm "criterion" [1] formulates a necessary condition for a stationary sheath. We reinvestigate the problem of sheath formation accounting for emitting and reflecting walls and find a generalized sheath condition. By a kinetic analysis of the presheath we show that this condition is usually fulfilled marginally and connected with a sheath edge field singularity on the pre-sheath scale. An analogous result was obtained earlier for absorbing walls. [2]

[1] E. R. Harrison and W. B. Thompson, Proc. Phys. Soc. London 74, 145 (1959).

[2] K.-U. Riemann, Phys. Fluids B1, 961 (1989).

NA-14 A Micro-Pyrometer System for Measuring the Temperature of F-Lamp Electrodes. A. AWADALLAH and A.K. BHATTACHARYA, GE Lighting, Cleveland, OH -- A Micro pyrometer capable of measuring time-resolved temperature profiles of the hot spot on the electrode of a fluorescent lamp is described. The system has a spatial resolution of .0008 inch in diameter and is capable of following the temperature excursions of the hot spot over 60 Hz AC frequency. It is capable of measuring temperatures as low as 1000° K. The instrument is simple to construct and easy to operate. It was used to measure the temperature variations of the cathode spot as a function of the phase of the lamp current and a temperature averaged over 60 Hz. The hot spot temperature was fairly constant in the cathode and anode half cycle. The average hot spot temperatures of an electrode surface covered with emission mix in F40W lamps operating on reference and 2-lamp rapid start ballasts were consistently measured in the range of 1400-1500 K.

NA-15 Mercury Pressure Effects on Convection in Horizontal Discharges, M.E. DUFFY and P.Y. CHANG, G.E. Lighting — A three-dimensional convection model has been developed and used to investigate horizontal, high pressure mercury vapor arcs. The model solves the coupled momentum, mass continuity, energy and electric field equations. The numerical approach is capable of handling irregular geometries of offset electrodes as well as curvature of arctube. The effects of mercury pressure on arc centering and wall temperature are reported by both the theoretical model and by measurements of curved arctubes with offset electrodes and varying dose weight. Aquadag spot temperatures on the arctube wall verify qualitative model predictions. Line of sight arc intensity measurements show the effect of increased buoyancy with higher mercury pressure. A similar trend is also obtained from the model. The data are used to set a geometry dependent model parameter approximating the effect of radiation absorption by the cold gas surrounding the arc.

NA-16 Short-Gap Breakdown in He: the Effect of Impurities*, J.P. NOVAK and R. BARTNIKAS, IREQ, Varennes, Québec, Canada --The experimental arrangement consisted of a pyrex glass vacuum chamber and two stainless steel electrodes of 5.08 cm diameter with the edges rounded to a 0.32 cm radius, separated by a 0.48 mm gap; limit pressure was below 1×10^{-4} Torr and before experiments the gap was degassed by a glow discharge. Working pressure was 760 Torr with relative pressure of the added dry air between ≈ 0 and 3×10^{-3} . The evaluated breakdown voltage U_{br} of the mixture was 250, 259, 268, 285 and 309 V for the relative pressures ≈ 0 , 10^{-4} , 3×10^{-4} , 10^{-3} and 3×10^{-3} , respectively. The initial current increase (recorded up to about 500 μ A) was very nearly exponential. The inverse time constant of the current rise as measured at the voltage $U_{br} + 10$ (V) was 0.051, 0.15, 0.26, 0.47 and 0.96 μ s $^{-1}$ at the corresponding relative pressures as above. In the near proximity of the breakdown voltage (measured up to about $U_{br} + 25$ V), the inverse time constant was approximately a linear function of the overvoltage with the slope rapidly increasing with the relative pressure of the air.

* This work was supported by CEA (Canada).

NA-17 Line Broadening in Laser-produced Oxygen Plasmas*,
L.S. Dzelzkalns and W.A.M. Blumberg, Geophysics
Laboratory (AFSC), P.C.F. Ip and R.A. Armstrong, MISSION
Research Corp., W.T. Conner and C.C. Lin, U. of Wisconsin
-- Ultra-broad spectral lineshapes have been measured in
the short- to medium-wavelength IR for laser-produced
oxygen plasmas. Atomic oxygen emissions were observed in
the GL LINUS facility in which O₂ at pressures of 30-190
torr was irradiated with a pulsed Nd:YAG laser with peak
laser intensities of $(1-10) \times 10^{12}$ W/cm². Time-resolved
spectra were obtained over the wavelength range 1.5-8.5
microns. The IR observations are being analysed using a
line broadening theory which treats the interactions of
the emitting oxygen atom with both the plasma ions and
electrons. The effect of the ions is calculated in the
quasi-static approximation using perturbation theory and
the electron broadening is obtained from impact-parameter
calculations of electron collision cross-sections. The
method will be applied to our observations of oxygen atom
Rydberg state emissions to determine the relative impor-
tance of ion versus electron broadening.

*Supported by the Air Force Office of Scientific Research
and the Defense Nuclear Agency.

NA-18 Time Dependent Solution of Boltzmann Equation in
Self-sustained XeCl Discharges Coupled to Plasma
Chemistry and Circuit Equations, C. GORSE and M.
CAPITELLI, U. of Bari, Centro Studio Chimica Plasmi
(CNR) --Time dependent Boltzmann equation, including
electron-electron and superelastic collisions, coupled
to plasma chemistry and circuit equations has been
solved for a self-sustained XeCl discharge. The main
results can be summarized as follows 1) the time
dependent solution of Boltzmann equation is necessary
during part of the temporal evolution specially when the
electric field drops to small values 2) superelastic
vibrational and electronic collisions play a non
negligible role during the laser action. The accuracy of
the code has been tested by comparing theoretical
results with the corresponding experimental ones
obtained in the National Laboratory of Frascati, showing
in general a satisfactory agreement for the behaviour of
laser output i) versus charging voltage (30 V₀ 50kV)
at fixed pressure (P=3atm) ii) versus pressure (1.5 P
3 atm) at fixed charging voltage (V₀=45kV).

NA-19

Study of UV and VUV fluorescence of high pressure rare gases excited by dielectric controlled discharge : third continuum of Argon *, C. Cachoncinlle and J.M. Pouvesle, CNRS/University of Orléans, France, and F. Davenloo, J.J. Coogan and C.B. Collins, The University of Texas at Dallas -- We report the observation of the third continuum of Argon centred at 188 nm (FWHM \approx 20 nm) in plasmas excited in high pressure (100 to 4000 torrs) Argon and Argon-reactant gas mixtures by fast high voltage pulses in a dielectric controlled discharge. The effect of various reactants, such as He, Xe, N₂ and H₂, on the fluorescence yield and decay has been studied leading to the determination of the corresponding rates. In contradiction to what has been reported previously (1), under our discharge conditions, the presence of large amounts of helium doesn't affect significantly the argon fluorescence in that domain. This and other experimental results necessitate a reexamination of the last assignment (1) of the origin of this third continuum to a transition between Rg²⁺Rg and Rg⁺Rg⁺ molecules. Analysis is presently in progress.

* Work supported in part by NATO grant n° 890508.

(1) H. Langhoff, Optics Comm., 68, 31 (1988).

NA-20

Model of electrons, ions, and fast neutrals in H₂ at very high E/n, A.V. PHELPS, JILA, University of Colorado and NIST. -- Previously assembled¹ cross sections and swarm coefficients for electrons, H⁺, H₂⁺, H₃⁺, H, H₂, and H⁻ in H₂ are used to model the current growth and spatial dependence of light emission for low current discharges in H₂ at very high E/n. At E/n < 1000 Td the H₃⁺ ion is dominant, but for E/n > 3000 Td H₂⁺ ions are dominant. The H⁺ to H₃⁺ ratio² increases with E/n to about 30% at 1000 Td. H⁻ ions can be neglected. At E/n > 10 kTd the predicted excitation of Balmer- α emission is primarily by fast H₂ and fast H. The predicted spatial dependence of the H₂ a³ Σ_g^+ \rightarrow b³ Σ_u^+ , near UV transition by electrons peaks sharply near the cathode and is very small elsewhere. This result is inconsistent with measurements³ for D₂ and with initial data⁴ for H₂. We propose that this UV excitation is caused by fast H or H₂ collisions with H₂.

¹A.V. Phelps, Int. Conf. Physics of Electronic and Atomic Collisions, New York, July, 1989.

²J. Fletcher and H. A. Blevin, J. Phys. D 14, 27 (1981).

³B.M. Jelenković and A.V. Phelps (unpublished).

⁴Z.Lj. Petrović and A.V. Phelps, 1989 Gaseous Electronics Conference.

NA-21

Density Measurement of the Metastable Hg(6^3P_2) in a Hg-Ar Low-Pressure Discharge. P. MOSKOWITZ, GTE Products Corp., Danvers, MA 01923 -- The radial density distribution and absolute density for the 6^3P_2 metastable level of mercury in the positive column of a low-pressure mercury-argon discharge has been measured using the modulated linear absorption (MLA) method.¹ The 6^3P_2 level is one of three closely spaced levels ($6^3P_{0,1,2}$) that play a crucial role in the operation of a fluorescent lamp. Knowledge of the metastable state density can aid in the validation of models for fluorescent lamps. In the MLA technique, the output of a tunable dye laser is split into pump and probe beams. The pump is 100% modulated, and saturates the atomic transition of interest, while the weak probe intersects the pump at right angles inside the discharge. Synchronous detection of the probe yields pinpoint density information at the intersection zone, obviating the need for Abel inversion of the data. This reduces the error propagation and inherent uncertainties associated with Abel inversion. Model predictions and experimental results² for the density of Hg(6^3P_2) have recently appeared in the literature. Densities measured under varying discharge conditions are compared with these published results.

1 P. Moskowitz, Appl. Phys. Lett. 50(14), 891 (1987)

2 J. T. Dakin and L. Bigio, J. Appl. Phys. 63, 5270 (1988)

NA-22

Study of Negative Ion Formation by Electron Impact on Dichloromethane, Toluene, Xylene and Trichloroethane,* C. TIMMER and S.K. SRIVASTAVA, Jet Propulsion Laboratory, California Institute of Technology -- A crossed electron beam and molecular beam collision geometry has been employed to study the process of negative ion formation from the above molecules. Cross section data on these molecules are not readily available. It is found that both dissociative attachment of electrons and polar dissociation are responsible for the production of negative ions. In the case of dichloromethane and trichloroethane, the cross sections are very large for the appearance of Cl^- (masses 35 and 37). Cross sections for the production of the various negative ions from toluene and xylene are small. The various negative ion spectra and cross sections will be presented at the conference.

*Work supported in part by Environmental Protection Agency.

NA-23

Plasma Line Broadening in Molecular Spectra in D.C. Glow Discharges, W. T. CONNER and R.C.WOODS, U. of Wisconsin-Madison--Certain nearly degenerate molecular states can be perturbed by the modest plasma densities in glow discharges. We have studied the millimeter wave rotational spectra of the *l*-doublets of HCN and HCO⁺ in excited states of their bending vibrations. These transitions are much broader and weaker than their unperturbed counterparts, due to their fast Stark effect. This broadening was measured as a function of plasma density. Models of this effect based on the impact and quasi-static limits have been developed. The impact approximation is favored, for both ions and electrons, on theoretical grounds and is supported by the data. Surprisingly, the quasi-static model simulates the observed spectra fairly well too. We have also applied both models to atomic oxygen, see the poster *Line Broadening in Laser-produced Oxygen Plasmas* by L. S. Dzelzkalns et.al.

NA-24

Stark Broadening in High Pressure Helium Plasmas -L.W. Downes, S.D. Marcum and W.E. Wells, **Miami University, Oxford OH**, and J.O. Stevefelt, **GREMI, Université d'Orleans, France**--We have investigated the electron, atomic (2^3S) and molecular ($2^3\Sigma$) metastable densities in high pressure (100 - 4000 Torr) helium plasmas during the discharge and afterglow periods of a long pulsed (900 ns) electron beam discharges (250 KeV, 10 A/cm²). Using the broadening of the 388.9 nm ($2^3S \rightarrow 3^3P$) line and removing the pressure broadened and instrument (gaussian) components, we have found the lorentzian that fits the Stark broadened spectrum. Those fits suggest electron densities in the range of 10^{14} - 10^{15} cm⁻³. Metastable densities were also determined from the lorentzian fit to the lines. We present the results of the study along with the pressure broadening parameters for high pressure helium plasmas. Comparisons with calculated densities from a kinetics model of such plasmas are also presented and discussed.

NA-25 The Effect of Radiative Cascade on Cesium Excited State Populations in Thermionically Assisted Ar-Cs Discharges.* M.L. TACKETT, S.D. MARCUM, **Miami University, Oxford, OH**, B.N. GANGULY, **AFWAL, WPAFB, OH** -- A model has been constructed that allows calculation of cesium excited state densities in low pressure (0.1 Torr Cs, 2 Torr total pressure) Ar-Cs discharges that use a heated cathode (700-1200 K). The model assumes that the dominant creation processes are electron impact excitation from the ground state and radiative cascade from higher levels while destruction is by spontaneous emission. Results are reported for the range $N_e = 10^8 - 10^{11} \text{ cm}^{-3}$ and $T_e = 2000 - 4000 \text{ K}$. The model indicates cascade contributions to excited state densities in the range of 30% for a number of cesium levels. Predicted emission spectra show similar cascade contributions to line emission intensities and agree well with measured spectra. Electron temperatures and densities based upon comparison of predicted and measured spectra are presented and discussed.

*Work supported by U.S. Air Force (WPAFB).

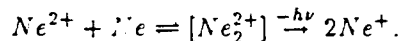
NA-26

A Study of the Influence of 3P_2 population of Mercury on the Electron Temperature in a Hg-Ar rf discharge, L. Maleki, B. Blasenheim and G. Janik, Jet Propulsion Laboratory-- We have studied the influence of laser irradiation on the line emission of an rf excited mercury-argon discharge. The discharge is produced by inductively coupling rf power to a closed cell containing a small amount of Hg and Ar at 1 Torr of pressure. The laser excites the $7 \ ^3S_1$ level of mercury from the 3P_2 metastable level. The influence of the depletion of the metastable population on the discharge parameters is determined through monitoring changes in the intensity of lines present in the discharge emission. By examining this effect we have determined that: 1) electron impact excitation from 3P_2 level is the dominant mechanism for the excitation of upper levels in neutral mercury, but not in the singly ionized mercury or neutral argon; and 2) depletion of metastable population by laser light closes the excitation channel mentioned above and thus increases the electron temperature in the discharge.

The Research described in this paper was carried out by the Jet Propulsion Laboratory, California Institute of Technology, under a contract with NASA.

NA-27

Multiply Charged Noble Excimers, P. D. HAALAND and R. A. DEEMER, Air Force Institute of Technology - Radiative charge transfer from He^{2+} to He has been experimentally probed by Johnson *et al.*^a and theoretically characterized by Cohen *et al.*^b The quantum constraints on radiative charge transfer from heavier multiply charged ions are less well defined. We report the results of *ab initio* electronic structure calculations for the reaction of Ne^{2+} with Ne :



Potential energy surfaces, transition moments, and the implications of radiative charge transfer kinetics for the extraction of stimulated vacuum ultraviolet radiation will be described.

^aR. Johnson and M. Biondi, *Phys. Rev.* **A18**, 194 (1978)

^bJ. Cohen, J. Wadehra, and J. Bardsley, *Phys. Rev.* **A18**, 996, 989 (1978)

NA-28 Global Potential Energy Surfaces of H_2Cl^+ and Comparison with Experiments Th. Glenewinkel-Meyer, P. Knowles¹, Ch. Ottinger, P. Rosmus² and H.J. Werner³ MPI für Strömungsforschung, Göttingen, FRG

The three lowest H_2Cl^+ -PES of A' -Symmetry were calculated using the *ab-initio* MCSCF (CAS) and MR-CI approaches. The Gaussian basis set for the H atom consisted of 10 s-functions (Huzinaga) and additional 4 p- and 2 d-functions; for the Cl atom a slightly modified and augmented Partridge 17-12 basis set was used combined with additional 4 d- and 2 f-functions. This set was contracted to Cl [7s,7p,4d,2f], H [7s,4p,2d]. The calculations were done pointwise for H-Cl distances ranging from 2 to 6 bohrs at 0.2 bohr intervals. For different C_s geometries, e.g. $\angle HClH = 90^\circ$ and $\angle HClH = 175^\circ$, the behaviour of the three PES was studied. In particular, the presence and location of conical intersections was investigated.

Experiments done in our group on luminescent charge transfer of $H^+ + HCl(X^1\Sigma^+)$ were compared to the theoretical results. The observed high rotational excitation of the product $HCl^+(A^2\Sigma^+)$ at low collision energies is due to an avoided crossing which allows the reaction to take place only in a bent configuration, with an HClH angle somewhere between 60° and 100° .

¹U. Cambridge, UK; ²U. Frankfurt, FRG; ³U. Bielefeld, FRG

NA-29 Formation of XeCl and Xe₂Cl During Three Body Recombination of Xe₂⁺ and Cl⁻, W. L. MORGAN, JILA, Univ. of Colorado & NIST and Kinema Research, Monument, CO 80132 and D. R. BATES, Queen's University of Belfast--Recent measurements¹ have shown XeCl to be a product of the three body recombination of the xenon dimer ion and the chlorine negative ion. This is in contrast to the conventional wisdom where we would expect the molecular ion to simply recombine to form Xe₂Cl. We have performed many body Monte Carlo simulations of the trajectories of Xe-λe⁺ and Cl⁻ as a function of pressure in a xenon buffer gas in order to study the recombination process. We find for low pressures that enough energy is gained between collisions with the background gas to rotationally excite and eventually dissociate the Xe₂⁺ ion; this leads to XeCl being a more probable recombination product than it might otherwise be.

¹S.P. Mezyk, R. Cooper, and J. Sherwell, submitted to J. Phys. Chem.

NA-30 Radiation Trapping under conditions of Low to Moderate Optical Depth,* T. COLBERT and J. HUENNEKENS, Lehigh U. --We have studied trapping of resonance radiation under conditions of moderate to low line-center optical depths in sodium argon mixtures. We report measured effective radiative decay rates which are compared to predictions of the Post and the Milne theories of radiation trapping. These theories are expected to be valid for lineshapes with low to moderate line-center optical depths, where the Holstein theory of radiation trapping is expected to break down. The experiment is performed under conditions where the radiation trapping is dominated by either the Doppler-broadened Gaussian or by an impact-broadened Lorentzian lineshape function. The measured effective radiative rates agree well with rates predicted by the theories over the range of low to moderate optical depths.

*Work supported by GTE Laboratories Inc., General Electric Corporate Research and Development, and the National Science Foundation under grant PHY-8451279.

NA-31

Collisional Relaxation of $\text{NH}(^3\Sigma^-, v=1-2)$ by N_2 and H_2 , * D. J. FLANAGAN, S. J. LIPSON, J. A. DODD, and W. A. M. BLUMBERG, Geophysics Laboratory (AFSC), J. PERSON and B. D. GREEN, Physical Sciences Inc.,-- The rate constants for the relaxation of vibrational levels $v=1$ and 2 of $\text{NH}(^3\Sigma^-)$ by N_2 and H_2 have been measured. Vibrationally-excited NH was produced by the $\text{N}(^2\text{D})+\text{H}_2$ reaction in N_2/H_2 mixtures irradiated by a pulsed 35 keV electron beam in the GL LABCEDE facility. Time-resolved spectra of NH fundamental band emission were observed using a slow-scanning Michelson interferometer. Time-resolved histories of the populations of NH vibrational levels $v=1-3$ were obtained using a synthetic spectral fitting code. Rate constants for the relaxation of vibrational levels $v=1$ and 2 by N_2 and H_2 were determined from the population histories by kinetic modeling. Additional kinetic analysis was required to infer the effects of quenching by beam-created N and H atoms. These results are important for predicting the IR spectra of NH produced by combustion processes.

*Supported by the Air Force Office of Scientific Research.

SESSION NB

3:45 PM - 5:16 PM, Thursday, October 19

Hyatt Rickeys Hotel - Camino Ball Room D

NOVEL PLASMAS

Chair: C. B. Fleddermann, University of New Mexico

NB-1

Relativistic Plasmas Produced by Intense Lasers,* J. N. BARDSLEY and B. M. PENETRANTE, Lawrence Livermore National Laboratory -- The quiver motion of electrons in the focal regions of intense lasers can be disturbed significantly by space-charge forces and spatial inhomogeneities in the laser field. Independent-electron simulations of these effects have been performed¹, and a multi-electron particle-in-cell code has been developed. These codes are being applied to analyze laser-induced nuclear reactions, the production of high-order harmonic radiation, and the use of short-pulse lasers to pump short-wavelength recombination lasers.

*Work performed under the auspices of the U.S. Department of Energy by the Lawrence Livermore National Laboratory under Contract No. W-7405-ENG-48.

¹J. N. Bardsley, B. M. Penetrante and M. H. Mittleman, Phys. Rev. A 40 (1989) in press.

NB-2

Wide Area Disc Shape Plasma Source for Energy Assisted CVD,* Z. YU, T. SHENG, H. ZARNANI, B. PIHLSTROM and G. J. COLLINS, Department of Electrical Engineering, Colorado State University, -A wide area disc shape plasma source up to 20 cm in diameter is generated by a ring cathode electron beam. VUV photons, excited species, and radicals created from the disc plasma can all assist dissociation of chemical vapor deposition feedstock reactants via volume photo-absorption and sensitized atom-molecule collisions, respectively. In addition, the excited radical flux and VUV impingement on the film may also assist heterogeneous surface reactions and increase surface mobility of absorbed species. Microelectronic thin films including amorphous silicon, AlN and Si₃N₄ have been deposited at temperatures between 100°C-400°C. The deposited films show significant improvement over other photo-assisted CVD processes in the film quality, low substrate temperature and the maximum deposition rates achieved.

*Work supported by National Science Foundation, Naval Research Laboratory and Applied Electron Corporation.

NB-3

Plasma Processes in Soft Vacuum Electron Beams Used for Microelectronic Film Processing, G. J. COLLINS, Colorado State University -- Soft vacuum (0.05 ~ 3 Torr) glow discharge generated electron beams are employed to create a large area plasma for assisting chemical vapor deposition (CVD) of microelectronic thin films, zone melt recrystallization, hardening of polymer films, and pattern definition in polymer films. The electron beams are operated on both a continuous and a pulsed (20-100 nsec) basis. The electron beam spatial intensity and energy profiles have been quantified from generation in the cold cathode sheath to impingement on the substrate surface for each unique application. The properties of electron beam assisted CVD films are cataloged and compared to conventional plasma assisted CVD films. Zone melt recrystallization silicon films are compared to those using conventional strip heaters. Submicron features ($\sim 0.5 \mu\text{m}$) from a stencil mask have been transferred into PMMA by the pulsed electron beam. Pulsed electron beam hardening of AZ-type resist patterns were also achieved with hardened resist patterns stable to the temperature up to 350°C .

NB-4

Electron Beam Generation by Electron Bombardment Induced Cathode Emission,^{*} B. SZAPIRO, C. MURRAY, and J.J. ROCCA, Electrical Engineering Department, Colorado State University—We have demonstrated that intense pulsed electron beams can be created by multiplication of a lower current density primary beam impinging on a high electron yield target. A 17 A electron beam of 1 μs pulse width was generated from a 2.5 A beam bombarding an activated Ag-Mg alloy target 2.5 cm in diameter at an energy close to that required for maximum emission of secondary electrons. The surface activation technique for Ag-Mg is similar to the one used for photomultiplier tubes, providing reproducible yields greater than 5 that remain stable under bombardment by the intense (A/cm^2) primary beam. The maximum electron beam current densities were limited by the onset of electron current oscillations probably associated with the development of beam-plasma instabilities.

^{*} Work supported by Wright Research and Development Center.

NB-5

The Effects of adding Xe to a H₂ Discharge. A.A. Mullan, University of Ulster, Coleraine, N. Ireland and W.G. Graham, Queen's University, Belfast, N. Ireland

Recently in attempting to understand the basic processes producing negative hydrogen ions in intense ion sources and in trying to optimize the total negative ion production, small percentages of other gases have been added to the hydrogen discharges and the changes in the extracted positive and negative ion concentrations monitored¹. We have now measured the plasma parameters and the relative positive and negative ion concentrations in a hydrogen multipole filament driven discharge with additional small percentages of Xe gas. The main features of the present results are the increased electron density, electron temperature and plasma potential when Xe is added. This latter effect is important in interpreting our mass spectrometry data.

1. K.H. Leung et al. Rev. Sci. Instrum. 56, 2097 (1985) and S.R. Walther et al. J. Appl. Phys. 64, 3424 (1988).

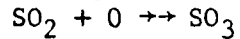
NB-6

Removal of SO₂ from Flue Gases Using Combined Plasma and Optical Processing.* Jeanne H. Balbach, Mark J. Rood and Mark J. Kushner. University of Illinois, Urbana, IL. Combined plasma photolysis (CPP) is a method that has the potential to remove SO₂ from flue gases at lower capital and operating costs, with a higher degree of safety, and higher electrical efficiency than current methods. CPP consists of a device that produces a pulsed discharge in the flue gases (Air/H₂O/SO₂/NO_x =90/10/10⁻³/10⁻³) followed by irradiation with UV photons. The irradiation photolyzes O₃ producing O(¹D). Further reaction with H₂O forms OH radicals which react with SO₂ to form H₂SO₄. This acid reacts with NH₃ to make a particulate material which is easily removed with filters. The plasma chemical reactions that occur between the gas phase radicals and SO₂ as a result of CPP are numerically simulated. The results of the model are compared to experimental results.

*Work supported by Advanced Environmental Control Technology Research Center.

NB-7

Plasma Oxidation of SO₂ in Flue Gas,* S.K. DHALI and I. SARDJA, Southern Illinois University -- The experimental results of the removal of SO₂ from a synthetic flue gas using a dielectric-barrier discharge will be reported. The dielectric-barrier discharge is an efficient means for producing atomic oxygen by electron impact. A high voltage line transformer is used for power, and the discharge geometry is co-axial. The following reactions accounts for the reduction of SO₂ concentration in the flue gas:



A typical measurement shows a 65% reduction in SO₂ concentration for a sample gas of 6400 parts per million of SO₂ in air. We will report the results of SO₂ removal for different flows, gas mixtures, and applied voltage. Also, we will report the results of emission and spectroscopy of atomic oxygen.

*Work supported by DOE.

SESSION P

7:30 PM - 10:00 PM, Thursday, October 19

Hyatt Richeys Hotel - Camino Ball Room C and D

CROSS SECTIONS I WISH I KNEW

Chair: C. C. Lin, University of Wisconsin

P-1

Cross Sections of Great Interest to Aeronomy and Astrophysics. * J. P. Doering, Dept. of Chemistry, Johns Hopkins U.

-- The need for electron impact cross sections in aeronomy and astrophysics arises from the ubiquitous nature of electron collision processes. In environments as different as the thermospheres of the planets and supernova remnants, excitation by electrons is controlled by the interaction of the ambient electron energy distribution with the available atomic and molecular species. The ambient electron energy distribution is in turn produced by the balance of electron production and loss functions where the production mechanism can be either photoionization or impact of high energy particles accelerated by electromagnetic fields. Understanding of the loss function requires knowledge of electron inelastic cross sections and emission cross sections are necessary to predict the observed radiation. Cross sections can be divided into those which are possible, very difficult, or probably impossible to measure in the laboratory depending on the nature of the species excited. Present work will be reviewed and examples of each class will be given to stress the need for cooperative experimental and theoretical work.

*Work supported by NSF Grant ATM-8605992.

P-2

Cross-sections I Wish I Knew in Discharge Light Sources. JOHN F. WAYMOUTH, 16 Bennett Rd, Marblehead, Mass 01945. Highly sophisticated computer models are available for most electric discharge lamps. In low pressure discharge lamps, such as the Hg-RG fluorescent lamp, and the low-pressure sodium lamp, most of the ionization and much of the excitation of upper energy levels occurs stepwise via resonance or metastable states. There is very little experimental data on the necessary cross-sections. Similarly, in some parameter ranges, associative ionization is significant; only a few of the cross-sections are known. In metal halide high-pressure discharge lamps, diffusion of molecules, radicals and atoms through mercury vapor controls species concentrations in the arc. There is no experimental data on diffusion coefficients. To calculate rate processes for which cross-section data is absent, models use everything from quantum-theoretical calculated values to outright guesses.

P-3

Electron-Molecule Collision Cross Section Needs for Etching Gases*, KURT H. BECKER, City College of New York -- It is the objective of the presentation to give an assessment of the electron impact cross section needs for molecules that play an important role in the areas of plasma etching and deposition. Two aspects will be addressed. Firstly, an attempt is made to identify and categorize those target molecules for which cross section data are needed most regularly. Secondly, the current availability of cross sections and the future needs for particular types of cross sections will be discussed in detail for each molecule.

* Work supported by NSF-CBT and PSC-CONY.

P-4

Cross Section Needs for Modeling Etching and Deposition Discharges, L. E. KLINE, Westinghouse STC, Pittsburgh, PA 15235 -- Many gases are used in plasma processes for microcircuit fabrication. Plasmas are used for both etching and thin film deposition. The gases used include halogens, freons, silanes as well as the rare gases and H_2 , N_2 , NH_3 , N_2O and O_2 . Cross section data is available for H_2 , N_2 and O_2 . Recent cross section, swarm and discharge dissociation measurements and theoretical studies have provided cross sections for HCl , Cl_2 , CH_4 , CF_4 , SiH_4 , CCl_2F_2 , SF_6 , C_2H_6 , C_2F_6 , Si_2H_6 and N_2O . The available data suggest that electron impact neutral dissociation, where the dissociation products are all in their ground electronic state, is a key channel in for chemical activation of N_2 , O_2 , CH_4 , CF_4 , SiH_4 , SF_6 , and N_2O . The neutral dissociation rate is comparable to or larger than the dissociative ionization rate for these gases. Neutral dissociation is also likely to be important for many of the other feed gases used in plasma etching and deposition. The limited available data and the data needs for this important process will be reviewed.

P-5

Cross Sections and Moments of Importance

A. GARSCADDEN, Wright Research and Development Center, Wright-Patterson AFB, OH--The relevance of, and need for low energy electron collisional cross sections for plasma processing applications are illustrated by their influences on the electron energy distribution function (EEDF) and the subsequent excitation, dissociation and ionization rates. Low energy ion collisions such as dissociative charge transfer are also important in plasma reactors. In many situations there is a need for information on the cross sections of the principal products of dissociation, the volatile products of surface reactions, and of complex molecules used in processing. Adding to the difficulty is the fact that one is really interested in data for excited gases, especially vibrationally excited gases. Self-consistency tests of the data are emphasized, especially when the cross sections are derived from different experiments. In order to maintain contemporary relevance to the technology, the need to measure other non-traditional moments of the distribution function is outlined.

P-6

A Status Report on the Availability and Needs of Electron Impact Cross Sections for Modeling Plasma Deposition *Mark J. Kushner, University of Illinois, Urbana, IL -- Reliable electron impact cross sections for momentum transfer, attachment, electronic and vibrational excitation, dissociation and ionization are prerequisites for developing models of plasma deposition systems. We will briefly review the availability of cross sections for deposition of silicon and carbon films. Gas mixtures containing silane, disilane, methane, and higher hydrocarbons, and typical additives (e.g., H_2 , N_2O , O_2 , NH_3 , PH_3 , BH_3) will be discussed. The availability and need for partial cross sections and cross sections for electron-radical processes will also be discussed.

*Work supported by the National Science Foundation.

SESSION QA

8:00 AM - 9:39 AM, Friday, October 20

Hyatt Rickeys Hotel - Camino Ball Room C

SINGLE WAFER PLASMA PROCESSING

Chair: J. H. Keller, IBM, East Fishkill

QA-1

ECR and Other High Density Plasmas for Single Wafer Plasma Processing, W.M. Holber and J. Forster, IBM T.J. Watson Res. Ctr. and East Fishkill, -- The trend in plasma processing for semiconductor applications has been towards higher plasma density, lower neutral pressure operation. This is driven by several different requirements. Single wafer operation requires far greater rates than for batch tools - in order to maintain reasonable throughput for manufacturing. Submicron features require tighter control over etch and deposition profiles. Finally, more delicate and complex structures require that the energy of ion bombardment be minimized. The challenges of higher plasma density, lower neutral pressure, and lower ion energies have been addressed primarily through the use of magnetized plasmas - both in the MHz and low GHz frequency regime. Particular emphasis will be placed in this talk on Electron-Cyclotron-Resonance (ECR) plasmas, operating at 2.45 GHz. Results obtained in a divergent magnetic field ECR system will be reported. It has been found that plasma densities up to 10^{12} cm⁻³ can be achieved with uniformities required for single-wafer processing. Several unique features of such plasmas will be discussed.

QA-2

RF Excited Diffusion Plasmas, R.W. BOSWELL, PRL, RSPHYS5, Australian National University - With appropriately designed extended antennas rf power from 2 to 20 MHz can be used to create large volumes of high density plasmas at low pressures ($< 10^{-2}$ Torr). Peak densities of $\sim 10^{14}$ cm⁻³ at a few 10^{-3} Torr argon have been achieved in 5 cm diameter sources. With larger sources coupled to a diffusion chamber surrounded by permanent magnets, ion current densities of a few ω A cm⁻² uniform over a 20 cm substrate have been measured in O₂, SF₆, CHF₃ and SiCl₄. Etch rates for Si, SiO₂, GaAs, Al and resist are between 0.5 and 1.0 μ m min⁻¹ for gas pressures of $\sim 10^{-3}$ Torr and rf powers between 500 and 1000 watts. The substrate bias voltage can be varied independently of the plasma density thereby minimizing ion induced damage. The system can operate without metallic containments. The theory and operation of this type of plasma will be reviewed.

QA-3

Low Pressure RIE using an RF Plasma Source with Surface Magnetic Confinement - A. Wendt, M. H. Cho, N. Hershkowitz, and H. Persing, University of Wisconsin, Madison. Reactive ion etching (RIE) of silicon in CF_4-O_2 and SF_6 plasmas using an RF, capacitively coupled, multidipole magnetic confinement plasma system will be reported. Our investigation of RIE at low pressures ($\sim 10^{-4}$ Torr) addresses processing concerns as microelectronic devices become smaller, faster, and packed more densely on an IC. Etch rates and trench etch profiles will be presented for a range of processing and plasma conditions (etch chemistry, pressure, flow rate, plasma density, and substrate bias). Etching of Si has been carried out with Al, SiO_2 , and photoresist etch masks with feature sizes as small as $0.8\mu m$. Attention will be given to the advantages and limitations of low pressure etching.

*Work supported by NSF

QA-4

Characteristics of Inductively Excited Discharges with a Drift Space, P. Bletzinger and M. E. Dunnigan, Wright Research and Development Center WPAFB, OH. For applications in plasma etching and thin film deposition the parallel plate reactor does not offer separate control of plasma density and ion energy. This can be achieved with a microwave exciter (ECR) and an added DC or rf drift field. We have investigated a simpler system using an inductor (3" dia. by 3" length) over a section of a 2" dia. glass tube with electrodes spaced 2" away from the inductor ends. With one tube, permanent magnets in multipole configuration were placed inside the inductor. Using the electrodes with an applied sweep voltage, the collected current peaks at .3 Torr, decreasing slowly at higher pressures but increasing monotonically with power ($40mW/cm^3$ max). Using time averaged double probes will allow more accurate electron density measurements and permit measurements at higher power. We hope to also report on time resolved single probe measurements.

QA-5

RF Induction/Multipole LPSWE System, J. H. Keller
IBM - E. Fishkill, Hopewell Jct., NY -- A low pressure single wafer etching system has been designed and tested. The plasma is inductively excited with 13.56 MHz rf power and the wafer is rf biased. This gives independent control of the plasma density and ion energy. The wafer is electrostatically clamped and cooled with helium. The plasma is surrounded in the radial direction by a multipole magnetic field which confines the plasma electrons thus producing a uniform plasma. Ion densities of approximately 5×10^{11} /cc and ion currents of 1 amp over a 125 cm wafer have been achieved in both electro-positive and electronegative gases, in the 1 to 20 mTorr pressure range¹. Uniformities of 7% (3 sigma) and etch rates of over 1 micron / min have been achieved for both Si and SiO₂. RF induction is a very simple and efficient means of producing high plasma densities. It is competitive with both Magnetron and ECR type plasmas but does not have the problem of a magnetic field at the wafer. In the rf induction mode (no rf bias power) the floating potential and plasma potential are typically 13 and 30 volts respectively.

¹ Ajit Paranjpe, to be published.

SESSION QB

8:00 AM - 9:30 AM, Friday, October 20

Hyatt Richeys Hotel - Camino Ball Room D

COLLISIONS BETWEEN ATOMS, MOLECULES, AND IONS

Chair: J. R. Peterson, SRI International

QB-1

IR Excitation Cross Sections from Fast O-Atom Collisions,^{*}
G.E. CALEDONIA, B.L. UPSCHULTE, R.H. KRECH, and B. CLAFLIN,
Physical Sciences Inc., and G. BURGESS, MIT/Lincoln Laboratory --
Experimental measurements of the cross sections for vibrational
excitation of molecules by energetic oxygen atoms have been suc-
cessfully performed. A crossed molecular beam apparatus utilizing
both a supersonic target molecular beam and a fast O-atom source
was developed for these measurements. The fast O-atom source is
generated by focusing a high power pulsed CO₂ laser into a nozzle
containing expanding molecular oxygen. Inverse Bremsstrahlung
absorption of the 10.6 μm radiation produces a laser breakdown of
the O₂; dissociation, and ionization occurs very rapidly. The
nozzle expansion is tailored to provide sufficient time for ion-
electron recombination but insufficient time for atomic recombina-
tion. Instantaneous fluxes of 10²² atoms/cm²s with velocities
variable throughout the 6 to 10 km/s range have been obtained. The
target molecular beam was generated from a pulsed free jet expan-
sion. A calibrated radiometer, utilizing an InSb detector and
bandpass filters, viewed the collision perpendicular to the inter-
secting beams. A circular variable filter (CVF) radiometer was
used to provide spectral bandshapes. Measurements were performed
with CO, CO₂, CH₄, and H₂O target beams in the single collision
regime. Cross section and reaction path observations are
discussed.

^{*}This work was sponsored by the Department of the Army under con-
tract number F19628-85-C-002. The views expressed are those of
the author and do not reflect the official policy or position of
the U.S. Government.

QB-2

The Dependence of Spacecraft Glow On the Spacecraft Velocity,
R.E. MEYEROTT AND G. R. SWENSON, Lockheed Palo Alto
Research Laboratory -- The extent to which spacecraft glow depends on
the spacecraft velocity, and hence the kinetic energy of the ramming
participants to the spacecraft surface recombination reactions, has a large
impact on the difficulty in conducting laboratory simulations. If the
dependence on the kinetic energy is minimal, as suggested by Kofsky
and Barrett, then much of the previous work on recombination catalyzed
by laboratory substrates can be applied with any little modification.
However, if the kinetic energy is an important part of the glow
producing mechanism, laboratory reactors will require intense sources
of atoms and molecules with kinetic energies of up to ~10eV. Such
sources are difficult to constrict.

The pseudo-continua red spacecraft glow in the 0.4 to 0.8μm is
believed by many investigators to be due to the surface recombinations
of O and NO atoms to form excited NO₂. However, this glow has a
spectral distribution that does not completely agree with that produced
by three body gaseous recombination or by low energy surface
recombination. A model for the N₂ Lyman-Birgel-Hopfield spacecraft
glow will be presented in which the upper state of the LBH bands is
populated by radiation transition from higher levels. The higher levels
are populated as a consequence of the high kinetic energy of incident N
atoms. The model predicts additional radiations that are associated with
the LBH glow. The application of this model to the red glow will be
discussed.

QB-3

Ion and Fast Neutral Excitation in N₂ at Very High E/n, * V.T. GYLYS** and A.V. PHELPS, JILA, University of Colorado and NIST. -- Measurements are made of the pressure dependence of the time integrated emission of the 1st and 2nd positive bands of N₂ at 670 and 337 nm and the 820 nm line of NI following a photon initiated, pulsed discharge through N₂ at E/n = 52 kTd. The pressures are 10 to 35 mTorr, i.e., well below the 60 mTorr at breakdown. The photocurrent pulse is ≈ 10 mA for ≈ 10 ns. The emission is normalized to the time integrated 391 nm emission of the N₂ 1st negative band which is excited only by electrons.¹ The 337 to 391 nm emission ratio is proportional to the N₂ density at low pressures as expected for 337 nm excitation in N₂⁺ collisions with N₂, but increases more rapidly at higher pressures as is consistent with efficient excitation of N₂ by fast N₂. The relatively rapid increase with pressure of the ratios of 670 nm and 820 nm emission to 391 nm emission are not yet understood.

* Supported in part by Lawrence Livermore Laboratories.

** Now at Rockwell International/Rocketdyne Division, Canoga Park, CA.

¹ V.T. Gyls, B.M. Jelenković and A.V. Phelps, J. Appl. Phys. 65, 3369 (1989).

QB-4

Rotational excitation of N₂⁺ in N₂ at E/n ≈ 100 Td, * JACEK BORYSOW[§] and A.V. PHELPS, JILA, University of Colorado and NIST. -- The rotational temperature of N₂⁺ ions in N₂ drifting in an electric field is measured using the absorption of A²Π(v = 2) ← X²Σ(v = 0) lines near 780 nm. The ions are in a pulsed, positive column discharge with 1.5 Amp cm⁻² current, 10 μs duration, and 0.3 torr pressure. A single-mode, tunable diode laser source propagates parallel to the electric field with an absorption S/N > 10⁵:1 for 1 μs resolution. Densities of rotational levels with quantum numbers up to 20 obey Boltzmann distributions with temperatures of 360 ± 15 K during the discharge and 305 ± 15 K in the afterglow. The change in temperature determined from the higher levels is 57 ± 2 K. The E/n from Doppler profiles¹ and N₂⁺ drift velocities is ≈ 105 ± 5 Td. The ion drift energy corresponds to a temperature of 1200 ± 80 K during the discharge. The results yield the ratio of rotational excitation to charge transfer collisions.

*Supported in part by the Wright Research and Development Center.

[§]Now at Michigan Technological University, Houghton, MI.

¹J. Borysow and A.V. Phelps, Bull. Am. Phys. Soc. 34, 293 (1989).

QB-5

Energy Transfer in the B²Π State of NS, INGRID J. WYSONG, JAY B. JEFFRIES, and DAVID R. CROSLEY, SRI International--Quenching and vibrational energy transfer in the B²Π state of the NS free radical have been studied using temporally and spectrally resolved laser induced fluorescence in a low-pressure discharge flow reactor. The collision partners were He, Ar, H₂, N₂, O₂, SF₆, CO₂, and N₂O. Total removal cross sections show an oscillatory behavior with v' in the range of unperturbed levels, v'=4-7, for all colliders studied save O₂ where a nearly monotonic increase is seen. Significant vibrational transfer occurs for H₂ and the polyatomics; the rates vary little with v'. Δv=2 transfer occurs with the polyatomic colliders for v'=5. Time-resolved fluorescence traces from the perturbed v'=3 and 8 levels differ from the unperturbed levels and from each other: v'=3 is perturbed by quartet states and shows "gateway" transfer behavior, whereas v'=8 is perturbed by a doublet and shows efficient interelectronic transfer for all rotational levels.

Supported by the Air Force Office of Scientific Research.

QB-6

Temperature Dependent Quenching of NO A²Σ⁺ and B²Π by H₂O, GEORGE A. RAICHE, GREGORY P. SMITH, and DAVID R. CROSLEY, SRI International-- Quenching cross sections for electronically excited nitric oxide have been obtained from measurements of the pressure dependence of time decays of laser-induced fluorescence. The temperature range 300-750K was covered using a heated flowing gas cell; gas temperatures were measured using rotational excitation spectra. Results in Å² are given in the table. Although the sizes of the cross sections suggest the influence of attractive forces, only for H₂O collider is there a decrease with increasing temperature (i.e., collision velocity).

Collider	300K: NO	O ₂	H ₂ O	750K: H ₂ O
σ _Q (A ² Σ ⁺)	37	21	103	34
σ _Q (B ² Π)	46	3	17	5

Supported by the U.S. Army Research Office.

SESSION RA

10:00 AM - 11:44 AM, Friday, October 20

Hyatt Richeys Hotel - Camino Ball Room C

RF DISCHARGES: MODELS AND EXPERIMENTS

Chair: M. A. Lieberman, University of California

RA-1

An Experimental System for RF Discharge Physics Research, V.A. GODYAK, R. B. PIEJAK, B. M. ALEXANDROVICH, GTE Laboratories Inc., Waltham, MA -- An experimental system has been designed and built to comprehensively study the electrodynamic and plasma characteristics of capacitively coupled electroded RF discharges at low gas pressures. The system consists of a glass discharge cell, a vacuum station, a controllable gas flow system for precise gas flow, a tuneable matcher-coupler with voltage, current and power sensors, a two channel precision RF power meter, a wideband RF source and RF amplifier and a data acquisition, processing and display system based on a multi-channel waveform analyzer connected to a PC. A previously developed plasma probe diagnostic station has been modified for plasma density and electron energy distribution measurements in this system. The following range of RF discharge parameters can be studied with this system: gas pressure .001-10 Torr, RF power, .01-100 watts, RF frequency .5-150 MHz.

RA-2

Frequency effects in a RF Discharge* M. SURENDRA and D. B. GRAVES, University of California, Berkeley - A study of frequency effects in a RF discharge using a self-consistent particle-in-cell simulation is presented. Electron-neutral interactions are included through realistic differential cross sections for both elastic and ionizing collisions. The importance of secondary electron emission at the electrode in sustaining low frequency discharges (in particular, below the ion plasma frequency) is discussed. At higher frequencies, where the RF sheath velocities can be appreciable, electron heating (stochastic heating or wave riding) by the moving sheaths plays an important role. The different heating mechanisms at the high and low frequencies influence the time dependent behavior of the electron energy distributions. The effects of frequency and pressure on spatial and temporal profiles of the ionization rate are also presented.

*Work supported in part by San Diego Supercomputer Center.

RA-3

DC Self Bias Formation in Symmetric Parallel-Plate RF Glow Discharges, J.W. BUTTERBAUGH and H.H. SAWIN, Massachusetts Institute of Technology - The formation of DC self bias in well-confined, symmetric, parallel-plate RF (13.56 MHz) glow discharges has been investigated. At narrow spacings of 3-4 mm and pressures of 2-6 torr, stable discharge operation in CF₄ is obtained with either a positive or negative self bias on the capacitively coupled powered electrode. It is believed that the presence of negative ions are important in the formation of this electrical asymmetry since the same effect can be observed with a gas feed of 96% Ar and 4% SF₆. The energy and flux of positive ions striking the grounded electrode has been measured by orifice sampling and retarding grid analysis and correlates with the magnitude and sign of the self bias of the powered electrode. Spatially resolved plasma induced emission has also been measured from a small amount of Ar added to the CF₄ discharge indicating the most intense glow nearest the electrode with the higher DC potential.

*IBM Burlington, Resident Study Program

RA-4

The Spatial and Temporal Variation of Plasma Parameters in an rf Discharge. C.A. Anderson, University of Ulster, Coleraine, N. Ireland and W.G. Graham, Queen's University, Belfast, N. Ireland. - Our time resolved Langmuir probe technique has been extended to higher frequencies and used to study the spatial variation of plasma parameters in a rf discharge operating at frequencies of up to 1 MHz. This time resolved technique can be used to investigate the fundamental processes driving the parallel plate discharge. The dependence of the plasma parameters on the gas used, gas pressure, rf frequency and method of driving the electrodes has been studied. Measurements of the electron energy distribution function shows the electron distribution to be non Maxwellian and time dependent. It is found that time averaged measurements tend to overestimate all the plasma parameters particularly the electron temperature and plasma potential when compared with measurements made using the time resolved technique.

¹C.A. Anderson, W.G. Graham, and M.B. Hopkins. Appl. Phys. Lett 52, 783 (1988).

RA-5

Ion Bombardment Angle and Energy in Argon rf Discharges, J. LIU, G.L. HUPPERT, and H.H. SAWIN, M.I.T. -- The measured ion angle distribution shows that a significant portion of bombarding ions impinge at angles greater than 10° from the surface normal, even at pressures below 20 mtorr. The ions with large incident angles have lower energies than those incident perpendicular to the surface. Monte Carlo simulations of the sheath kinetics predict the trends shown in the experimental data for ion energy and angle distributions. Fine structures in the ion energy distribution were observed below 50 mtorr and are attributed to charge-exchange collisions in the sheath. The average energy can be correlated directly to the applied voltage across the electrodes for measured plasma pressures up to 500 mtorr.

RA-6

Particle Modeling of an ECR Reactor,* R. K. PORTEOUS and D. B. GRAVES, Chemical Engineering, U. of California, Berkeley -- The high frequencies and plasma densities which characterize an ECR reactor challenge conventional particle modeling techniques. The electrons must be followed on a timescale of the plasma and cyclotron periods ($< 10^{-9}$ s) while the plasma as a whole comes to equilibrium in 10^{-4} s (around the mean ion residence time). The particle flux to the walls depends on sheaths 0.1 mm thick which in turn depend on the ion diffusion in the whole chamber.

A 2D3V model of a cylindrical ECR reactor has been developed. Electric fields are calculated self-consistently with the motion of ions and electrons, while localized ECR heating is introduced heuristically. Electrons are strongly confined by a uniform axial magnetic field whereas ions are only weakly magnetized. Both electrons and ions may have elastic and inelastic collisions with neutrals. Innovative techniques to handle the disparate time and length scales are introduced. Results showing the effect of the microwaves on the electron velocity distribution will be presented.

*Work supported in part by IBM.

RA-7

Two-Dimensional Simulations of RF Glow Discharges,* J. H. Tsai and C. Wu, Electrical Engineering Department, Auburn University.--Self-consistent two-dimensional numerical simulations of rf glow discharges have been carried out in nonattaching (N_2) and attaching (SF_6) gases using a single moment fluid model. The More Accurate Flux Corrected Transport¹ and Reconstructed Fast Fourier Transform techniques² have been used to solve the fluid and Poisson's equations, respectively, in the presence of large gradients and dynamic range. The Glow discharge in SF_6 has been observed to be considerably different from those in N_2 . The results obtained further illustrate the radial-axial flow dynamics of charged particles.

*Work supported by CRAY Research, Inc.

¹E. E. Kunhardt and C. Wu, J. Comput. Phys. 68, 127 (1987).

²C. Wu and E. E. Kunhardt, J. Comput. Phys. 83, (1989) (in press).

SESSION RB

10:00 AM - 11:43 AM, Friday, October 20

Hyatt Richeys Hotel - Camino Ball Room D

OPTICAL DIAGNOSTICS

Chair: J. T. Dakin, GE Lighting

RB-1

UV Emission from a Discharge in N₂O and Electron Detachment. T.H. TEICH, Swiss Federal Institute of Technology, Zürich. - Determination of discharge parameters/swarm coefficients for gases in which unstable negative ions are formed may present considerable difficulties, particularly when detachment rate coefficients are high as, for instance, in N₂O where the secondary ion NO⁻ is the principal electron donor. Some access to rate coefficients may be gained from the measurement of local light emission from suitable excited states¹. For N₂O, such states were assessed by means of spectrally resolved synchronized single photon counting applied to emission from a Trichel pulse corona discharge. The dominant emission is found to originate from NO(B²Π, v'=0) and is indirectly excited, probably via formation of O('S); the relatively slow decay corresponds to a quenching density of the order of $3 \cdot 10^{17} \text{ cm}^{-3}$ for a B state natural lifetime of 2μs. Besides emission NO (B→X), there are minor shares of emission from N₂O⁺(2Σ) and N₂(C³Π); the latter emission N₂(C→B) occurs promptly and with a fast decay and should thus give access to local electron density data useful for discharge parameter determination.

¹ M.J. Brennan and T.H. Teich, Proc. 9th Int. Conf. Gas Discharges and Their Applications, Benetton Editore, Padova 1988, pp. 343-346.

RB-2

Gas Temperatures from Vibrational Temperatures, M. PASSOW, M. L. BRAKE, and P. LOPEZ, Dept. of Nuclear Eng., U. of Michigan -- Gas temperatures (T_g) of low pressure (0.5 - 100 Torr) microwave (2.45 GHz) discharges in nitrogen can be estimated from measurements of the vibrational temperature (T_v). The dependence of T_v on T_g is calculated by modeling the excitation and de-excitation mechanisms of the vibrational levels. Included in the model are electron excitation, V-V and V-T transfer. The model shows that at low electron densities (10^{10} - 10^{13} #/cc) and low T_v's (<4000K) that T_v and T_g are equal. At higher temperatures (>8000K), T_v is equal to the electron temperature. The T_g's predicted by this model (1000K-2000K) for T_v's measured in a low pressure microwave discharge (5000K - 15,000K) match the measured rotational temperatures very well. Thus, estimates of T_g can be made from T_v and the relationship between the two, without having to go to the extra work to measure the rotational temperature.

RB-3

Temperature Profiles in N₂ and N₂-Ar DC Discharges Using Coherent Anti-Stokes Raman Spectroscopy (CARS). P. P. YANEY and B. L. Epling,* U. of Dayton**; S. W. KIZIRNIS, USAF Aero Propulsion Lab. -- Spatially resolved CARS measurements provided non-equilibrium rotational and vibrational temperature profiles in glow discharges stabilized by glass electrode caps which constrained the discharge to about 10 mm diameter. Both axial and radial profiles were determined. The doorknob-shaped Ni-Fe electrodes were spaced 14 mm. Nominal conditions were 40 Torr total pressure, 0.08 A/cm² and E/N=60 Td. The influence of gas flow rate and changes in the Ar-to-N₂ ratio were studied. The temperatures were obtained from computer fits to spectra recorded with a narrow-band, scanning, folded BOXCARS system. The length of the control volume (dia. \approx 20 μ m) was measured to be 1 mm by scanning a 6 mm by 0.38 mm Ar jet through the beam crossing in air. A computer model of the laser beam geometry agreed with these results.
* In partial fulfillment of the requirements for the M.S. degree in Electro-Optics.
** Supported by USAF Contract F33615-86-C-2722.

RB-4

Time Resolved Two-Dimensional Emission Spectroscopy of a LF Asymmetric H₂ Discharge -- B. N. GANGULY, J. R. SHOEMAKER, and A. GARSCADDEN, Aero Propulsion and Power Laboratory, WPAFB, OH. -- Two dimensional emission intensities of H α and the 540-550nm H₂ molecular band have been measured in a 0.75 Torr H₂ discharge with 4:1 electrode area ratio, driven at 50 kHz, using a time-gated (400nsec) intensified CCD imaging system. The 18mm diameter photocathode (570 X 380 pixels) allows temporal and spatial resolutions simultaneously of the entire powered discharge volume, including behind the electrodes. Nearly symmetric sheaths and negative glows about the front and back surfaces of either powered electrode are observed for abnormal glow discharge conditions. The emission profiles show that the discharge is focussed to the anode, especially when the large electrode is cathode and that there is also simultaneous excitation on both sides of the anode. Decay of the cathodic cycle shows bright plasma regions "trapped" behind the cathode. The presence of strong atomic and molecular excitation in the sheath regions indicates a highly collisional sheath for electrons and ions.

RB-5

Emission spectra of laser produced plasmas used in producing high T_c thin films.
H.F. Sakeek, W.G. Graham and T. Morrow, Physics Department, Queen's University, Belfast, Northern Ireland. The emission from plasmas created during KrF laser ablation of high temperature superconducting material ($YBa_2Cu_3O_7$) has been studied. The aim is to obtain a fundamental understanding of the laser ablation process and to correlate the elemental abundance in the plasma with the stoichiometry of the thin films produced. Currently the spatial variation of the emission lines and its dependence on laser power is being investigated. The effect of operating in an oxygen environment will be studied.

RB-6

Imaging of Laser-Produced Plasmas Using Planar Laser-Induced Fluorescence. P. H. PAUL, M. A. CAPPELLI and R. K. HANSON, Stanford University -- Planar laser-induced fluorescence (PLIF) provides a powerful, non-invasive technique for probing complex, high-speed flowfields with excellent spatial and temporal resolution. We report recent PLIF imaging of Ba and Ba^+ in a laser-produced plasma, obtained by focusing a XeCl laser onto a barium target in vacuo. PLIF imaging is performed using an intensified CCD array and an excimer-pumped dye laser. We discuss the application of laser ablated films to the formation of dense focused neutral atomic beams.

*Work supported in part by AFOSR, Aerospace sciences directorate.

RB-7

Optogalvanic Line Profile of Cu Autoionization Levels, R. SHUKER and M. HAKHAM-ITZHAQ, Physics Dept., Ben-Gurion University, and A. BEN-AMAR, NRCN, Beer-Sheva, Israel -- Autoionization levels are generally very broad, long lived and have characteristic asymmetric line profile, the well known Fano-shape.⁽¹⁾ We present measurements of the lineshape of autoionization levels of Cu atom using pulsed optogalvanic technique⁽²⁾, whereby a discharge response to changes in the level population and electron distributions induced by laser absorption is utilized as spectroscopic tool. We use a 15 nsec, 7 GHz linewidth pulsed dye laser to scan the transition profile of two autoionization transitions of copper. A one cm^{-1} tuning of the dye laser is used across the broad transition profiles. The results exhibit the characteristic Fano-shape for these transitions. This demonstrates the usefulness of this technique in the study of lineshapes and line-profiles.

- (1) U. Fano and J.W. Cooper. Phys. Rev **136A**, 1364 (1965)
- (2) A. Ben-Amar et al., J. Appl Phys Rev. **54**, 1473 (1983)

INDEX OF AUTHORS

A

Aggarwal, I. J-9
 Ajello, J. M. J-25, LB-3
 Alexandrovich, B. M. RA-1
 Alford, W. J. KA-3, LA-3
 Alston, S. J-20
 Alves, M. V. E-1
 Anderson, C. A. RA-4
 Anderson, H. M. BA-7
 Anderson, L. W. LB-4, NA-7
 Anicich, V. G. E-43
 Armstrong, R. A. NA-17
 Awadallah, A. NA-14

B

Bacal, M. E-15
 Bailey, W. NA-9
 Balbach, J. H. NB-6
 Bannister, M. E. E-25
 Baravian, G. E-32
 Bardsley, J. N. BC-3, MA-4, NB-1
 Bartnikas, R. NA-16
 Baston, L. D. J-3
 Bates, D. R. NA-29
 Becker, K. J-21, J-23, P-3
 Beckes, B. R. KB-5
 Bederson, B. LB-6
 Ben-Amar, A. RB-7
 Benjamin, N. J-32
 Benze, J. W. KB-5
 Berlemont, P. E-15
 Bénétruy, P. E-22
 Bhattacharya, A. K. NA-14
 Biblarz, O. E-18
 Birdsall, C. K. E-1
 Bischel, W. K. A-2
 Bjerre, N. E-47, E-48
 Blasenheim, B. NA-26
 Bletzinger, P. QA-4
 Blumberg, W.A.M. NA-17, NA-31
 Bodette, D. E. KA-3
 Boesten, L. E-35, E-36
 Bonham, R. A. J-22
 Bonin, K. D. E-17
 Borysow, J. QB-4
 Boswell, R. W. FB-1, QA-2
 Brake, M. L. RB-2
 Brannon, P. J. KA-4
 Brault, J. W. MA-2
 Brenna, J. T. A-6
 Brown, R. A. J-2
 Brunet, H. FB-2
 Brunteau, J. E-15
 Burgess, G. QB-1
 Burrow, P. D. MB-5
 Butterbaugh, J. W. RA-3

C

Cachoncinlle, C. NA-19
 Calabrese, D. E-45
 Caledonia, G. E. QB-1
 Capitelli, M. NA-18
 Cappelli, M. A. BA-2, RB-6
 Carl, D. NA-5
 Carron, N. J. E-16
 Carter, J. G. MB-6
 Cartwright, D. C. MB-3
 Cecchi, J. L. E-25
 Chang, J. S. J-5
 Chang, P. Y. NA-15
 Chantry, P. J. GB-3
 Chapman, B. J-32
 Chatterjee, B. K. E-41, E-42
 Cho, M.-H. J-7, NA-3, QA-3
 Christophorou, L. G. MB-6
 Chu, H. N. NA-7
 Chu, S. C. MB-5
 Claflin, B. QB-1
 Clark, J. D. J-28
 Clark, R.E.H. J-27
 Clark, S. BB-2
 Colbert, T. NA-30
 Colgan, M. J. E-12
 Collins, C. B. NA-19
 Collins, G. J. J-9, NB-2, NB-3
 Conner, W. T. NA-17, NA-23
 Conrad, J. R. J-12, NA-12
 Coogan, J. J. NA-19
 Corr, J. J. J-30
 Cosby, P. C. CB-2, J-24
 Crosley, D. R. QB-5, QB-6
 Csanak, G. FA-2, J-27
 Czerny, T. E-31

D

Dakin, J. T. J-13
 Darnelincourt, J. J. E-22
 Datskos, P. G. MB-6
 Davenloo, F. NA-19
 Daviaud, S. E-24
 Dawson, J. M. NA-8
 Deemer, R. A. NA-27
 DeJoseph, C. A. J-28
 Denman, C. A. BC-2, FB-5, MB-7
 DeTemple, T. A. KA-1
 Devynck, P. E-15, E-44
 Dhali, S. K. J-19, NB-7
 Diebold, D. NA-3
 Dillon, M. A. E-34, E-35, E-36
 Dodd, J. A. NA-31
 Doering, J. P. P-1
 Downes, L. W. NA-24
 Duffy, M. E. NA-15
 Dunkel, E. A. GA-7
 Dunning, F. B. CB-3
 Dunnigan, M. E. QA-4
 Dyer, M. J. A-2
 Dzelzkalns, L. S. NA-17

E

Eckstrom, D. J. NA-6
Eliasson, B. GA-2
Elizondo, J. M. KB-4, KB-5
Emmert, G. A. E-10
Epling, B. L. RB-3
Ernie, D. W. E-8

F

Fagen, B. E-27
Faris, G. W. A-2
Feldman, B. J. KA-2, KA-5
Fincke, J. R. LA-6
Fitaire, M. E-46
Flanagan, D. J. NA-31
Flannery, M. R. GB-2
Fleddermann, C. B. CA-6
Forster, J. QA-1
Freidhoff, C. B. GB-3
Freund, R. S. FA-1
Friedmann, J. B. A-6
Frömling, G. NA-10
Fucaloro, A. F. MB-2

G

Ganguly, B. N. GA-4, NA-25, RB-4
Garscadden, A. GA-4, J-6, NA-9, P-5,
RB-4
Gastineau, J. E. J-29
Gekat, F. FB-3
Gellert, B. GA-2
Gerardo, J. B. J-26
Gilliard, R. P. J-13
Gist, T. NA-9
Glenewinkle-Meyer, Th. NA-28
Godyak, V. A. E-11, J-1, NA-2, RA-1
Gogolides, E. E-6, J-2
Gordon, M. BA-2, GA-6
Gorse, C. NA-18
Goto, T. BA-5
Gottscho, R. A. CA-1
Gousset, G. E-24
Graham, W. G. E-44, NB-5, RA-4,
RB-5
Graves, D. B. E-7, E-20, NA-1, RA-2,
RA-6
Green, B. D. NA-31
Greenberg, K. E. A-4, A-5, J-4
Gyls, V. T. QB-3

H

Haaland, P. D. NA-27
Hakham-Itzhaq, M. RB-7
Hanson, R. K. RB-6
Harbison, B. J-9
Hargis, Jr., P. J. A-4, A-5, J-4
Harman, G. CA-7

Hay, P. J. MB-3
Hays, G. N. J-26, KA-3
Helm, H. CB-2, E-47, E-48
Henchman, M. GB-5
Herron, J. T. J-15
Hershkowitz, N. J-7, NA-3, QA-3
Hirota, E. BA-5
Hitchon, W.N.G. BB-1, J-8, J-16
Holber, W. M. QA-1
Hudson, D. J-17
Huennekens, J. NA-30
Huestis, D. L. A-2, E-47
Hui, P. E-13
Huo, W. M. E-40
Huppert, G. L. RA-5
Hussein, M. E-10

I

Ibrahim, M. J-26
Ingold, J. BC-1
Inokuti, M. NA-11
Ip, P.C.F. NA-17
Ishii, M. A. NA-11
Itabashi, N. BA-5

J

Jaacks, D. H. E-45
Jaffe, S. M. E-28
Jain, A. K. E-37, MB-4
Jairath, R. BA-7
James, G. K. J-25, LB-3
Janik, G. NA-26
Jeffries, J. B. A-1, A-3, QB-5
Jellum, G. M. E-20
Jiang, T. Y. LB-6
Johnsen, R. CB-4, E-41, E-42
Jolly, J. E-32
Jorda, M. E-46

K

Kadar-Kallen, M. A. E-17
Kaneda, T. J-5
Kannari, F. LA-2
Karabourniotis, D. J-14
Kato, K. BA-5
Keehan, M. S. GB-2
Kegelman, T. E-27
Keller, J. H. QA-5
Kimura, M. E-35, E-36, NA-11
Kizirmis, S. W. RB-3
Kline, L. E. E-14, P-4
Knowles, P. NA-28
Kocecic, J. E-21
Koch, D. J. J-16
Kogelschatz, U. GA-2
Kojima, H. BA-4
Komatsu, K. LA-2
Krech, R. H. QB-1

Kruger, C. H. BA-2, GA-6
 Kulkarni, S. V. E-33
 Kunhardt, E. E. BB-2, BC-4, KB-7
 Kunkel, W. B. E-30, NA-8
 Kushner, M. J. BB-3, BB-4, FB-6,
 FB-7, KB-3, LA-4,
 LA-5, LA-7, NB-6, P-6

L

Lacour, B. FB-2
 Lagally, M. G. NA-7
 Lakdawala, V. K. E-33
 Lam, K. W. E-26
 Lawler, J. E. BB-1, J-8, LB-4,
 MA-2, NA-7
 Leduc, E. E-46
 Lee, H. S. CB-4
 Lefkow, A. R. NA-7
 Legentil, M. FB-2
 Lembo, L. J. E-47, E-48
 Leone, S. R. GB-1
 Leroy, R. E-15
 Leung, K. N. E-30, NA-8
 Levine, M. A. MA-4
 Lichtenberg, A. J. J-11, NA-5
 Lieberman, M. A. E-2, E-3, J-11, NA-5
 Liescheski, P. B. J-22
 Lima, M. LB-1
 Lin, C. C. LB-4, NA-17
 Lin, T. H. CA-5
 Lipson, S. J. NA-31
 Litzenberger, L. LA-1
 Liu, J. E-6, RA-5
 Lockwood, R. B. LB-4
 Lopez, P. RB-2
 Lorents, D. C. E-48
 Lowenthal, M. NA-8

M

Ma, C. J-22
 Mahajan, S. M. E-26
 Maleki, L. NA-26
 Mann, J. B. FA-2
 Marconi, M. C. GA-3
 Marcum, S. D. NA-24, NA-25
 Marec, J. E-24
 Marrs, R. E. MA-3
 Martus, K. E. J-21, J-23
 Matsui, E. LA-2
 McArthur, D. A. KA-3
 McCaughey, M. J. BB-4
 McClelland, T. KA-5
 McConkey, J. W. J-30, J-31
 McEwan, M. J. E-43
 McGeoch, M. LA-1
 McKoy, V. LB-1
 McNaughten, P. MB-4
 McNeil, J. R. J-9
 McVittie, J. P. E-9
 Mentel, J. FB-3, J-18

Merts, A. L. FA-2
 Meyerott, R. J. QB-2
 Meytlis, V. E-27
 Michels, H. H. E-39
 Miller, T. GB-5
 Miller, T. A. E-31
 Mitchell, A. CA-1
 Mitchell, J.B.A. FA-3
 Mitchner, M. E-28
 Mizzi, S. FB-2
 Moeny, W. M. KB-4, KB-5
 Moore, J. H. BA-3, LB-2
 Morey, I. J. E-2
 Morgan, T. J. FA-3
 Morgan, W. L. CA-3, E-19, J-10, NA-29
 Morris, R. A. GB-5
 Morrow, T. RB-5
 Moskowitz, P. NA-21
 Msezane, A. Z. E-38
 Mueller, H. GA-1
 Mueller-Markgraf, W. CA-4
 Mullan, A. A. NB-5
 Murnick, D. E. E-12
 Murray, C. NB-4

N

Neal, D. R. KA-3
 Neiger, M. GA-1
 Nesnidal, M. P. J-29
 Neuman, W. A. LA-6
 Newman, L. A. KA-1
 Nicolai, J.-P. J-3
 Nishiwaki, N. BA-5
 Norcross, D. W. J-20
 Novak, J. P. NA-16

O

O'Brian, T. R. MA-2
 Obara, M. LA-2
 Ohwa, M. LA-4, LA-5, LA-7
 Olthoff, J. K. J-15
 Oskam, H. J. E-8
 Ottinger, Ch. NA-28
 Owano, T. BA-2, GA-6

P

Pack, J. L. E-14
 Pak, H. KB-3
 Palladas, A. J-14
 Palmer, B. A. MA-1
 Paranjpe, A. P. E-9
 Pasquiers, S. FB-2
 Passow, M. RB-2
 Patterson, E. L. KA-4
 Paul, P. H. RB-6
 Paulson, J. F. GB-5
 Pearton, S. J. CA-1
 Penetrante, B. M. BC-3, MA-4, NB-1

Persing, H. M. NA-3, QA-3
 Person, J. NA-31
 Persuy, P. E-32
 Peterkin, F. E. KB-6
 Peterson, J. R. E-44
 Petrović, Z. Lj. KB-2
 Phaneuf, R. A. MB-1
 Phelps, A. V. E-14, KB-2, NA-20,
 QB-3, QB-4
 Piejak, R. B. E-11, J-1, NA-2, RA-1
 Pihlstrom, B. NB-2
 Poor, M. R. CA-6
 Popovic, S. E-21
 Porteous, R. K. E-7, RA-6
 Pouvesle, J. M. NA-19
 Preppernau, B. L. E-31
 Pritchard, H. LB-1
 Puech, V. FB-2

R

Raiche, G. A. QB-6
 Rata Booshanam, A. J-19
 Rathge, R. D. GA-7
 Redwing, R. NA-7
 Reich, N. FB-3
 Reicher, D. W. J-9
 Riemann, K.-U. E-5, NA-13
 Riley, K. KA-2
 Rocca, J. J. FB-4, GA-3, NB-4
 Rodriguez, A. E. KB-4
 Romo, W. J. LB-5
 Rood, M. J. NB-6
 Roque, M. J-21
 Rosmus, P. NA-28
 Rossi, M. J. CA-4
 Rudolph, R. N. BA-3
 Ruskell, T. G. J-29

S

Sakeek, H. F. RB-5
 Samlin, G. E. KA-4
 Sappey, A. D. A-1, A-3
 Sardja, I. NB-7
 Sato, H. E-35, E-36
 Sauers, I. CA-7, J-15
 Savas, S. E. E-3
 Sawin, H. H. CA-2, E-6, J-2, J-3,
 RA-3, RA-5
 Schaefer, G. E-13
 Scheller, G. R. CA-1
 Scheuer, J. T. J-12, NA-12
 Schlachter, A. S. E-30
 Schlie, L. A. BC-2, FB-5, GA-7,
 MB-7

Schmerge, J. F. GA-3
 Schorpp, V. GA-1
 Schulman, M. B. GA-5
 Schwirzke, F. KB-1
 Scoles, G. E-25
 Self, S. A. E-9, E-28
 Sen, A. D. E-43
 Shamim, M. J-12, NA-12
 Sharp, W. E. GB-4
 Sharpless, R. L. E-29
 Sharpton, F. A. LB-4
 Shemansky, D. E. J-25, LB-3
 Sheng, T. NB-2
 Shoemaker, J. R. E-23, GA-4, RB-4
 Shohet, J. L. A-6
 Shuker, R. RB-7
 Shyn, T. W. GB-4
 Siegel, R. J-21
 Smith, G. P. QB-6
 Smith, P. A. J-9
 Snitchler, G. J-20
 Sommerer, T. J. BB-1, J-8
 Spence, D. E-34, E-35, E-36
 Srivastava, S. K. MB-2, NA-22
 Stalder, K. R. E-29, NA-4
 Steinhauer, J. NA-5
 Stern, R. A. E-15
 Stevefelt, J. CB-1, NA-24
 Stevens Miller, A. E. GB-5
 Stockwald, K. GA-1
 Stockwell, W. NA-8
 Stutzin, G. C. E-30
 Suda, A. KA-2
 Sugai, H. BA-4
 Sultan, G. E-32
 Surendra, M. NA-1, RA-2
 Swenson, G. R. QB-2
 Szapiro, B. NB-4

T

Tackett, M. L. NA-25
 Takahashi, S. LA-2
 Tanaka, H. E-35, E-36
 Teich, T. H. RB-1
 Terai, K. J-5
 Thompson, D. G. MB-4
 Timmer, C. NA-22
 Tin, C. C. CA-5
 Tosh, R. E-42
 Toups, M. F. E-8
 Toyoda, H. BA-4
 Trainor, D. W. LA-2
 Trajmar, S. MB-3
 Tsai, J. H. RA-7
 Tsakonas, A. J-14
 Tserepi, A. E-31
 Tucker, J. E. KA-5
 Tzeng, Y. BA-1, CA-5

U

Upschulte, B. L. QB-1

V

Vahedi, V. E-1, E-2
Valluri, S. R. LB-5
Van Brunt, R. J. E-33, J-15
van den Berg, H. E-5
van der Burgt, P.J.M. J-30
van der Donk, P. FA-3
Verboncoeur, J. E-2
Viggiano, A. A. GB-5
Voshall, R. E. E-14
Vušković, L. LB-6

W

Wadehra, J. M. E-39
Wan, H. X. LB-2
Wang, C. J. E-4
Wang, M-C. KB-7
Wang, S. J-31
Watari, K. LB-1
Waymouth, J. F. P-2
Wells, W. E. NA-24
Wendt, A. A-6, J-7, NA-3, QA-3
Weng, Y. BB-3
Wengorz, Th. J-18
Werner, H. J. NA-28
Wernsman, B. FB-4
Wexler, B. L. KA-2, KA-5
Whaling, W. MA-2
Wickliffe, M. W. MA-2
Wiese, L. E-45
Williams, M. D. NA-8
Williams, M. S. NA-6
Williams, P. F. KB-5
Williamson, M. NA-5
Winstead, C. LB-1
Wood, B. P. J-11
Woods, R. C. NA-23
Woodward, D. R. GA-5
Wormhoudt, J. BA-6
Wright, M. W. FB-5, MB-7
Wu, C. E-4, RA-7
Wysong, I. J. QB-5

Y

Yamada, C. BA-5
Yaney, P. P. RB-3
Yenen, O. E-45
Young, A. T. E-30
Youngman, K. KB-5
Yousif, F. B. FA-3
Yu, Z. J-9, NB-2

Z

Zarnani, H. NB-2
Zau, G. CA-2
Zhu, P. FB-1
Zissis, G. E-22
Zuo, M. LB-6